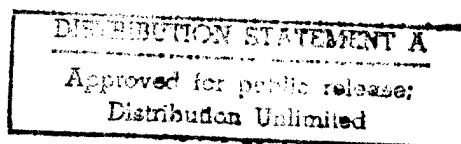172114

JPRS 83371

29 April 1983

USSR Report

ELECTRONICS AND ELECTRICAL ENGINEERING

No. 102

19980608 209

FBIS FOREIGN BROADCAST INFORMATION SERVICE

NOTE

JPRS publications contain information primarily from foreign newspapers, periodicals and books, but also from news agency transmissions and broadcasts. Materials from foreign-language sources are translated; those from English-language sources are transcribed or reprinted, with the original phrasing and other characteristics retained.

Headlines, editorial reports, and material enclosed in brackets [] are supplied by JPRS. Processing indicators such as [Text] or [Excerpt] in the first line of each item, or following the last line of a brief, indicate how the original information was processed. Where no processing indicator is given, the information was summarized or extracted.

Unfamiliar names rendered phonetically or transliterated are enclosed in parentheses. Words or names preceded by a question mark and enclosed in parentheses were not clear in the original but have been supplied as appropriate in context. Other unattributed parenthetical notes within the body of an item originate with the source. Times within items are as given by source.

The contents of this publication in no way represent the policies, views or attitudes of the U.S. Government.

PROCUREMENT OF PUBLICATIONS

JPRS publications may be ordered from the National Technical Information Service (NTIS), Springfield, Virginia 22161. In ordering, it is recommended that the JPRS number, title, date and author, if applicable, of publication be cited.

Current JPRS publications are announced in Government Reports Announcements issued semimonthly by the NTIS, and are listed in the Monthly Catalog of U.S. Government Publications issued by the Superintendent of Documents, U.S. Government Printing Office, Washington, D.C. 20402.

Correspondence pertaining to matters other than procurement may be addressed to Joint Publications Research Service, 1000 North Glebe Road, Arlington, Virginia 22201.

USSR REPORT

ELECTRONICS AND ELECTRICAL ENGINEERING

No. 102

CONTENTS

COMMUNICATIONS

SOLID STATE CIRCUITS

SONICS & ULTRASONICS

NEW ACTIVITIES: MISCELLANEOUS

USE OF ACOUSTOELECTRONIC CONVOLVERS IN PHASE LOCKING SYSTEMS

KUZICHKIN, A. V. and TARASOV, V. M.

[Abstract] The feasibility of an acoustoelectronic phase locking loop for
automatic frequency control is examined, such a conventional system consist-
ing of a phase detector, a low-pass loop filter, and a tunable self-excited
oscillator. The performance of this system is analyzed by assuming a narrow-
band signal at the detector input and calculating the signal at the filter
output. The same output signal is obtainable with detector and filter re-
placed by an acoustoelectronic convolver. The latter consists of a piezo-
electric plate with internal or external nonlinearity and an interdigital
array of electrodes deposited on it. The input signal and the oscillator
signal are applied to respective interdigital transducers, one at each end
of the plate, and are converted here to oppositely propagating surface
acoustic waves. The transfer function of this system depends on the phase
error (it does not with detector and filter in the conventional system) and
the width of the unilateral noise band is proportional to the length of the
nonlinear-interaction space. Figures 2; references 7: 6 Russian, 1 Western.
[134-2415]

MEASURING ACOUSTIC PARAMETERS OF SURFACE-ACOUSTIC-WAVE TRANSDUCER BY LASER
PROBING METHOD

VOROSHNIN, A. B. and FELINSKIY, G. S.

[Abstract] The laser probing method is applied to measurement of absorption,
transmission, and reflection coefficients, also insertion losses, in an
acoustic channel containing an interdigital SAW receiving transducer which
converts acoustic energy to electric energy. The method is based on the
proportionality relation between area of the SAW profile over the SAW flux
aperture and acoustic power of the SAW flux in the given section, on the
square-law relation between laser diffraction efficiency and SAW amplitude
at the laser probing point on the surface of the acoustic waveguide, and on
the dependence of the acoustic parameters of the output transducer on the
character of the electric load. Solutions to the corresponding equations of
interaction yield the degree of matching between SAW transducer and acoustic
channel as well as basic requirements for construction of the measuring
equipment. The experimental equipment includes a 10 mW LG-52A laser with
a focusing lens, a high-frequency oscillator for exciting surface acoustic
waves, a diaphragm for extracting diffracted light and an avalanche photodiode
for recording it, a low-noise amplifier for amplifying the photodiode output
signal and sending it to the Y-input of an XY-plotter, a displacement trans-
ducer with digital-scaler and a digital-to-analog converter sending the
transducer output signal to the X-input of that XY-plotter, also a frequency
meter, a digital voltmeter, and an oscillograph. The areas of SAW profiles
are measured within 0.1% accuracy, taking into account instrument errors.
The method is effective for solution of problems of acoustic and electric
matching. Figures 3; tables 1; references 9: 7 Russian, 2 Western.
[134-2415]

2

RS-3/RS-8 AMATEUR RADIO SATELLITE TELEMETRY

[Article by A.Papkov, DOSAAF Master Radio Designer]

[Text] The TLM-12 telemetry transmission system was developed for the
"Radio"-series amateur radio satellites. This is the system carried
aboard the "Radio-3" and "Radio-8" amateur satellites. The telemetry
produced by the TLM-12 is received with an ordinary communications
receiver without using any additional devices.

In simplified form, this system can be viewed as a digital millivoltmeter
with a measurement range extending from 0 to 990 mV and with its input
connected via a 35-channel two-stage analog switch to 31 points in the
on-board equipment one at a time. The status of each stage of the input
switch, and consequently the meaning of the parameter transmitted, are
designated by particular letters, and the measurement result is
represented by a two digit zero between 00 and 99. For example, a value
of 9.1 V is transmitted by the digits "9" and "1" (91). The data obtained
in this manner is translated into Morse code and used to key the
satellite transmitter.

The TLM-12, whose structural diagram is shown in the figure, transmits data
on the value of the voltage at its 31st input. The voltage applied to the
24 inputs of the switch is first reduced by a factor of 10-20. Six of the
inputs have no dividers and are used for direct connection to tested circuits
with output voltage not exceeding 1 V. Information from the relay transmitter
output power transducer is applied to a separate input. All of the input
signals are measured with respect to the common "negative" circuit of the
entire system. Currents, temperatures, pressure and other nonelectrical
parameters are first converted to corresponding voltage values by special
devices.

The voltage measurement error of the TLM-12 system is $\pm 1\%$ of the sample
with a supply voltage of 9+002 V. Deviation of the power supply voltage
beyond these limits increases the measurement error. The TLM-12 system does

not have its own power supply stabilizer, but rather is powered from the 9-volt satellite source. The system draws as much as 5 mA when making a measurement (200 msec), and 1 mA the rest of the time (2.5-3 sec).
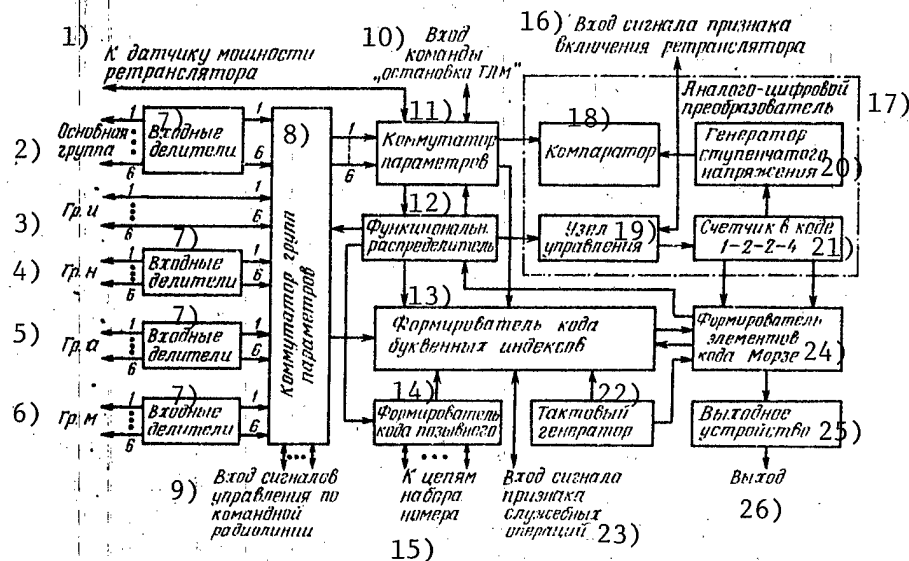
Figure 1 TLM-12 telemetry system

Key:

1 -- to relay power transducer
2 -- primary group
3 -- group i
4 -- group n
5 -- group a
6 -- group m
7 -- input dividers
8 -- parameter group switch
9 -- command link control signal input
10 -- "halt TLM" instruction input

11 -- parameter switch
12 -- functional distributor
13 -- literal index code generator
14 -- callsign code generator
15 -- to number dialing circuits
16 -- input for relay "on" flag
17 -- analog-digital converter
18 -- comparator
19 -- control unit
20 -- step voltage generator
21 -- 1-2-2-4 code counter

(continued)

4

Key to figure (continued)

22 -- clock
23 -- service operation flag
     signal input
24 -- Morse code element generator
25 -- output device
26 -- output

The telemetry frame of the TLM-12 system is divided into groups. Each
frame contains five groups of seven parameters. As was mentioned
earlier, each parameter has its own literal index. These indexes are
transmitted in the following sequence: K, D, O, G, U, S, V. The first
group of the telemetry frame is the primary group, and has no literal
index. The four remaining groups are given the indexes i, n, a, m. The
numerical value of each parameter is thus preceded by a one- or two-letter
index. This structuring of the telemetry data allows it to be received
under conditions of very strong noise and fading, and allows fragmentary
phrases to be put together to form a complete telemetry frame.

During reception there is no need to keep track of the alternation of
parameters: it is enough to receive one or two index letters and the
immediately following two digits in order to confirm unambiguously that the
value of a particular parameter has been received. If several operators
receive this data at the same time and compare their results, the accuracy
of the received data becomes higher.

After the parameters in each group have been transmitted there is a short
pause, after which the callsign of the satellite is transmitted, consisting
of the letters RS and the satellite number, e.g., for the fifth satellite in
the "Radio" series the callsign is "RS5".

The frequency with which the telemetry system inputs are sampled varies,
so that the transition from parameter to parameter is not uniform. This
rate is determined by the specific irregularity of the Morse telegraph
code which is used.

One advantage of the TLM-12 system is the capability for changing the
composition of the telemetry frame on line by sending signals over the
command radio link. In other words, a command from the ground can be
used to exclude from a telemetry frame any group in which the parameters are
not of current interest. It is also possible to exclude several groups in
any combination, or all groups, except for the basic group which is always
present in the telemetry frame.

TABLE OF RS-3/RS-8 SATELLITE TELEMETRY PARAMETERS

K	--	relay output power	mW	$0.2N^2$
D	--	power supply voltage	V	$0.2N$
O	--	load current	mA	$20(100-N)$
G	--	service parameter	-	-
U	--	"	-	-
S	--	stabilizer unit temperature	°C	N
V	--	transmitter radiator temperature	°C	N
iK	--	relay output power	mW	$0.2N^2$
iD	--	calibration	-	00
iO	--	beacon output power	mW	$0.2N^2$
iG	--	relay sensitivity	dB	N
iU	--	AGC for command link receiver	rel. un.	N
iS	--	AGC for robot receiver	rel. un.	N
iV	--	AGC for service channel receiver	rel. un.	N
nK	--	relay output power	mW	$0.2N^2$
nD	--	solar battery current	mA	$50N$
nO	--	temperature of first solar battery	°C	$2.7(N-26)$
nG	--	temperature of second solar battery	°C	"
nU	--	temperature of third solar battery	°C	"
nS	--	equipment temperature	°C	$0.8(N-5)$
nV	--	gas temperature	°C	$0.8(N-10)$
aK	--	relay output power	mW	$0.2\ N^2$
aD	--	relay voltage 1	V	$0.1\ N$
aO	--	relay voltage 2	V	$0.1\ N$
aG	--	voltage of stabilizer 1	V	$0.1\ N$
aU	--	voltage of stabilizer 2	V	$0.1\ N$
aS	--	voltage of stabilizer 3	V	$0.1\ N$
aV	--	voltage of stabilizer 4	V	$0.1\ N$
mK	--	relay output power	mW	$0.2\ N^2$
mD	--	fill out on-board robot log	QSO	N
mO	--	engaged heater power	W	$0.1\ N$
mG	--	robot transmitter power	mW	$20\ N$
mU	--	service channel transmitter power	mW	$20\ N$
mS	--	robot receiver sensitivity	dB	N
mV	--	service channel receiver sensitivity	dB	N

When performing various experiments with the satellite, e.g., tracking its position in space, the amount of data on a particular parameter can be increased significantly by blocking the input switches. When this is done, the literal indexes and digital value of only one particular parameter are transmitted continuously. This blocking is done by an instruction from the ground, which is transmitted when the telemetry system is sending the parameter of interest. The system is also unblocked via the command link.

The distribution of the parameters in a complete telemetry frame and the formulas for translating them to the required quantities are shown in the table.

The parameter "K" in each group contains information about the output power of the transmitter, allowing radio amateurs to judge the loading of the relay channel and the required signal power. However, it must be recalled that the total power of the output stage of the transmitter, which emits beacon and robot signals in addition to the relay signals, is what is measured. If the parameter "K" in each group is followed by two zeros (00), this means that the relay channel is off.

When the command point is executing service operations, the literal index of the basic group is preceded by the index ye, and the literal indexes of the other groups are changed as follows: s replaces i, r replaces n, u replaces a and v replaces m.

The paramters iG, mV and mS provide information about signal attenuation conditions at the inputs of the satellite receivers in decibels. When these parameters have values of zero, the sensitivity is at its maximum.

COPYRIGHT: Radio No 9, 1982

6900
CSO: 1860/115

7

PROBABILITY OF CUTOFF OF TRACKING PROCESS IN MULTIDIMENSIONAL RADIO
TRACKING SYSTEMS

VAGAPOV, V. B., Ukrainian SSR

[Abstract] Cutoff of the tracking process in radio systems is defined as
the first excursion of at least one component of the vector of regulation
errors beyond the tolerance limits, the tolerance region being defined in
the form of a rectangular hyperparallelepiped. With the frequency of such
excursions equal to the ratio of the mathematical expectation of their
number within a given time interval to that time interval, the probability
of cutoff is calculated first for a stationary tracking process and then
for a nonstationary one. It is assumed in the latter case that the dynamic
deterministic components of the regulation error vary more slowly in time
than does its fluctuation components. For illustration, the results are
applied to a two-dimensional tracking system responding to a given harmonic
input signal. Figures 4; references: 3 Russian.
[135-2415]

AUTOCORRELATION FUNCTION FOR SIGNAL SCATTERED BY LARGE BODY IN MOTION

VOROB'YEV, V. I. and MASLAKOVA, N. A., Belorussian SSR

[Abstract] In order to determine the dependence of the statistical charac-
teristics of an electromagnetic or acoustic field scattered by a large body
on the transmitter-receiver-body configuration, the autocorrelation function
for a reflected (scattered) signal is derived so as to apply to a sufficiently
general arbitrary configuration. A scattering region is considered which

consists of N point reflectors, each moving along a random trajectory while the entire region (its center) moves at a constant velocity. The field intensity vector of a scattered signal is calculated by the electrodynamic method, applicable to a staggered radar system. Figures 2; references 5: 2 Russian, 3 Western (all in translation).
[135-2415]

ACTION OF NOISE ON DISCRETE VELOCITY TRACKING SYSTEMS WITH DISCRIMINATORS OF CORRELATION TYPE

MELEZHIK, V. A.

[Abstract] An analysis is made of the effect that noise has on discrete velocity tracking systems with frequency discriminators of correlation type. A single frequency measurement is made on the pulse reflected from the target with each exposure by a probe pulse. To smooth errors and accomplish velocity tracking, these measurements are processed by recurrence equations. This procedure reduces the variance of signal frequency measurement errors at the output of the tracking system by a known amount. An expression is given for the dynamic error in the steady state, assuming that the target moves with constant acceleration. It is shown that an AGC system maintains the signal power constant at the input in the presence of noise. Comparative analysis shows that the main factor responsible for malfunction of such tracking systems in the presence of noise is failure of the discriminator rather than increased error fluctuations. This becomes a problem under dynamic conditions when the target moves with an acceleration that gives rise to a change in the Doppler frequency of the reflected signal. Figures 3.
[128-6610]

DYNAMIC PROGRAMMING IN PROBLEMS OF SYNTHESIS OF MULTICHANNEL PHASING DEVICES

KAKHANOVICH, V. A. and TSARYUK, D. A., Belorussian SSR

[Abstract] The method of dynamic programming is applied to synthesis of multichannel microwave phasing devices capable of realizing M different amplitude-phase distributions in N elements in a radar system. As the

quality criterion serves a functional proportional to the rms error of all distri tions, which is to be minimized. The minimization process is broken up into several iterations with groups of vectors in each fixed sequentially according to the optimum strategy. The problem of synthesis reduces to search for this optimum strategy. The method was used for synthesis of an optimum multibeam linear antenna array with $N = 15$ elements spaced uniformly (period $d = 0.5\lambda$) and with a feedthrough system for optical excitation. Figures 2; references 3: 1 Russian, 2 Western (both in translation).
[135-2415]

ANALYSIS OF THRESHOLD SETTLING PROCESS WHEN NOISE INTENSITY CHANGES IN ADAPTIVE AND ROBUST RADAR SIGNAL DETECTORS

VOLKOV, V. Yu. and OVODENKO, A. A.

[Abstract] Adaptive threshold regulation is used to maintain a predetermined probability of false alarm during the inevitable changes in statistical characteristics of noise that occur during radar signal detector operation. The authors consider an algorithm of adaptive regulation of the post-detector threshold in accordance with an estimate of the quantile of one-dimensional noise distribution by discrete steps. This algorithm ensures automatic establishment of a predetermined probability of occurrence of noise spikes at the detector input with comparatively slow changes in noise characteristics. An analysis is made of the process of settling of the threshold and corresponding change in the probability of false alarm with a stepwise change in noise intensity. It is found that a jump in noise intensity does have an effect on changing the probability of a false alarm, although this influence is slight. Figures 1; references 8: 7 Russian, 1 Western.
[128-6610]

PRECISE MEASUREMENT OF RADIOTELESCOPE ANGLES

GIPPIUS, A. A., SAFONOV, L. N. and SEVRYUKOV, B. N.

[Abstract] A standard instrument has been developed and is commercially
produced for precise measurement and plotting of the angular coordinates
of large radiotelescopes. The instrument contains two inductosyns (rotating
multipole air-core transformers with pancake coils) as primary angle trans-
ducers, each with a coarse-reading transducer and an extension line to a
common digital data processing module. This module is interfaced with a
corrector consisting of an input device, an instructions memory, a control
device, an arithmologic unit, a data memory, and an output device. Time and
temperature stability of the analog part of the fine-scale phase measuring
channel is ensured by differential compensation of the parametric phase lead.
The rms intrinsic instrument error does not exceed 5", the error of individual
measurements being determined principally by the inductosyn accuracy and
not exceeding 10". The rms error of rotation angle measurements must still
be reduced further, to 1", which can be achieved either by increasing the
intrinsic inductosyn accuracy or by compensating and correcting the systematic
errors. At least three variants of a corrector design are proposed:
1) with the space distribution of errors determined directly through control
measurements with geodetic instruments and stored in the form of corrections;
2) with only the interpolar $2\pi/p$-periodic error corrected, by amplitude modu-
lation of the phase shifter output signal; 3) with use of an array of medium-
precision transducers. Figures 1; references: 3 Russian.
[134-2415]

EXACT AND APPROXIMATE METHODS OF CALCULATING MICROWAVE GROOVE IC MICROSTRIP
LINE

YASHIN, A. A.

[Abstract] Procedures are given for designing solid-state IC microstrip
lines for microwave antenna applications. Formulas are derived for calculat-
ing the major parameters of groove striplines with rectangular and curved
channels. The expressions given for the rectangular case are exact, while
the curvilinear relations are approximate with accuracy of 0.25-0.5%. The
given algorithms can be programmed, and standard software is available in
the YeS EVM computer complex for calculating the pertinent special functions.
Figures 2; references 8: 6 Russian, 1 Western in translation, 1 Japanese.
[128-6610]

DECOUPLING OF ANTENNAS BY MEANS OF PLANE DEVICES

LOMUKHIN, Yu. L., VOLKOVYSSKIY, Yu. I., CHIMITDORZHIYEV, N. B. and
BADMAYEV, S. D., Buryat ASSR

[Abstract] The feasibility of reducing the coupling between antennas near a
plane conducting surface by means of diffracting structures was studied in
experiments with plane shields oriented either transversely or longitudinally
between the plane metal surface of slot antennas. The experimental data ob-
tained with rectangular and circular shields, supported by theoretical cal-
culations of field attenuation between antennas coupled in the E-plane, in-
dicate that shields in either configuration can be effective in correcting
the radiation pattern of such antennas. The degree of decoupling depends on
the shield dimensions and on the distance between antenna and shield,
relative to the wavelength, and can be maximized by optimum shield design
for a given wavelength (frequency) of radiation. Figures 7; references 10:
8 Russian, 2 Western.
[135-2415]

DEPHASED HORN RADIATOR WITH MAIN LOBE OF ELLIPTIC CROSS SECTION

ZHULIDOVA, I. I. and TIMOFEYEVA, A. A.

[Abstract] Formulas are given for calculating the geometric dimensions of
antennas with low gain in which the width of the main lobe of the radiation
pattern is polarization-independent and is considerably different in mutually
perpendicular planes. The simplest type of antenna that produces the re-
quired radiation pattern is a dephased horn with broken generatrix that has
different flare angles in the principal planes. The authors consider two
modifications of such horns: with elliptic and with pyramidal apertures.
Experimental measurements based on the proposed computational technique
show that the radiation patterns of the two modifications are similar. The
formulas derived in the paper can be used with practical accuracy for
determining dimensions of horns to give a radiation pattern of predetermined
width and shape in the main lobe which differs appreciably in different
planes but is the same in different polarizations. Figures 4;
references 3: 1 Russian, 2 Western.
[128-6610]

PERFORMANCE OF STROBOSCOPIC CONVERTER USING FIELD-EFFECT TRANSISTOR WITH SCHOTTKY BARRIER

STAROSEL'SKIY, V. I., SUETINOV, V. I. and KOZLOV, A. T.

[Abstract] The availability of GaAs high-speed field-effect transistors with Schottky barrier has made it possible to develop a wideband stroboscopic converter of analog signals. Such a device consists of a transistor switch and an emitter follower, the latter with a current source and a high-resistance or transistor load. The circuit includes also a biasing resistor and a buffer resistor between the storing capacitor and the gate of the transistor in the emitter follower stage. The performance of this device is analyzed on the basis of an equivalent circuit with two identical voltage-dependent nonlinear resistances and one time-dependent capacitance representing the transistor channel. During operation the strobe pulse shifts periodically relative to the input signal, thus in effect leading it. The dependence of the transient time on the transistor width has been calculated and measured with the size of the storing capacitor ranging from 0.01 to 0.1 pF. Also the optimum transistor width, for minimum transient time and maximum bandwidth, has been determined. An experimental stroboscopic converter was designed and built for a bandwidth of 0.5 GHz, but an analysis of data indicates that a bandwidth of 5 GHz is feasible. Figures 4; references: 5 Russian.
[134-2415]

NONUNIFORMITY OF OUTPUT SIGNAL IN VIDICON DELAY DEVICES

ATAMUKHAMEDOV, M. B. and ZUKHRIDINOV, T. Kh., Moscow Electrical Engineering
Institute of Communications

[Abstract] Deviation from orthogonality of electron beam incidence on the
plane of the target during recording and readout of video signals in a
vidicon gives rise to nonuniformity of the output signal in vidicon delay
devices. This nonuniformity can be described by a combination of an additive
and a multiplicative component. In the first approximation, the shape of the
resultant nonuniformities is approximated by a parabolic equation. Thus the
nonuniformity can be reduced by applying a signal of parabolic shape to the
vidicon cathode. When this is done, the residual nonuniformity at the edges
of the raster may reach 5%. Experiments have shown that this residual non-
uniformity can be considerably reduced by using compensation signals that
have steeper than parabolic drop on the edges of the TV raster. A compensating
function that is more convenient than the parabolic is
$\xi(x, y) = (2e^{-\alpha|x|} - e^{-2\alpha|x|})(2e^{-b|y|} - e^{-2b|y|})$, where $b = 0.75$, $\alpha = 2\ln$
$(1 - \sqrt{1 - \beta})$ are coefficients determined from the condition of the extremum
of the function in the center of the raster, $\beta = u_{edge}/u_{center}$ is the relative
value of signal nonuniformity on the edges of the raster with respect to
the center. A block diagram is given of a TV test pattern generator used
to check the efficacy of such parabolic and exponential compensation signals.
Experiments confirm the sup riority of the exponential signal. Figures 2;
references: 5 Russian.
[130-6610]

USING GAME THEORY TO SYNTHESIZE OPTIMUM SYMBOL-BY-SYMBOL DATA TRANSMISSION
SYSTEM

ZHODZISHSKIY, M. I.

[Abstract] The author considers the problem of determining the optimum
algorithm which minimizes a certain criterion functional not to be exceeded
for any interference distributions in operation of a receiver acted on by
an additive mixture of signal and artificial interference. Such an
algorithm can be determined by game theory methods because the communication
line is attempting to minimize the criterion functional (error probability),
while the interference source attempts to maximize it. This conflict

situation can be analyzed by the mathematical theory of antagonistic games with complete information, the first player being the source of interference, and the second the [designer of the] communication line, where all invariable parameters are known to the players. Necessary and sufficient conditions are derived in terms of player strategies for extrema of the error probability in symbol evaluation in symbol-by-symbol data transmission for each player. Figures 1; references 5: 3 Russian, 2 Western (in translation).
[128-6610]

METHODS OF MULTIPLEXING COMMUNICATION CHANNEL WITH TELEVISION SIGNALS

NOVAKOVSKIY, S. V. and LITVINOV, G. K.

[Abstract] An analysis is made of three methods of transmitting more than one television signal over a single communication channel with minimum distortion of the image: 1) alternation of two color TV signals on the frame frequency using the effect of frame correlation with consideration of the characteristics of human perception of moving image components; 2) transmission of two programs over a standard communication channel by periodically forming a multiplexed signal common to two independent color TV programs from the signals of six fields; and 3) simultaneous transmission of four TV programs via one satellite communication channel by sequential time and frequency multiplexing. It is found that only analog systems can be used for transmitting several color TV programs over a single communication channel because present-day digital TV systems need a frequency passband of about 20 MHz for transmitting only one program, and therefore cannot utilize existing communication channels. Figures 5; table 1; references 5: 4 Russian, 1 Western.
[128-6610]

INTERFACE FOR TELEVISION CAMERA BUILT WITH CHARGE-COUPLED DEVICES FOR
AUTOMATIC PROCESSING OF IMAGES OF PARTICLE TRACKS

ASTAKHOV, A. Ya. and KOMOV, G. M., Joint Institute of Nuclear Research,
Dubna

[Abstract] An interface has been developed for a television camera built
with charge-coupled devices which transfers binary images of tracks of
particles from such a camera to the memory of a computer. The camera
characteristics are a sensitivity of 2 lx or better, a 3.89x4.83 mm^2 area
of image projection, and 144 lines with 232 elements/line in the photo-
sensitive compartment. Data output from the array occurs in intervals of
two lines at a frequency of 4.6 MHz. The memory for storing an array of
M rows and N columns is determined accordingly in order to facilitate
coding by either of two methods: 1) each array element at two levels (white
0, black 1); 2) linewise the coordinates of transitions from white image to
black image and from black image to white image. The television camera
operates on-line with a 1001-TPA/i minicomputer, with a program channel and
an autonomous channel. The interface is built with series 155 TTL micro-
circuits, assembled into a 1M wide CAMAC module. Tracks of particles are
extracted from the data array, the FILTR program for this purpose having
been written for this particular computer and occupying 600_8 words of the
memory. The algorithm extracts track elements in accordance with the
connectedness criterion. Processing is simplified and shortened by elimina-
tion of the mathematical apparatus, least squares or other, required in
conventional filtration of track center coordinates. The projector-camera-
interface-computer system is eminently suitable for use in spark chambers
and for processing laser Fourier images much more accurately and with much
better reproducibility than semiautomatic instruments such as PUOS and BPS-
75 (Soviet-made) or CAMET. Figures 4; references 2: 1 Russian, 1 Hungarian.
[140-2415]

TELEVISION CHARACTER GENERATORS

SHENGELAYA, V. A., Georgian Republic Radio-Television Center

[Abstract] The author reviews the principles of various systems for imaging
characters on a CRT screen. The method of raster character generation is
singled out as the best for use in broadcast television. A conventional TV

receiver equipped with small character generators and memory units can be
easily converted to a passive terminal of an information system or data
imaging device. Character generators now used in TV centers perform the
following functions: 1) Introducing up to 96 or 128 letters or special
characters in the image; 2) Changing the scale of the generated character
within certain limits; 3) Creating a library of type-styles on external
media (floppy disk, cassette, and so on); 4) Recording, storing and revising
150-400 pages of text on an external magnetic medium with subsequent page-
by-page sampling; 5) Automatic centering of the text relative to the vertical
axis of the screen; 6) Displacement of the text to any area of the screen;
and 7) Scrolling. A description is given of a TV display which permits on-
line complete or partial modification of the character library. Figures 3;
references 11: 10 Russian, 1 Western in translation.
[130-6610]

NEW MODULATION SYSTEM FOR TELEVISION TRANSMITTERS WITH SIMULTANEOUS
AMPLIFICATION OF IMAGE SIGNALS AND SOUND TRACK SIGNALS

GLAZMAN, E. S. and POPOV, A. A.

[Abstract] A new modulation system has been developed for television trans-
mitters which is compatible with simultaneous formation and amplification of
image signals and sound track signals. It involves quadrature modulation of
the image carrier frequency ω_{ic} at the difference audio frequency Ω_{au},
adding three auxiliary signal components at the combination frequencies
$\omega_{ic} - \Omega_{au}$, $\omega_{ic} \pm \Omega_{au}$, respectively, to the two main ones at the frequencies
ω_{ic} and $\omega_{ic} + \Omega_{au}$ so as to reduce signal fluctuations and amplitude peaking,
and appropriately shaping the signal envelope without undesirable widening
of the frequency spectrum with the minimum number of stages (tubes). Inter-
modulation interference and thus also moire are suppressed through quadrature
modulation of the brightness signal with the color signal, which eliminates
the need for precorrection. Excellent energy characteristics are attained
by quadrature pulse-modulation of the brightness signal frequency at the
difference frequency between stage carrier frequencies and sound track signal
frequency. The new system has been designed on a basis of a thorough analysis
of all energy relations and all sideband signal components, the latter in-
cluding those generated in the process of nonlinear amplification. The new
system has been tested, comparatively with the existing system, in an
ATRS-5/1 kW television transmitter in the III-rd frequency band. The appro-
priate modifications of the transmitter equipment include insertion of a
quadrature color-signal shaping circuit between i-f modulator output and
step-up frequency converter in the image channel, insertion of a quadrature
pulse-signal shaping circuit into the sound track channel, addition of a

band elimination filter for the lower color subcarrier frequency to the common output feeder, and replacement of GU-73B and GU-74B tubes with GU-93B and GS-42B tubes, respectively. The performance characteristics are: power requirement for simultaneous amplification with transmission of black-out level 18 kVA, power factor 0.94, output power 5.5/0.55 kW, intermodulation interference level -55 dB. They meet specifications of GOvernment Standards 20532-75 and 11515-65 as well as CMEA and IRCC requirements. Figures 9; tables 3; references 6: 4 Russian, 2 Western.
[126-2415]

TELEVISION CAMERA FOR PHOTOGRAPHY OF FAST MOVING TRAINS

IVANUSHKIN, Yu. M., senior scientific associate, KOSILOV, R. A., candidate of technical sciences, docent, and TERESHIN, N. V., junior scientific associate, all at All-Union Correspondence Institute of Railroad Transportation Engineers, and KISELEV, L. M., chief engineer, experimental-test loop of All-Union Scientific Research Institute of Railroad Transportation

[Abstract] A television system with a vidicon camera has been designed for recording images of fast moving trains in traffic control. A plain vidicon would be inadequate for this application, because at a high train speed (up to 220 km/h) the rate of signal current decay would be too low and the rate of image displacement on the transmitter tube screen would be too high. The problem is solved by separating the process of image exposure on the transmitter tube screen and the process of electric profile readout from the vidicon memory. The exposure time is reduced, to 1 ms if necessary, by means of an electromechanical modulator of the train image: a disk with a hole rotating behind the input objective. The disk, driven by a d.c. motor, is synchronized with the camera by half-frame pulses and stabilized through an automatic control system which receives redtangular pulses at a rate of 25 Hz from a tachometer (optical rpm transducer) tracking the disk and rectangular pulses at a rate of 50 Hz from the camera synchronizer. An experimental camera, low-inertia vidicon with electromechanical modulator, has been installed at the test loop in the Shcherbinka station, together with a recording system. The latter includes narrow-band frequency modulation of the telecamera signal, input to magnetic storage of the YeS 5081 computer, output from storage, demodulation, and control of video tracking of train. No blurring of images has so far occurred with camera 8 m away from the track and a train moving at 80 km/h. The possibility exists of registering trains, the speed of which exceeds 100 km/h. Figures 4.
[139-2415]

HIGH-EFFICIENCY FREQUENCY CONVERTER

DROZDOV, V. (UA3AAO) and ZHUKOV, S. (UA3ACV), Moscow

[Abstract] A schematic diagram of a frequency converter with wide dynamic range is given with a brief explanation of the basic circuitry. The converter consists of two switches connected in a bridge circuit and transformer-coupled to a control circuit. Sine-wave voltage from a heterodyne is converted to square-wave pulses with rise time of no more than 2 ns. The resultant control pulses are amplified by a transistorized differential amplifier, and balanced by a resistor that equalizes the durations of positive and negative control pulses. Resistors limit the maximum current through the open diode switch, while the voltage incident on these resistors, which is the reverse voltage for the closed diode switch, determines the maximum amplitude of the input signal to be converted, the input and output being mutually reverse. Tests wtih a crystal-controlled oscillator as the heterodyne on a frequency of 5.2 MHz showed sensitivity of 1.8 µV at a signal-to-noise ratio of 10 dB. The level of the converted useful signal fell by 1 dB when the level of an interfering signal outside the passband of the IF channel reached 1.6 V. The level of third-order intermodulation components was no more than 100 dB. The latter parameter can be improved by 6-10 dB if a low-loss IF filter and more sensitive IF amplifier are used. Practical recommendations are given for construction. Figures 2.
[129-6610]

LED-BASED LINEAR SCALES

[unsigned article]

[Text] An LED-based linear scale is an integrated circuit formed of LED structures (segments) arranged sequentially, and the required electrical connections.

Discrete LED structures are turned on by a control device. When turned on, they have the appearance of a solid glowing line which becomes longer or shorter depending upon the number of LED activated.

Linear scales are used to display continuously varying information: the rate of movement of an object, liquid or temperature level, the composition of a gaseous medium, output channel signal levels, etc.

These scales are analogs of pointer-type indicators, and make it possible to read out information rapidly, to fix the peak values of measured quantities and to monitor the containment of modes within acceptable limits. The impossibility of obtaining a reading with high accuracy is one shortcoming of linear scales.

Linear scales can be placed horizontally, as well as vertically.

The original material used to make series linear scales is gallium phosphide (GaP), which can produce light ranging from red to green, as well as solid suspensions of GaAsP and GaAlAs, which are used to obtain structures which glow red.

The most important parameter of linear scales is the strength of the light, measured in millicandles (mcd). The strength of the light is a function of the amount of d.c. passing through the segments. This is a linear function on the operating section of the curve. The strength of light produced by this device drops off sharply as temperature increases.

One specific characteristic of linear scales is the relative dispersion of the strength of the light between the glowing segments (elements) making

up one scale, which is defined by the ratio

$$\frac{I_{v_{max}} - I_{v_{min}}}{I_{v_{max}} + I_{v_{min}}} ,$$

where $I_{v_{max}}$ is the strength of the light of the brightest segment under nominal d.c., $I_{v_{min}}$ -- strength of light from dimmest segment under nominal d.c.

The relative dispersion and the strength of light between glowing segments in the same device does not exceed 50%.

Type ALS317A-G, 3LS317A-B and 3LS345A linear scales are produced in rectangular plastic cases, with the light coming from the side opposite the leads.

Type ALS343A-5 and 3LS343A-5 linear scales are produced in the form of chips with flat glowing elements and contact areas. These devices are designed for use in hybrid integrated microcircuits or equipment units providing sealing and moisture protection. The chips are mounted with a conducting adhesive (K-3, AS-40V, etc.). It is recommended that the leads be secured by thermocompression or ultrasonic welding.

When installing encapsulated linear scales, the soldering should be done no closer than 4 mm from the case at temperatures not exceeding 260°C for no more than 3 sec employing a heat sink. The heat sink can be a flat clip with jaws at least 3 mm wide. No electrical current can be allowed to pass through the device during soldering, and solder and flux must be kept away from the illuminated surface of the device. After soldering, the glowing surface of the linear scale must be cleaned with a soft tightly woven cloth soaked in alcohol.

The basic parameters of linear scales at an ambient temperature of 25°C are given in tables 1-4; figures 1-3 provide dimension drawings, lead numbering and connection diagrams.
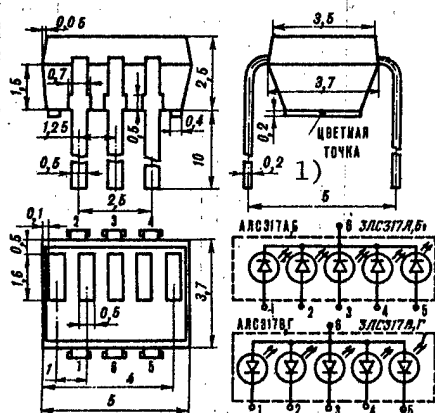
Figure 1

Key: 1 -- colored dot
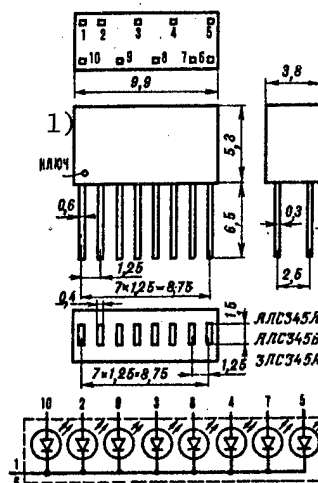
Figure 2

Key: 1 -- switch

Figure 3
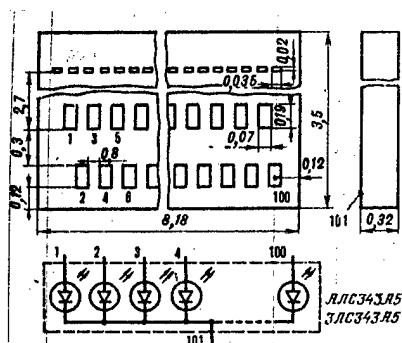
TABLE 1

PARAMETERS OF 5-SEGMENT LINEAR SCALES

Type of Device	Material	Color	Strength of light, mcd, with I_{dc}=10 mA	For fixed voltage, V, with I_{dc}=10 mA	Maximum spectral distribution, μm	Conventional type designation — Case color	Number of colored dots
ALS317A	GaAlAs	red	> 0.16	< 2	0.665	red	one black
ALS317B	GaAlAs	red	> 0.35	< 2	0.665	red	two black
ALS317V	GaP	green	> 0.08	< 3	0.568	green	one black
ALS317G	GaP	green	> 0.16	< 3	0.568	green	two black
3LS317A	GaAlAs	red	> 0.16	< 2	0.665	red	none
3LS317B	GaAlAs	red	> 0.35	< 2	0.665	red	one blue
3LS317V	GaP	green	> 0.08	< 3	0.568	green	none
3LS317G	GaP	green	> 0.16	< 3	0.568	green	one blue
3LD317D	GaP	green	> 0.32	< 3	0.568	green	two blue

Light strength and fixed voltage values shown for one segment. Dispersion of light strength not exceeding three-fold within one device.

Currently produced only with common anode.

Maximum Modes

Forward d.c. at t_{env}=+70°C for one segment, mA 12

Operating temperature range, °C . . . . -60 - +70

TABLE 2

PARAMETERS OF 8-SEGMENT GaAlP-BASED LINEAR SCALES

Type of Device	Light strength, mcd, for I_{dc}=10 mA	Fixed direct voltage, V, for I_{dc}=10 mA
ALS345A	> 0.3	< 2.2
ALS345B	> 0.2	< 2.2
3LS345A	> 0.3	< 2.2

Display color red. Maximum spectral distribution 0.6 μm. Light strength and fixed direct voltage values shown for one segment.

Maximum Modes

Forward d.c. at t_{env}=+70°C (for one segment), mA .   .   .   [sic]

Fixed reverse voltage, V   4

Operating temperature range, °C   .   .   .   . -60 - +70

TABLE 3

PARAMETERS OF 100-ELEMENT CASELESS GaAlP-BASED LINEAR SCALES

Type of Device	Light strength, mcd, for I_{dc}=1 mA	Fixed direct voltage, V, for I_{dc}=1 mA
ALS343A5	> 5	< 2.5
3LS343A5	> 5	< 2

Display color red. Light strength and direct fixed voltage values shown for one element. Dispersion of light strength in one device not over three-fold.

TABLE 4

MAXIMUM MODES (For One Element)

Pulsed d.c., mA	Type of Device	ALS343A5	3LS343A5
	for τ_{imp} = 1 msec, t_{env} = + 70°C	30	20
Forward d.c., mA	at t_{env} = + 35°C	2	–
Forward d.c., mA	for t_{env} = +70°C	1	–
Fixed reverse voltage, V	–	3	–
Operating temperature range, °C	–	–60 – +70	–

6900
CSO: 1860/115

INTEGRATED CIRCUITS FOR MILLIMETER-WAVE BAND (SURVEY)

YEMEL'YANENKOV, B. N., KOSHEVAYA, S. V., GASSANOV, L. G. and
OMEL'YANENKO, M. Yu.

[Abstract] The basic electrodynamic components available for monolithic
circuit integration and hybrid circuit integration are microstrip lines,
coplanar structures, fin lines for centimeter and long millimeter waves,
"dielectric" structures (cubes, cylinders, spheres), for short millimeter
waves, and quasi-optical resonators. The main structural and design charac-
teristics of these components are reviewed, as well as methods fo their
excitation. Active elements now used for the millimeter-wave band, in such
devices as oscillators and mixers, are primarily Gunn-effect and IMPATT
diodes and Schottky-barrier field-effect transistors. The unique properties
of GaAs make this material preferred, but other semiconductor and dielectric
materials with negative differential conductance are also suitable where
nonlinearities are required. The main development trends are miniaturization
through monolithic circuit integration with increasing functional capability,
with optimization of component matching for any given wave band, including
signal receiving and processing devices. Figures 12; references 83:
28 Russian, 55 Western (1 in translation).
[127-2415]

PHYSICAL PRINCIPLES OF PRODUCING INTEGRATED CIRCUITS FOR MILLIMETER-WAVE
BAND

YEMEL'YANENKOV, B. N., KOSHEVAYA, S. V., GASSANOV, L. G, and
OMEL'YANENKO, M. Yu.

[Abstract] Production of integrated circuits for the millimeter-wave band is
made possible by the availability of active solid-state devices for signal
generation and processing such as amplification and of solid-state electro-
dynamic transmission lines. Energy transfer between electromagnetic oscil-
lations or waves is effected either by conduction electrons or by a non-
linearity mechanism. Transverse electromagnetic waves have so far received
most attention, but propagation of optical and acoustic as well as spin and
magnetoelastic waves through various crystals has also been established, quasi-
surface waves of all these types being especially advantageous in integrated
microwave electronics. The main two problems relevant to design and per-
formance of integrated microwave circuits are wave instability modes,
negative differential conductance being a possible cause of absolute or
convective instability during electron drift in complex GaAs crystals, and
nonlinearities of semiconductor devices such as nonlinear current-voltage
characteristics and nonlinear piezoelectric or electrostrictuve effects.
A survey of studies made on this subject indicates that oscillation pro-
cesses in lumped elements and wave processes in distributed elements can
serve as basis for microwave circuit integration. References 55: 40 Russian,
15 Western (6 in translation).
[127-2415]

TUNABLE NARROW-BAND RADIO-FREQUENCY FILTER

GOLENISHCHEV-KUTUZOV, V. A., MIGACHEV, S, A., TARASOV, V, F. and
SHAMUKOV, N. A., Kazan Physico-Technical Institute, Kazan branch,
USSR Academy of Sciences

[Abstract] A tunable narrow-band filter for radio frequencies has been
developed for operation at room temperature. It consists of two piezoelec-
tric (quartz) transducer plates separated by a sound guide, with one low-Q
variable-capacitor LC-circuit across the input transducer and another one
across the output transducer. Signals are selected through the mechanism

of dimensional acoustic resonance attending the propagation of volume
acoustic waves in a sound guide between two parallel plates. Both LC-
circuits are tuned simultaneously for matching the two transducers with the
signal source and the signal receiver respectively. A mercury column serves
as the sound guide. It has a characteristic impedance higher than that
of quartz ($19.7 \cdot 10^6$ kg/m^{2}s) and makes good acoustic contact with a quartz
surface which has been polished to optical precision, even though it does
not wet it. The two X-cut quartz disks are 10 mm in diameter and have
silver coating on their outside faces, for electrical connection to the
matching capacitors, the mercury column between their inside faces serving
as their other common electrode. Mechanical adjustment is provided by a
plunger and three screws, electrical trimming is provided by a piezoceramic
(TsTS-19 material) cylindrical bushing with silver coating on both inside
and outside surfaces. The operating range of the filter is 1 ÷ 100 MHz, the
tuning range is +10% of the operating frequency and the trimming precision
is within +0.1%. Passband and attenuation are determined by the length of
the sound guide and on the closeness of coupling between the acoustic
resonator and the matching circuits. When designed for 5 MHz, the filter
has a bandwidth not exceeding 1.6 kHz and inserts an attenuation of 25 dB.
Figures 2; references: 1 Russian.
[140-2415]

DIGITAL MATCHED FILTER

MAKAROV, S. B. and MEDVEDEV, B. M., Leningrad Polytechnic Institute

[Abstract] A digital matched filter has been designed for optimal processing
of discrete signals coming from an analog-to-digital converter in the form
of an m-digit code. In addition to the converter in the input stage, the
device contains a digital multiplier, a 256x8-bit direct-access memory, a
digital adder, a pulse response shaper between memory and multiplier, and
a digital-to-analog converter in the output stage. The pulse response
shaper, with 16 selectable quantization levels, is tunable to various forms
of signal modulation. The filter maximizes the signal-to-noise ratio at the
output in the presence of an additive signal+noise mixture at the input. It
is programmable for operation in the recording mode and in the readout mode.
The components are built with series K564 microcircuits, but its speed can
be increased through substitution of K130, K133, or K530 series, or with
fewer quantization levels and fewer selectable pulse response values. Its
structure is universal, inasmuch as components can be added for any specific
application. Figures 2; references 5: 4 Russian, 1 Western in translation.
[140-2415]

TUNING EQUATIONS FOR SINGLE-RESONANCE CIRCUITS

MACHUSSKIY, Ye. A.

[Abstract] The tuning range is established for single-resonance circuits, a parallel one with a variable capacitance and a series one with variable inductance. The respective formulas are $f_{max}/f_{min} = (C_{max}/C_{min})^p$ and $f_{max}/f_{min} = (L_{max}/L_{min})^p$, where p is the ratio of energy stored in the tuning element to total energy stored in the circuit. When the derivative of the susceptance of the external circuit with respect to frequency remains proportional to the susceptance of the tuning element, then p remains constant throughout the tuning range. In real circuits p varies, but these formulas are still very accurate when the variation of p remains small or the frequency dependence of the susceptance of the external circuit can be approximated with a curve corresponding to a constant p. Figures 2; references 3: 2 Russian, 1 Western.
[127-2415]

WIDE-BAND AMPLIFIERS DESIGNED AROUND MOS FIELD-EFFECT TRANSISTORS

GOLOVKOV, A. A. and PIVOVAROV, I. Yu.

[Abstract] An approach is proposed to the synthesis of equivalent circuits of the input and output impedances of MOS field-effect transistors in a common-source hookup, and expressions are derived that relate the maximum frequency band of an amplifier to the parameters of the transistor. It is assumed in the analysis that the voltage gain of the transistor is greater than unity, and that gate-source and gate-drain leakage resistances are equal to zero. It is shown that for most microwave MOS power transistors, the limitations imposed on the working band of an amplifier by reactive components are more relaxed for the output circuit, and it is the input circuit that determines amplifier bandwidth. The graphs and formulas given in the paper can be used to determine the maximum possible working band of an amplifier or the limiting permissible parameters of the transistor. Figures 5; references 5: 4 Russian, 1 Western.
[128-6610]

COMPENSATION LIGHT FILTERS FOR COLOR MOTION PICTURE PHOTOGRAPHY

KAPKINA, A. A., KURITSYN, A. M. and SHLYAKHTER, Ye. M., All-Union Scientific
Research Institute of Motion Picture Photography

[Abstract] Motion picture color film is generally balanced for artificial
lighting, and trimming filters are used for daylight or for sources with
different color characteristics. In this paper a comparative analysis is
made of the characteristics of trimming filters produced in the Soviet
Union and elsewhere. It is concluded that non-Soviet filters are made in
excessively narrow steps. Such fine corrections are not necessary in profes-
sional color photography. It is recommended that Soviet light filters
should be supplemented with a series providing the necessary steps for
compensating mixed illumination. Considerable shifts should be made with
interference coatings, and intermediate steps can be covered by combining
these coatings with film light filters designed for minor conversions.
Figures 6; tables 7; references 13: 11 Russian, 2 Western.
[130-6610]

NEW SERIES K174 MICROCIRCUITS

SADOVNIKOV, I.

[Abstract] The concluding part of a data sheet on series K174 ICs. The
first part of the sheet was printed in RADIO, No 10, 1982. This part gives
schematic diagrams and characteristic curves for the K174UN12 stereophonic
volumen and tone control, and the K174KhA6 chip for IF channels in UHF FM
broadcast receivers. The K174UN12 meets GOST specifications for first and
second class receivers and amplifiers. Nominal supply voltage is 15 V,
current consumption is 40 mA, range of volume control at least 77 dB,
range of channel balance control at least ±6 dB, signal-to-noise ratio at
100 mV input, at least 52 dB, and working frequency range at least 20-
20,000 Hz. The K174KhA6 amplifies, limits and detects FM IF signals, pro-
vides noiseless tuning to the received station, generates field strength in-
dicator signal voltages, and provides AFC. This chip has a nominal supply
voltage of 12 V, current consumption of 16 mA, input voltage limitation of
60 μV in frequency range of ±50 kHz, and a coefficient of attenuation of
parasitic amplitude modulation of at least 46 dB. Figures 11.
[129-6610]

THIRTY-TWO-CHANNEL ELECTRONIC MODULE FOR WIRE CHAMBERS

BARTIKYAN, M. V., MIRZOYAN, S. S., MATEVOSYAN, E. M., OGANYAN, K. Sh..and
SHIKHLYAROV, K. K.

[Abstract] An electronic device has been developed for recording signals
from a multiwire proportional chamber. This 32-channel MKE-32 device is
built with complete large-scale hybrid integration, for operation with a
sequential-sampling module in conformance with the CAMAC system. The record-
ing module consists of one horizontal board and four vertical boards, each
vertical one carrying eight channel and connected through an RLMI-2 connector
to the horizontal one carrying converters and branchers of "fast OR",
"record", "read", "clear" signals. The module has an input impedance of
1.3 kohm and a recording threshold of $1.5\pm15\%$ mV. It is mounted directly
on the chamber and connected to the latter through RLMI-2 connectors in two
planes. Its performance with a 256-channel orthogonal XY chamber was tested
with an automatic CAMA - Computer ("Elektronika-100/16I") system.
Figures 3; references: 2 Russian.
[140-2415]

UNDERGROUND CORROSION AND ELECTROCHEMICAL PROTECTION OF ARMORED CABLE WITH
LEAD SHEATH

LUNEV, O. A., MISHCHENKO, V. I. and NIKOL'SKIY, K. K.

[Abstract] A study was made of underground corrosion of cables, specifically
of the role played by the sheath-armor pair in KMB-4 cables with lead sheath.

The experimental data were interpreted in terms of theoretical relations on the basis of an equivalent electrical resistance network with signal current, polarization and leakage currents, and potentials of all the current sources. Calculations were made on a Nairi-2 computer. The results of this analysis reveal that the effectiveness of electrochemical protection increases with a decreasing number of leakage paths between armor and sheath. The effectiveness can be further increased by insertion of resistances between them at the locations of protective anticorrosion devices. A more elaborate design procedure is required for protection of cable segments also exposed to stray, lightning, and electromagnetic pickup currents. Figures 4; tables 4; references: 3 Russian.
[126-2415]

EXPERIENCE IN OPERATION OF HERMETICALLY SEALED SINGLE-QUAD CABLES IN RURAL COMMUNICATION SYSTEMS

VOSS, M. A. and PARFENOV, Yu. A.

[Abstract] Hermetically sealed KSPPZ single-quad cables with copper conductors 0.9 and 1.2 mm in diameter, a polyethylene insulation sheath, and a hydrophobic filler have been designed for transmission of analog signals at frequencies up to 550 kHz and digital signals at repetition rates up to 700 kHz, underground or overhead at ambient temperatures from -50 to +50°C. On the basis of actual operation in rural communication networks covering over 100,000 km cable length, data have been obtained pertaining to:
1) Defectiveness in manufacture, defectiveness in installation, defectiveness of terminal equipment; 2) Mechanical defects in cable sheath and core caused by extraneous construction work along cable route; 3) Defects caused by rodents; 4) Defects caused by lightning; and 5) Loss of hermeticity. These data are compared with those for other types of cables (KSPP, KSPPB, KSPPBZ). Standard relations are given which define unit and complex reliability parameters, the operating data covering the 1975-79 period are evaluated in these terms, and the stability of electrical cable characteristics are projected for a period extending over more than 10 years. Figures 1; tables 3; references: 4 Russian.
[126-2415]

ALGORITHM OF TWO-DIMENSIONAL FOURIER TRANSFORMATION WITH MIXED BASE

VASYUK, G. I.

[Abstract] When a multidimensional discrete Fourier transformation is to be
performed, algorithms with mixed base become most expedient. This is demon-
strated in this brief communication on two-dimensional arrays $N_1 = 3 \times 2^r$ and
$N_2 = 3 \times 2^r$, for which an algorithm with mixed 2,3 base can be very economical
in terms of arithmetic operations, especially in terms of the number of
multiplications. As proof, an economical algorithm is devised first for a
square NxN array ($N = 3 \times 2^r$) and then for a square 3Nx2N array. General
expressions are derived for the number of multiplications of complex numbers
by one another, the number of multiplications of complex numbers by $\pm j$ or $1/2$,
and the number of additions of complex numbers. The actual numbers of these
operations are tabulated for r = 4,6,8. Figures 1; tables 2;
references: 1 Russian.
[134-2415]

INTERFERENCE IMMUNITY OF PHASE-KEYED SIGNAL RECEPTION IN CHANNEL WITH GAMMA
FADING

KROTOV, A. V.

[Abstract] In studying interference immunity of phase-keyed signals, gamma
distribution is taken as the probabilistic model of a signal that has passed
through a channel with fading because experimental research has shown that
such a model gives a good description of the actual situation in real
channels, and because this model is a generalization of some fading models
that have already been thoroughly studied. Also, gamma fading is a two-
parameter distribution, which enables high-accuracy approximation of experi-
mental curves for signal level distribution. The analysis covers both gamma
fading (where the model described fluctuations of signal amplitude) and
gamma attenuation (where the distribution applied to fluctuations of average
power of the signal). It is found that the depth of fading increases with
decreasing parameter η of the gamma distribution. Figures 3; references:
4 Russian.
[128-6610]

ENERGY CONTROL DURING SEARCH FOR SIGNAL IN MULTICHANNEL SYSTEM

TONKONOGOV, Yu. M.

[Abstract] An algorithm of search for a signal in a multichannel system is
proposed which not only takes into account the possibility of signal commu-
tation over channels but also provides energy control during each step of
the search, with invariance of the average power stipulated as constraint.
The time saved by using this algorithm instead of the algorithm of sequential
scanning of channels increases with decreasing frequency of false alarms and
with an increasing rate of signal commutation. Figures 1; references:
1 Russian.
[134-2415]

ESTIMATION OF SIGNAL PARAMETER ON BASIS OF ORTHOGONAL WALSH TRANSFORMATION

SENATOROV, A. K.

[Abstract] Use of the discrete orthogonal Walsh transformation for estimating
the parameters of a radio signal according to the maximum-likelihood
principle is demonstrated on an additive mixture of radio signal
$S(t,\vec{l}_0) = A(t,\vec{l}_0)\cos[\omega_0 t + \psi(t,\vec{l}_0) - \varphi_0]$ with a uniformly distributed random
initial phase φ_0 and white noise $n(t)$ with a unilateral spectral density N_0
appearing at the receiver input. The structure of the device for estimating
a nonenergy parameter consists of an analog-to-digital converter, an
orthogonal transformation module, and a weighting multiplication module.
The efficiency of the orthogonal Walsh transformation compares favorably with
that of the Fourier transformation, the accuracy of frequency estimation
being only slightly worse in the case of radio signals of finite duration
and even slightly better in the case of radio signals with phase keying.
Figures 2; references: 4 Russian.
[134-2415]

NECESSARY AND SUFFICIENT CONDITIONS FOR OPTIMALITY OF PHASE KEYED SIGNALS

MITSEL'MAGER, E. Ye. and MUKHAMEDYAROV, R. D.

[Abstract] A complete set of conditions is established, each necessary and
all together sufficient for optimality of phase keyed signals according to
the minimax criterion. A binary pulse code sequence and the corresponding
autocorrelation function are considered, an important universal property
of optimum phase keyed signals being that the number of blocks (longest
sequences of consecutive identical elements) is related to the number of
elements in the signal. A lemma and two theorems are proved which yield
these conditions, Expressions for specific values of the autocorrelation
function and corresponding sets of optimality conditions illustrate this
relation. References: 5 Russian.
[134-2415]

PARAMETRIC DISCRETE FOURIER TRANSFORMATION

PONOMAREV, V. A.

[Abstract] The discrete Fourier transformation is generalized into a parametric
one and applied to analysis of discrete signals given on the interval
[0,N-1] ($N = 2^n$, n = 1,2...) and complemented with N(r-1) (r = 1,2,...) null
readings. The properties of parametric discrete exponential functions are
described and, on their basis, the concept of periodicity is extended so as
to make N-periodicity a special case. The linearity theorem, the shift
theorem, and the correlation theorem are formulated and proved for the
parametric discrete Fourier transformation. From the shift theorem invariance
of the energy spectrum follows with respect to shift of a parametric N-
periodic function. These tools are useful for evaluating, for instance, the
aperiodic correlation function of a discrete signal x(n) (n = $\overline{0,N-1}$).
Figures 2; references 5: 4 Russian, 1 Western (in translation).
[134-2415]

INTERFERENCE IMMUNITY OF RADIO TRANSMISSION LINES WITH WIDEBAND SIGNALS

TEPLYAKOV, I. M., RSFSR

[Abstract] The performance of radio lines for continuous transmission of
digital messages is analyzed from the standpoint of interference immunity.
Transmission of pseudo-noise signals is treated as the reference base, by
means of which transmission of "jumping"-frequency signals and transmission
of hybrid signals are compared. Pseudo-noise signals can be generated
from a flux of binary input symbols either by means of a filter with a nearly
rectangular amplitude-frequency characteristics or by 180° phase-shift keying
of the carrier according to the law of pseudo-random sequences. "Jumping"-
frequency signals can be generated by frequency keying in the case of fast
"jumping" with only one binary symbol at any one frequency or by relative-
phase keying in the case of slow "jumping" with several symbols at any one
frequency. For either type of signals, including hybrid ones, 3 methods of
transmission are available: 1) Without redundant symbols; 2) Repetition
with a symbol split into subsymbols; and 3) Use of codes with error correc-
tion. A comparative evaluation of all modes of message transmission must
also take into account additional signal losses in the respective equipment.
Figures 3;   ables 3; references 7: 2 Russian, 5 Western (all in translation).
[135-2415]

USING DIGITAL-ANALOG ALGORITHMS TO EVALUATE INTERFERENCE IMMUNITY OF CONTINUOUS
MESSAGE TRANSMISSION

BRONNIKOV, V. N.

[Abstract] Among the disadvantages of pulse-code phase modulation is the
necessity for a considerable increase in spectral width and threshold power
of the received signal. Also, the quality of the communication channel is
not fully utilized because of the quantization error. Digital-analog al-
gorithms of message transmission can considerably alleviate these problems
by transmitting the quantization error simultaneously with the quantization
code, and by analog coding. In this paper a method is proposed for calculat-
ing the generalized gain in average transmitter power that is realized in using
a digital-analog algorithm for message transmission, and results of gain cal-
culations are given for specific algorithms in a defined class for signal
reception in the region above the threshold. The change in threshold power

of the received signal is evaluated. It is shown that a communication system with the proposed class of digital-analog algorithms for continuous signal transmission is competitive with other types of low-interference transmission such as frequency modulation where signal registration is not required, and there are restrictions on expansion of the signal spectrum. The range of gain in average transmitter power is 13-160 with signal spectrum expansion by a factor of 4, and an increase in threshold power of the received signal by a factor of 2-12. Tables 1; references: 3 Russian. [128-6610]

STATUS OF AND OUTLOOK FOR DEVELOPMENT OF HIGH-POWER RADIO BROADCASTING TRANSMITTERS

VOROB'YEV, A. A., GLUSHKO, M. M., SOKOLOV, E. P., SUDARIKOV, A. A., KHVILIVITSKIY, T. G. and TSEKHANOVICH, G. S.

[Abstract] During the 1970s Soviet industry developed and built radio broadcasting transmitters with power ratings from 5 to 2000 kW for both low-medium and high frequencies. Particularly successful is the PSV-2000 medium-frequency design serving as a basis for 500-1000 kW and 1000-2000 kW equipment. Further developments must increasingly cover the reliability and the degree of automation for eventual transition from continuously attended to completely unattended operation, improving the energy performance indicators, and reducing the design and production costs through standardization as well as the installation and operation costs. Achievement of these goals primarily requires systematic effort in the area of components, search for an use of new materials, adaptation of microelectronics and fiber optics to low-power circuitry as well as streamlining the construction of heavy-power equipment. A case in point is intensive current scientific-research and experimental-engineering activity in the development of new Class D radio amplifiers for operation in the switching mode with pulse-code-modulation of the input signal at constant amplitude and amplitude-modulation of the output signal. Three types of modulator are considered for such an amplifier: (1) Tube of half-wave modulator in series with tube of high-frequency power amplifier tube, operating like an amplifier plate supply with audio-frequency control for carrier-frequency power as well as sideband-frequency power; (2) Full-wave modulator in parallel with high-frequency power amplifier, operating like Class B device for sideband-frequency power only; and (3) Modulator in parallel with an amplifier, connected so that both can be grounded and require only one common plate supply, operating at variable carrier-frequency power with proportional percentage modulation. Version (2) is most advantageous in transmitters with power ratings up to 150 kW, version (3) is most advantageous in transmitters

with power ratings above 150 kW. Figures 4; references 18: 9 Russian,
9 Western (3 in translation).
[126-2415]

GUARANTEED DETECTION CHARACTERISTICS OF NONPARAMETRIC SIGNAL DETECTORS

BRIKKKER, A. M.

[Abstract] A procedure is outlined for determining conditions under which
the probability of signal detection is no less than a preassigned level for
devices or algorithms of nonparametric type which are designed to make a
decision on the presence or absence of a signal in a waveform observed for
a given duration, where the process may be either interference or a combina-
tion of signal and interference. The proposed method is based on the concept
of guaranteed detection characteristics determined by assigning classes of
possible received signals and distribution functions of interference.
Techniques are given for calculating the guaranteed detection characteris-
tics that are asymptotically optimum for certain signals and interference
distributions, with examples of construction of such characteristics, which
involves finding the minimum of the detection probability functional that
can be represented as the product of two functionals, one of which depends
only on the shape of the signals being received, while the other depends
only on the density of the interference. The Chebyshev inequality can be
usedcto construct guaranteed detection characteristics in isolated cases
where the detection probability can be represented as a function of many
variables that depends on a single random parameter. References: 4 Russian.
[128-6610]

INTERFERENCE IMMUNITY OF WIDEBAND DIGITAL HONEYCOMB STRUCTURE OF MOBILE
COMMUNICATION NETWORK

VARAKIN, L. Ye.

[Abstract] Subdivision of a territory into a honeycomb of many small
hexagonal service districts with a base station at the center of each is
a very effective way to maintain a reliable radio link with a subscriber

station installed on an object moving around this territory. The radio link is automatically relayed from one base station to the next as the subscriber moves from one hexagon into another, this arrangement making it possible to utilize repeatedly the same frequency channels in a relatively narrow assigned frequency spectrum. Here the essential design and performance characteristics of such a structure for transmission of digital information by noiselike spread-spectrum signals are evaluated, with particular emphasis on proper spacing of base stations and frequency channels to ensure sufficient interference immunity. CCalculations are based on a "spider web" pattern of interfering stations around the communicating one. The frequency spectrum is found to be much more efficiently utilized in such a system than in a centralized one. Figures 4; tables 1; references 15: 13 Russian, 2 Western.
[126-2415]

INTERFERENCE IMMUNITY OF DIGITAL SYNCHROPHASE SIGNAL DEMODULATORS WITH ANGLE MODULATION

KHOROSHAVIN, A. I. and FOMIN, A. F.

[Abstract] The paper deals with some untreated aspects of digital systems of phase synchronization involving analysis of the interference immunity of digital phase AFC systems that operate in the FM demodulation mode with consideration of the major forms of errors: dynamic, noise, time discretization and level quantization. The problem is formulated as applied to digital synchrophase signal demodulators, consisting in determining the optimum demodulator parameters and the coefficient of transmission of the filter such that the threshold effect occurs at the minimum signal-to-noise ratio at the demodulator input. This problem is solved by methods of the theory of digital automatic control systems, using the frequency technique in the z-transformation. The results can be used to calculate the optimum parameters of second-order digital synchrophase demodulators used for reception of angle-modulated signals with uniform message spectrum as a function of preset bandwidth and given method of digital integration. It is shown that the interference immunity of such demodulators is appreciably dependent on the frequency of time discretization, number of quantization levels and the methods of digital integration. Other things being equal, the most interference-immune demodulators are those in which digital integration is done by the trapezoidal method. Figures 2; tables 1; references: 6 Russian, 4 Western in translation.
[128-6610]

RADIOCOMMUNICATION IN MOUNTAINOUS TERRITORY OF TRANSCAUCASIAN TRUNK LINE

BIBILEYSHVILI, E. G., department head, Radio Communication and Automation of Signalization and Communication for Passenger Service on Transcaucasian Railroad

[Abstract] Existing ZhR-1 radio stations on steam locomotives in the Transcaucasian railroad system, installed during the nineteen sixties, are being replaced with much more modern ZhR-5M radio stations featuring better design and performance characteristics, operating with ultrashort waves and having a farther range. Already about 150 such radio stations for shunting operations have been installed, on locomotives and on ground in over 50 railroad stations. At the same time, a radio communication system for passenger service has been in operation here since the middle nineteen sixties, with ZhR-3 radio stations serving 78% of the Vesoloye-Samtredia line. Other railroad stations such as Tbilisi-freight, Tbilisi-junction, Tbilisi-sorting, Samtredia II, and Batumi-freight are to be similarly equipped. The main problems of organizing these train communication systems lie in the design, construction, installation and operation of radio transmission lines according to requirements imposed by this mountainous region which has a subtropical climate in its western part. Particularly interesting and challenging is the Zestafoni-Khashuri line with numerous artificial structures such as bridges, tunnels, galleries and sharp curves along the way, the most difficult having been supporting the waveguide inside the Surami tunnel. Another important problem is ensuring stability of ultrashort-wave radio communication in such a region. Along the 13 km long Chiatura-Sachkhere line and the 25 km long Chiatura-Zestafoni line this is not possible, because of the extremely rugged mountain reliefs, so that radio stations operating at the frequency of 2,130 Hz have been installed here. For shunting operations in large junction yards are recommended ZhR-U-LS and ZhR-U-SS radio stations with carefully mounted transmitter and receiver antennas. Outstanding contributions to development and installation of the communication system for the Transcaucasian railroad have been made by veteran radio operators T. S. Mandzavidze, Yu. A. Simkhovich, B. B. S. Dzhanpoladov, K. Ya. Alimbarashvili and I. P. Chalyy and others, as well as by highly skilled young radio operators V. Ukhanev, E. Soselia, G. Khurtsilava, Yu. Kolosovskiy, N. Titishvili, V. Megrelishvili, Sh. Martirosov, P. Purtseladze, G. Koroshinadze, Kh. Arabadzhan, A. Khachatryan, Yu. Oganesyan, and S. Agamiryan, and others.
[139-2415]

CLASSIFICATION OF TWO-DIMENSIONAL IMAGES

OSTROVSKIY, A. S., KURASHOV, V. N., MAKAROVSKIY, A. P, and ZINCHENKO, O. A.

[Abstract] An important part of automatic processing of two-dimensional signals is image recognition and classification. Design of an image calssifier is intimately associated with selection of informative indicators and can either be treated as the design of such a selector which maps m indicators into a single one or be treated as a problem separate from that of indicator selection. Classification of optical Fourier spectra by means of the Karunen-Loewe expansion may be adequate with not more than three coefficients-indicators and thus, with the optimum basis, be more efficient than with any other conventional basis. Calculation of the Karunen-Loewe functions requires solving a Fredholm integral equation of the second kind. Here use of a two-dimensional basis with Hermite functions is proposed, as a special case of this solution, and is applied to an array of images $\{X_n(u,v)\}$ with a factorizable correlation function $R_x(u-u',v-v') = R^I_x(u-u') \cdot R^{II}_x(v-v')$. An efficient orthogonal basis can be constructed with a suitable approximation of the correlation function. An interesting case is that where the partial correlation functions R^I and R^{II} can be approximated with Gaussian distributions, the Fredholm equation being solvable analytically. References 6: 3 Russian, 3 Western (2 in translation).
[134-2415]

POWER SUPPLY WITH AUTOMATIC FREQUENCY CONTROL FOR KLYSTRON OSCILLATORS

KABDIN, N. N., ORANSKIY, L. G. and SOLENYY, V. N.

[Abstract] A new power supply has been made available for klystron oscillators
used in radiospectrometers. It is designed for klystrons operating in the
2-mm wave band, but can also be used for any other millimeter-wave klystron.
During modulation of the repeller voltage the klystron frequency is stabilized
from an external resonator through an astatic automatic control system. A
crystalline or low-temperature n-InSb device can serve as the microwave
detector. It supplies: 1) 0-7 V to the filament with maximum current of
8 A and maximum instability $\leq 5 \cdot 10^{-5}$; 2) -20-(-500) V to the focusing system
with a maximum current of 10 mA and maximum instability of $\leq 10^{-4}$; 3) 100-
4000 V to the resonator with maximum current of 80 mA and maximum instability
$\leq 5 \cdot 10^{-5}$; and 4) -20-(-500) V to the repeller with maximum current of 10 mA
(gain 1000 with respect to control input, bandwidth 500 kHz, load capacitance
≤ 30 pF). The automatic frequency control provides a stability factor of at
least 1000 at 50 Hz, a dynamic range of 40 dB and a response speed of
50 microsecond. All stabilizer controls and the automatic frequency control
system are contained in the top cabinet, all power transformers with high-
voltage rectifiers and regulating transistors are contained in the bottom
cabinet. The unit draws 500 VA when plugged to a 380/220 V - 50 Hz line
and requires not more than 0.4 1/min of cooling water. A photograph of the
equipment is shown. Figures 1; references: 1 Russian.
[140-2415]

MEASUREMENT AND ABATEMENT OF NONLINEAR DISTORTIONS IN FM OSCILLATORS

VORONKOV, Yu. V.

[Abstract] Commercially available G4-107 and G4-116 FM oscillators generate
output signals with a high ripple factor in their frequency-modulation charac-
teristic. A device is proposed which can measure the second harmonic of
the modulating signal with high resolution and compensate this harmonic
very effectively. It consists of a low-frequency oscillator, two adders, an
FM oscillator, a distorter, a frequency deviation meter, two tuned ampli-
fiers, two phase shifters, two attenuators, and an output indicator. Its
operation is based on the principle of $n \cdot 180°$ phase change of the fundamental
modulating signal (n = 1) and of its harmonics upon retuning of the frequency
deviation meter from forward channel to mirror channel. The instrument can
also measure and compensate other even harmonics, but odd harmonics generated
in the oscillator cannot be separated from those appearing in the frequency
deviation meter. Figures 1;
[134-2415]

METHOD OF APPROXIMATING NONLINEAR CHARACTERISTICS OF ELECTRONIC COMPONENTS

ZUBCHUK, V. I. and SHPAKOVSKIY, A. A.

[Abstract] A method of approximating the characteristics of all passive and
active electronic components is proposed which, although not universally
applicable, yields in most cases a satisfactory analytical description of any
univalent dependence with weak or strong nonlinearity. The method is based
on using the function $y(x) = \alpha \ln[1 + e^{b(x - X0)}]$ so that

$$y(x) = \begin{cases} 0, & \text{if } x << X_0 \text{ and } e^{b(x-X_0)} \leq 1 \\ ab(x-X_0 & \text{if } e^{b(x-X_0)} >> 1 \end{cases}$$

This provides a smooth transition (coupling) from the straight line $y = 0$ to the asymptote through the point $(X_0,0)$ with a slope $\alpha = \tan^{-1}ab$. The form of the line depends on $Y_0 = y(X_0)$ and on a b. Numerical evaluation on a computer is possible as long as $b(X_{max} - X_0) < \beta = P_{max}\ln 10$ (X_{max} – maximum value of argument within the range of definition, P_{max} – maximum order of number with floating point for given computer). As a typical example, the input characteristics of K134TV14 JK-trigger is approximated in continuous and differentiable form with the sum of two variants of this function $(a_1,b_1; a_2,b_2)$ and some linear function. Figures 2; references 6: 3 Russian, 1 East German, 2 Western.
[134-2415]

MULTICHANNEL GENERATOR OF HIGH-VOLTAGE VOLTAGE PULSES

BEZUGLOV, V. G., GALAKHOV, I. V., GASHEYEV, A. S., IVANOV, V. I., KUZ'MICHEV, Yu. P., KUCHEROV, A. I., MASLOV, A. F. and MURUGOV, V. M.

[Abstract] A generator of firing pulses for dischargers has been built with a 3-electrode discharger and 118 coaxial cable segments as shaping lines. The discharger has a 9-mm long main gap between two ring electrodes. The high-voltage one is connected to the shaping lines in parallel and the other one is grounded. The firing electrode is separted from the high-voltage one by a ring insulator projecting into the main gap so as to allow a 10 ns delay from breakdown of the firing gap and turn-on of the discharger. The air in the working chamber is under a pressure of 10^6 Pa, which provides a 250% safety margin of electric strength. The inductance of the discharger is 30 nH. The 30 m long KVI-120 cable segments have a characteristic impedance of 50 ohm and a 120 kV insulation. The cables are precharged to -60 kV. With all of them connected to the discharger, the rise time of a voltage pulse at the open other end was measured as 0.18 µs and its amplitude was 120 kV. The rise time can be shortened by connecting fewer cables to the discharger. Figures 3; references: 4 Russian.
[140-2415]

MULTICHANNEL GENERATOR OF HIGH-VOLTAGE NANOSECOND PULSES

MATVEYEV, V. V., PRUT, V. V., SUSLOV, P. A. and SHIBAYEV, S. A.

[Abstract] A multichannel generator of high-voltage nanosecond pulses with
a rate of voltage buildup on the order of 10^{12} V/s and adjustable amplitude
of the control pulse has been developed where water replaces a coaxial cable
as the shaping line. It contains a storing capacitor with a capacitance
much higher than that of the shaping line, a controlled thyratron discharger,
a peaking discharger and a capacitive voltage divider. The peaking discharger
has a radial construction, ensuring low inductance, with insulators and with
stainless steel electrodes; it is filled with air under a pressure of 5 atm.
The shaping line is filled with water, after the latter had been purified
with ion-exchanging resins to an electrical resistivity of 1 Mohm·cm. The
voltage divider with a ratio 90:1 has an input capacitance of 22 pF and an
output capacitance of 2000 pF. Its lower cutoff frequency is determined by
the electrical conductivity of water, and its upper cutoff frequency is
determined by its natural frequency. The latter is approximately 10 GHz.
The charging time of the shaping line is 170 ns. The generator was tested
in a series of over 1000 discharges with a charging voltage of 45 kV and
pulse amplitude of 60 kV. Figures 3; references: 4 Russian.
[140-2415]

NOISE CHARACTERISTICS OF OSCILLATOR WITH GUNN-EFFECT DIODE IN 3-MM WAVEBAND

PUDALOV, V. M., Scientific Research Institute of Metrological Service,
Moscow

[Abstract] The noise characteristics of a 9 GHz oscillator with a Gunn-
effect diode (Soviet-made AA703) and varactor for frequency control over the
9.1-9.5 GHz range were measured and evaluated in accordance with IEEE defini-
tions and terminology. The measurements covered spectral density of power
fluctuations and spectral density of frequency deviations, the former
determined with the aid of a narrow-band Unipan-233 receiver with known
current-voltage characteristic and the latter determined with the aid of a
frequency discriminator. A comparison of the characteristics of this
oscillator with those of a similar 9 GHz oscillator without tuning varactor
and with those of two reflex klystrons (also a laboratory prototype of a

two-resonator klystron) indicates that this is indeed a low-power (3-5 mW) device. The fluctuations were also measured in the time domain, characterized and evaluated in terms of the Allen dispersion $\sigma_y(2,\tau)$, by mixing the output signal with one from an analogous oscillator with a 1000 times higher frequency stability in a superconducting resonator. Beat signals with difference frequencies of 50-200 Hz were passed through an amplifier-shaper with a 100 Hz - 1 MHz passband and at the TTL level sent to an NTA-1024 multiscaling analyzer. The characteristics of this oscillator should also be compared with those of low-noise cermet klystrons, but data on those are not yet available. The authors thank K. I. Andronik for assisting with measurements, I. Ya. Karsnopolin and S. G. Semenchinskiy for discussing the study, A. K. Yanysh and G. S. Chernyshev for technical assistance. Figures 3; tables 2; references 21: 7 Russian, 14 Western (1 in translation). [140-2415]

SHAPER OF CONTROL PULSES FOR HIGH-SPEED REGISTER ARRAYS OF CHARGE-COUPLED DEVICES

DIK, P. A., Moscow Institute of Engineering Physics

[Abstract] A shaper of two-level voltage pulses has been developed for controlling register arrays of charge-coupled devices with a p-channel. The device is also a level shifter, inverting the polarity of pulses from standard TTL elements. It is designed with maximum economy and with optimum phasing of the four output transistors in two KT339V-KT904A series pairs, one between the output center tap and the +5-(-5) V terminal and one between the output center tap and the -5-(-20) V terminal. The input stage contains one KT339B, one KT326A, one KP303B, and two KT316 transistors, also a KD503B diode. It is coupled to the upper output transistor pair directly and to the lower output transistor pair through a D312 diode. The pulse rise time and fall time depend on the load capacitance, both dropping to minimum under $C_L \sim 100$ pF (output voltage 18 V, switching frequency 1 MHz) and increase sharply as the load capacitance increases further. The maximum switching frequency is approximately 15 MHz until the load capacitance C_L exceeds 100 pF and decreases sharply as C_L increases further. The maximum amplitude of output voltage pulses must not exceed 20 V. Figures 3. [140-2415]

47

MILLIMETER-WAVE PULSE GENERATORS USING IMPATT DIODES (SURVEY)

KOTSERZHINSKIY, B. A., TARANENKO, V. P. and TRAPEZON, V. A.

[Abstract] Operation of IMPATT diodes in the pulse mode is characterized
by shift of the frequency during the presence of a radio pulse and by
dependence of the diode impedance on the supply current as well as on the
temperature. The frequency shift results in frequency modulation of the out-
put signal and the current-dependence of the diode impedance makes it possible
to control the frequency shift, as well as the rate of change of frequency,
by varying the shape of the current pulse. Two methods of controlling
the frequency shift are varying the current density, which is difficult but
expedient in the case of coherent generators, and injection of photons into
the active diode region by irradiation with a GaAs laser. Design of millimeter-
wave pulse generators involves calculating (in a quasi-continuous approxima-
tion) the length of the electron drift path for given current density and
junction temperature, calculating (through solution of the Poisson equation
by numerical methods) the impurity concentration for a given length of the
electron transit region, and optimizing (empirically) the area of the p-n
junction in the basic p^+-p-n-n^+ four-layer diode structure. The drift
region and the junction area must be larger for optimum performance than in
the case of continuous-wave operation. A generator consists of a diode
mounted in a waveguide under the supply stub, a filter in the supply circuit
(coaxial for frequencies up to 100 GHz, capacitive for frequencies above
100 GHz), a load matching transision, and a short-circuited tuning plunger.
Power compounding stages of a millimeter-wave pulse generator are assembled
into a coaxial waveguide structure. Existing devices deliver a power one
order of magnitude higher than corresponding continuous-wave generators,
the duration of current pulses ranging from 100 to 300 ns with a rise time
of a few nanoseconds and a 0.003-0.005 duty factor. Figures 11; tables 4;
references: 25 Western.
[127-2415]

GENERATOR OF PSEUDORANDOM SIGNAL

BESSONOV, S. A. and MARKELOV, A. S., Leningrad Institute of Mechanics

[Abstract] A generator of pseudorandom signals has been built using a
generator of maximum-length pseudorandom binary sequence and an analog

shaping filter. It includes a time base generator, a 24-digit shift register and a modulo-2 adder. The time base generator consists of two pairs of AND gates, the repetition rate f of time base pulses being determined by the parameters of the $R_1 C_1$ coupling circuit. The shift register consists of a chain of D-triggers connected in series. The maximum period of the pseudo-random sequence is $T = (2^{24} - 1)/f$, with triggers 19 and 24 connected to the adder. The pseudorandom sequence generator sends a signal to a scaling operational amplifier which, with the aid of a feedback capacitor and a trimming resistor, limits the signal spectrum at the high-frequency end. An output signal with a normal distribution is obtained by means of a low-pass filter with a cutoff frequency below 10^{-3} f and with an amplitude-frequency characteristics flat over the 0-50 Hz range. The output signal level is set by a 0-3 V potentiometer. Another trimming resistor compensates change in the time constant of the signal and an active high-pass filter centers the random process. The generator is supplied from three stabilized voltage sources: +5 and +15 V. A process of 2000 s duration with a readout frequency of 256 Hz has been produced at a time base frequency of 85 kHz, with the nonuniformity of its energy spectrum not exceeding ±1 dB over the 1-45 Hz range. The repetition period of the generator can be varied from 50 to 400 s. Figures 2; references 5: 4 Russian, 1 Western in translation.
[140-2415]

LIMITING PERFORMANCE PARAMETERS OF SOLID-STATE SWITCHES BUILT INTO RESONANCE-TYPE WAVEGUIDE ARRAY

ALYBIN, V. G.

[Abstract] A resonance-type waveguide-rod array with diodes at both ends of parallel rods inside, under the narrower waveguide walls, is an effective design configuration for high-power high-speed solid-state control devices such as switches and limiters, also reflection-type phase shifters. Its outstanding features are excellent heat dissipation and parallel-series connection of the switches with respect to the microwave current. The performance characteristics of such a device have been calculated, with the aid of PROTEC and PROCOM computer programs, on the basis of an equivalent circuit where each switching diode is in series with an inductance across a capacitance, each diode, each diode presenting in position 1 a resistance and in position 2 a resistance-capacitance series combination to the microwave current. From these characteristics and typical design data are determined the maximum attainable output power and frequency range of such a device, with forward, zero, or reverse bias. The results compare favorably with those for single-diode waveguide-pin structures. There are limitations on the array

structure and the feasible number of "tiers", diode and housing dimensions being the main constraining factor. Figures 3; references 8: 6 Russian, 2 Western (1 in translation).
[127-2415]

FREQUENCY CONTROL OF QUARTZ RF RESONATORS

POSTNIKOV, I. I.

[Abstract] Correctors are used in order to stabilize the emission frequency of crystal-controlled rf oscillators. The main stabilizing element is a quartz resonator with invariable characteristics. However, in oscillators with resonators in a glass envelope, the frequency can be varied by a local change in thickness of the field electrodes of the piezoelectric element by directed laser action. To do this, it is necessary to know the sensitivity of the piezoelectric element to a local change in thickness on both the fundamental (working) frequency and nearby side frequencies. The author derives expressions for determining this sensitivity, and finds the distribution of experimental values of sensitivity for anharmonics. The results can be used for correcting the frequency of crystal-controlled oscillators in adjustment or operation, precluding the use of additional correctors. When this technique is used in oscillators that incorporate correctors, discrete-analog frequency control can expand the frequency tuning range. Figures 7; tables 1; references: 5 Russian.
[128-6610]

AMPLIFIER-SHAPER OF HIGH-VOLTAGE PULSES FOR CONTROL GATE OF ELECTRON-OPTICAL CONVERTER

SHAMIS, V. I., SERBIN, I. S., KORNEYCHUK, V. V. and ZADOROZHNYY, I. S.

[Abstract] An amplifier-shaper of high-voltage pulses with a clamping diode has been developed for controlling the gate of electron-optical converters. It is designed to produce pulses of sufficiently high amplitude and with sufficiently uniform pulse top, without overshoots. It consists of a two-stage transistor amplifier matched, with respect to input

50

signal level, to a TTL logic built with series K155 or K133 microcircuits, an emitter-follower intermediate stage, and a transformer output stage. The output stage has a high-voltage transistor in the primary circuit and a diode across the secondary winding, with another diode between low-voltage terminal of the secondary winding and ground. The device can produce pulses with 1.6-2 kV amplitudes at repetition rates up to 5 kHz, with 100 ns rise time and 50 ns fall time. The width of the pulse top can be varied from 200 ns to 20 us. Figures 2; references: 3 Russian.
[140-2415]

HYPERSONIC DELAY LINE WITH PHASE STABILITY AND LONG DELAY OF MICROWAVE SIGNAL

GALUSHKO, V. S., GANOPOL'SKIY, Ye. M., KOROLYUK, A. P., NEVELEV, A. Ya. and TARAKANOV, V. V.

[Abstract] A new hypersonic delay line has been made available for storage of radio-frequency pulse signals in the 10-cm wave band. It contains a $LiNbO_3$ single crystal cooled to liquid-helium temperature. Time delays of 12 us to 2 ms, in 12 us steps, are achieved by multiple passage of a hypersonic wave through the crystal. The distinguishing feature of this device is that hypersound propagates here through a sound guide with a caustic surface, which minimizes the net attenuation and lengthens the total time delay. The minimum level of a signal that can be delayed is 10^{-10} V, with a microwave input pulse of up to 10 W power. The bandwidth is 25 MHz, with mechanical tuning up to 300 MHz. The maximum phase instability is 0.1°/min. Input and output terminals are superposed for operation in the "reflection" mode. The equipment includes an STG-10 vessel of 10 l capacity with liquid helium, enough for 20-30 days of operation. A photograph of the equipment is shown. Figures 1.
[140-2415]

COMPUTERS

UTILIZATION OF INTRAPERIOD SYMMETRY OF HARMONIC BASIS FUNCTIONS IN
CALCULATION OF DISCRETE FOURIER TRANSFORMS

SHUBS, Yu. V.

[Abstract] A major problem in performing the discrete Fourier transformation
is reducing the number of Fourier weighting factors. Here a method of cal-
culating a discrete Fourier transform is proposed which utilizes the intra-
period symmetry of Fourier weighting functions. It reduces the necessary
number of such factors to one fourth, without significant complication of
the classical procedure. This possibility is demonstrated by expanding the
complex weighting function in the transform into a product of two exponential
functions, one determining the absolute values of the Fourier weighting fac-
tors in the first quadrant and the other one representing the change of sign
upon crossover to another quadrant. All possible values of the coefficients
in the exponents form a table of rules for evaluating the Fourier weighting
factors. A digital processor with a parallel-series structure for perform-
ing the discrete Fourier transformation accordingly consists of two read-only
memories (values, signs), a multiplier, a local control, a commutator-
distributor, and two storing adders (real part, imaginary part) based on
arithmologic circuits such as type 155IPZ. Figures 1; tables 1; references:
2 Russian.
[134-2415]

EFFECT OF DISPERSION ERRORS IN MEMORIES ON ACCURACY OF DISCRETE SPECTRAL
ANALYSIS

SHUBS, Yu. V., Kiev

[Abstract] Data for discrete Fourier transformation in digital-analog and
hybrid processors are stored in digital-analog memories consisting of N
independent cells, N being the base of the signal to be analyzed. The
random dispersion of the transfer ratio of these cells produces a multi-
plicative dispersion error. Here the effect of this error on the accuracy
of a discrete Fourier transformation is evaluated by following through the
algorithm, the latter with and without this error taken into account. The
error can be minimized by splitting the memory into R parallel channels,
which is demonstrated in the worst case, the degrees of parallelization in a
practical situation being a tradeoff between error reduction and hardware
complexity. Figures 1; references 4: 2 Russian, 2 Western (1 in
translation).
[137-2415]

USE OF MULTIMICROPROCESSOR ARRAYS IN SWITCHING SYSTEMS

PASHKEYEV, S. D.

[Abstract] When a given set of problems to be solved by a switching system
imposes constraints on both time and the probability of their simultaneous
processing by existing computer facilities, one may consider the feasibility
of replacing these facilities with an array of available microprocessors and
then optimize the configuration of this array according to selected criteria.
Here such a multimicroprocessor situation is analyzed and a typical configura-
tion is established for a message switching center. It is assumed that all
algorithms of the problem solution are convertible to microprocessor al-
gorithms, that the dispatcher operation is equivalent to operation of a
single-channel single-phase queuing system, and that failure-free operation
of any single microprocessor has an exponential probability distribution.
Time and probability of problem solution by a single microprocessor are
selected as quality criteria for the array. Problems are solved at five
levels, without dispatcher (full duplication), partly without and partly with
dispatcher, or with dispatcher, the process including distribution of problems

between microprocessors. A procedure for estimating the performance characteristics and a procedure for determining the optimum microprocessor level are developed on the basis of relations for all relevant time and probability parameters. An array configuration is selected accordingly for a typical set of 20 problems, representable by a loaded graph of 4 s width and 64 s critical path, which consists of two microprocessors operating with either hardware or software dispatcher. References: 2 Russian.
[126-2415]

PROGRAMMATICALLY CONTROLLABLE INPUT OF ANALOG SIGNALS TO 'NAIRI-K' COMPUTER

BOGORODITSKAYA, R. A., VITEL'S, G. L., DOLOMANOV, V. G. and SHUL'MEYSTER, Yu. I., Scientific Research Institute of Mechanics and Physics, Oaratov State University, Saratov

[Abstract] An input-output interface for the "Nairi" computer has been developed which can also serve for programmatic control. One of its functions is input of a large array of analog signals (up to 128) from 8 analog-to-digital converters, each connectable to a 16-channel commutator. Implementation of programmatic control required expansion of the computer capabilities, including a control instruction with operation code 70_8 and an interlaced integrating microprogram as well as a permanent memory. The interface hardware, in addition to an adder, an instruction counter and an instruction register, also includes a data shaper with a two-way bus driven by I/O signals, an address and control shaper with bus driven by strobe signals, a synchronization lines, a state line, an error line, a strobe-pulse shaper and a "Tg Flag" trigger. The authors thank Yu. V. Voronkov and A. S. Velikanov for assisting with the construction of the device. Figures 2; references: 7 Russian.
[140-2415]

ANALYZER CONTROL DEVICE AI-1024-4 FOR OPERATION IN DATA GATHERING AND STORING MODE OF PREPROCESSING

CHAYKOVSKIY, M. G. and GLAGOLEV, A. Ye.

[Abstract] The control device AI-1024-4 has been developed which enables a data analyzer to operate as an autonomous memory and to store data arriving in the positional binary code. Its capability to handle multidigit (up to 2^{10}) numbers facilitates statistical estimation, with a 0.1-1% accuracy, of signals with large mean value and only slightly varying measured parameters. The device comprises a generator of rectangular pulses, a frequency divider, a 10-digit reversible counter and a recording-pulse shaper. It also includes an amplitude converter with blocking oscillator, trigger and pulse polarity inverter, and an analog to-digital code converter. All components are built with integrated microcircuits, most of them series K155 and K131. The device is suitable for x-radiographic inspection of low-contrast objects and measurement of the reflection coefficient of mirror surfaces. Figures 1; references: 2 Russian.
[140-2415]

RAISING DIFFRACTION EFFICIENCY AND REMOVING HIGHER-ORDER DIFFRACTIONS DURING RECONSTRUCTION OF IMAGES FROM SYNTHESIZED FOURIER HOLOGRAMS

MAYOROV, S. A., OCHIN, Ye. F., ROMANOV, Yu. F. and TROPCHENKO, A. Yu., Leningrad Institute of Precision Mechanics and Optics

[Abstract] The projection method of copying Fourier holograms with a single-objective optical system is analyzed, a plane Fourier hologram obtained with an oblique reference beam serving as example of an original. The quality of transmission-type and reflection-type copies of synthesized Fourier holograms, when recorded on thick films of photographic material is evaluated and found to improve with a filter-screen placed in the back focal plane of the objective so that only zeroth-order and +first-order diffraction occurs here. In an experiment using an LG-38 He-Ne laser for recording copies on LOI-2 photographic plates and a GP-2 agent as developer, copies in the form of phase holograms with a 10% diffraction efficiency were obtained from computer-synthesized Fourier holograms with a 0.3% diffraction efficiency.

The article was recommended by the Department (Kafedra) of Computer
Engineering. Figures 3; references 4: 3 Russian, 1 Western.
[145-2415]

LIQUID-CRYSTAL DISPLAYS

LISITSYN, B., Moscow

[Abstract] A brief explanation is given of the working principles of
reflective and birefringent field-effect liquid-crystal displays. Basic
construction is explained with present limitations on such parameters as
size, viewing angle, contrast, DC and AC voltage amplitudes, frequency,
current and operating temperature range. Definitions of response and
relaxation times are given. It is pointed out that these are strongly
temperature-dependent and increase with cold. Maintenance suggestions are
made for prolonging LCD life.
[129-6610]

ASTATIC PULSE-PHASE SYSTEM OF AUTOMATIC FREQUENCY CONTROL WITH BIPOLAR
PULSE-WIDTH MODULATION

KUZNETSOV, A. P. and BUS'KO, V. L., Belorussian SSR

[Abstract] A pulse-phase system of automatic frequency control is examined
in which an integrating filter with astatism of order r between the phase
detector (pulse-type static trigger) and the control device ensures precise
tuning of the output signal phase. Voltage buildup at the filter output is
avoided by use of bipolar pulse-width modulation in the system. Its stability
"in the small" is analyzed using the integral law of pulse-width modulation
in the locking mode and the transfer function of the linear part of the
system (integrating filter + control device). The transcendental nonlinear
difference equation of a closed feedback loop is linearized by means of an
expansion into a Taylor series. The test of asymptotic stability reduces
to a test of the roots of the characteristic equation, which is demonstrated
on the simple case of a transfer function $W(p) = p^{-1}K(T_1p + 1)$ of the linear
part. Figures 1; references 3; 2 Russian, 1 Western (in translation).
[135-2415]

PASSAGE OF NORMAL STATIONARY RANDOM SIGNAL THROUGH PSEUDOLINEAR CORRECTIVE
DEVICE

DONTSOV, I. I., KULICHENKO, A. G., KULICHENKO, T. A. and KOROLEV, G. I.,
Ryazan Higher School, USSR Ministry of Internal Affairs

[Abstract] The performance of a two-channel pseudolinear corrective device
in an automatic control system is analyzed, the object being to evaluate

its efficiency in a system which processes stochastic rather than deterministic signals. The device consists of a modulus converter in the amplitude channel, a linear filter and a sign selector in the phase channel, and a multiplier of the signals from both channels. A normal stationary random signal is assumed to enter the device and the multiplier output signal is calculated, the multiplicand signals being mutually independent in this case. The correlation function for the output signal is determined according to the method of delta function and its mathematical expectation is found to be zero. The results are applied to the specific case of an input signal with the correlation function $R(\tau) = e^{-\beta\tau^2}$ and an ideal differentiating filter in the phase channel. The spectrum of such a signal is found to become wider in a pseudolinear corrective device than in a linear one. The article was recommended by the Department (Kafedra) of Mathematical Methods and Computer Engineering. Figures 2; references: 2 Russian.
[145-2415]

DEVELOPMENT AND INTRODUCTION OF AUTOMATIC CONTROL SYSTEMS FOR TECHNOLOGICAL PROCESSES IN EXTRUSION LINE

SABURENKO, B. F., engineer, CHERNEVSKIY, I. N., engineer, CHUGANOV, K. A., engineer, KHAMITOV, Sh. Sh., candidate of technical sciences, and RAMAZANOV, R. Sh., candidate of physico-mathematical sciences, Scientific Research Institute of Power Engineering and Automation, UzSSR Academy of Sciences

[Abstract] Intuitive control of technological processes is being replaced with automatic control, especially where processes are subject to wide "swings" caused by transportation-related delays on the one hand and random variations of the product dimensions on the other. A typical example is extrusion of thermoplastic insulation for electric cables, the critical dimension here being the diameter. An automatic control system for such an extrusion line has been developed and designed utilizing the nonlinearities of this process, namely the flexible (elastic) coupling between current-carrying blank and insulated cable core and the non-Newtonian rheological characteristics of plastic melt. The problem of product size (diameter) stabilization and process optimization is formulated as a minimization problem, namely finding the vector of settings in the space of permissible settings which will minimize the mean-square deviation from nominal size. The problem is solved by nonlinear mathematical programming. The system operates in two modes: first informational tracking during process priming on the basis of experience and intuition with a relatively wide insensitivity zone, then informational-advisory tuning during process correction according to recommendations based on the preceding mode. The system has already been installed in one experimental production plant of the Tashkent Scientific

Research Institute of the Cable Industry, with complete recording of data on "start up", "follow up", "optimization", "interruptions", "emergency shutdowns", and "end" of process. Figures 3; tables 1; references: 5 Russian.
[138-2415]

ELECTROMAGNETIC CAPABILITY

METHOD OF DESIGNING RADIAL ELECTROMAGNETIC BEARINGS

LYSENKO, A. P., OBRAZTSOV, A. N. and TOROMANYAN, O. S., Leningrad Institute
of Mechanics

[Abstract] A radial electromagnetic bearing for an instrument is designed
which consists of a stator on a shaft with four salient poles carrying field
coils inside a hollow cylindrical rotor ring, separated by a narrow air gap.
The attraction force is calculated on the basis of the equivalent magnetic
circuit, with the reluctances expressed in terms of geometrical dimensions
and assuming a negligible flux leakage. Certain geometrical ratios are
selected so as to ensure best utilization of the magnetic flux, assuming a
1.0 lamination stacking factor. The current in the field coils is controlled
so that an adequate centering force will be produced to offset any mechanical
unbalance pull on the rotor. Curves representing the relations between
bearing dimensions facilitate the graphoanalytical engineering procedure
for the bearing design. The article was recommended by the Department
(Kafedra) of Electrical Engineering. Figures 3; references: 3 Russian.
[137-2415]

ELECTRON DEVICES

GENERALIZED METHOD OF CONSTRUCTING LIGHT RAYS REFLECTED BY SECOND-ORDER
ASPHERICAL SURFACES

ADAMYAN, V. G., Leninakan branch, Yerevan Polytechnic Institute

[Abstract] A second-order surface is considered which constitutes the
geometrical locus of points with the same ratio of distance from a directrix
plane to distance from a focus point. The geometrical problem of construct-
ing a light reflected by such a surface is shown for the case of an incident
light ray parallel to the directrix plane. The point of incidence and the
plane tangent to the surface at this point are drawn with the aid as a ruler
and compasses only. The article was recommended by the Department (Kafedra)
of Graphics. Figures 2; references: 6 Russian.
[145-2415]

POWER SUPPLY WITH AUTOMATIC FREQUENCY CONTROL FOR BACKWARD-WAVE TUBES

KABDIN, N. N., ORANSKIY, L. G. and SOLENYY, V. N.

[Abstract] A new power supply has been made available for backward-wave
tubes used in radiospectrometers which operates in the 2-mm wave band.
During voltage modulation at the retarding structure the frequency is
stabilized from an external resonator through an astatic automatic control
system. A crystalline or low-temperature n-InSb device can serve as a micro-
wave detector. It supplies: 1) 200-500 V to the grid with maximum current of
5 mA and voltage instability of 10^{-4} (amplitude of fluctuations within
$5 \cdot 10^{-4}$ V); 2) 0-7 V a.c. (50 Hz) to the filament with maximum current of 2 A

and voltage instability of $2 \cdot 10^{-4}$; 3) 5 A rms (50 Hz) to the getter at
7.5 V; and 4) 50-4000 V to the retarding system with maximum current of 80 mA
and a voltage instability of 10^{-4}. The automatic frequency control provides
a stability factor of at least 1000 at 50 Hz, with relative frequency
fluctuation of $5 \cdot 10^{-5}$, has a dynamic range of 35 dB and a response speed of
50 µs. The carrier frequency is 250 kHz and the initial retarding-system
voltage is recovered automatically during failure of frequency stabilization.
The unit draws 500 VA when plugged to a 380/220 V - 50 Hz line and requires
0.3 1/min of cooling water. A photograph of the equipment is shown.
Figures 1; references: 1 Russian.
[140-2415]

PARASITIC FREQUENCY MODULATION AND ITS ELIMINATION IN MILLIMETER-WAVE
BACKWARD-WAVE TUBES

MALYKH, N. I., MELETA, Ye. A., NAGORNYY, A. G. and YAMPOL'SKIY, Ye. S.,
Abkhaz ASSR

[Abstract] OV-622 backward-wave tubes, which have a wide operating frequency
range and other excellent performance characteristics, are widely used for
measurements in the millimeter wave band. A major obstacle to reduction of
the equipment size, which would be possible with a filament current of higher
than 50 Hz frequency, is the danger of strong parasitic frequency modulation
of microwave signals. This frequency modulation was measured with instru-
mentation consisting of a stabilized high-voltage power supply, a filament
supply, a waveguide-type bridge with unequal arms, a phase shifter in the
shorter arm, a microwave detector, a two-beam oscillograph and a micro-
phone. The microwave detector in such a measuring system converts frequency
modulation to phase modulation proportional to the latter under fixed condi-
tions, the instrument constant (ratio of frequency deviation to phase
deviation) being in this case equal to 0.1 with an L = 8.25 m difference
between the lengths of the two arms. Measurements made over the 0-10 kHz
range of filament-current frequency have revealed a series of subharmonic
resonance peaks, the fundamental highest and narrowest peak occurring at
0.9 kHz with a frequency deviation Δf = 250 MHz. The frequency deviation is
very small (Δf = 0.6 MHz) at 50 Hz and small ($\Delta f \doteq$ 6 MHz) at frequencies above
1.2 kHz, no resonance peaks occurring above 3 kHz. This behavior is attri-
butable to mechanical oscillations of the cathode relative to the retarding
structure, caused by vibrations of the current-carrying heater in a strongg
magnetic field and, in turn, causing variations of the electron beam
parameters with attendant variations of the signal frequency. On the basis
of the evidence that the parasitic frequency modulation is in phase with the
filament current throughout the entire frequency range of the latter, a

compensation circuit has been designed and tested for suppressing the former. A part of the voltage from the filament transformer is added to the high voltage, through a series connection, with the correct phase and with the magnitude controllable by a variable resistor. Figures 4; references 2: 1 Russian, 1 Western (in translation).
[135-2415]

MODULATION CAPABILITIES OF DENSELY SPACED RESONATOR ARRAYS

GRADOVA, S. N., ZAKHAR'YASHCHEVA, Ye. A., KOROTKOV, A. F., TRUSHIN, S. A. and FILIMONOV, G. F.

[Abstract] Modern traveling-wave pulse power tubes contain a retarding system which consists of a π-periodic chain of coupled resonators and a magnetic focusing system which also has a periodic structure. Better bunching characteristics are attainable with a chain of decoupled resonators, at some sacrifice in modulation capability. Here the modulation capability of such a chain is evaluated, assuming that the spacing period of the resonators can be maintained the same and need not be increased. Calculations have been made to determine the dependence of the maximum attainable modulation range on the wave impedance of the resonators and on the relative length of the buncher, also to determine the corresponding Q-factors. The results indicate that a 10-15% modulation of the electron beam by such a resonator chain is feasible, with necessary optimization of system parameters. They also indicate the possibility of further design improvements, namely shortening the total length of the resonator chain and decreasing the number of resonators. Figures 1; tables 1; references 4: 3 Russian, 1 Western (in translation).
[134-2415]

MODULATION OF DIELECTRIC PERMITTIVITY OF SEMICONDUCTOR BY STRONG MICROWAVE FIELD

BUSHKOV, A. A., IVANCHENKO, V. A., KLIMOV, B. N. and MIKHAYLOV, A. I.

[Abstract] Modulation of the dielectric permittivity of a semiconductor by a microwave field is considered, an important factor here being the

reactive component of semiconductor conductance associated with the inertia of charge carriers. Taking into account the contribution by free charge carriers, the modulation factor is calculated for an n-Ge device to which a strong constant electric field E_0 as well as a weak microwave signal field E_s (frequency ω_s) and a strong microwave pumping field E_p (frequency $\omega_p > \omega_s$) have been applied. The corresponding transient-state equations of energy and momentum conservation for drift electrons in a homogeneous semiconductor have been derived on the basis of a shifted Maxwell distribution and then solved according to the fourth-order Runge-Kutta scheme. The dependence of the velocity modulation factor and of the permittivity modulation factor on the pumping field intensity, also the dependence of the permittivity modulation factor on the free charge concentration, have been evaluated for $\omega_s = 3 \cdot 10^{11}$ s^{-1}, $\omega_p = 8.16 \cdot 10^{11}$ s^{-1}, $E_s = 30$ V·cm^{-1}, and E_0 from 900 to 2100 V·cm^{-1}, with a 77 K lattice temperature. Two situations are important from the practical standpoint: 1) Where the constant component of electron drift velocity and the amplitude of its pumping-frequency component have arbitrary signs; and 2) Where the constant component of electron drift velocity is positive. Figures 2; references 2: all Western (1 in translation). [127-2415]

CONTROL OF SEMICONDUCTOR POWER SWITCHES BY MEANS OF MICROWAVE RADIATION: PART 2

GREKHOV, I. V., KARDO-SYSOYEV, A. F. and KRIKLENKO, A. V., Physico-Technical Institute imeni A. F. Ioffe, USSR Academy of Sciences, Leningrad

[Abstract] The feasibility of controlling semiconductor p-n diode and p-n-p-n thyristor structures by means of microwave pulses was first studied theoretically and then experimentally. In the experiment p-regions were doped with a donor to a concentration $N_D \approx 10^{18}$ cm^{-3} and n-regions were doped with a donor to a concentration $N_D \approx 10^{14}$ cm^{-3}. Specimens with cylindrical symmetry were placed inside a 30Ω coaxial resonator tunable to minimum VSWR by a short-circuiting plunger and loaded by a resistor bank and a capacitor bank in parallel. Microwave pulses at a low frequency of 0.93 GHz were applied to the thyristor structures, the power absorbed by the latter dropping fast when coming from a 60 kW source and holding up when coming from a 30 kW source. Ionization was found to begin at a threshold microwave power level and the ionization current then to increase linearly with the microwave power, the threshold microwave power increasing and the rate of current increase decreasing as the initial applied bias voltage was decreased from 1000 to 250 V. Load current and voltage transients were measured in a circuit with two thyristors switched by incident and reflected microwave pulses. The duration of the load current was found to be determined by the time constant of the

load circuit, while the voltage across the thyristor structure increased linearly with the peak load current. An evaluation of the data yields a rate of load current buildup $dJ_L/dt \approx 3.75 \cdot 10^{11}$ A/(cm$^2 \cdot$s), which is one order of magnitude higher than the rate of buildup by the field-effect mechanism and corresponds to a buildup by the avalanche-injection mechanism with impact ionization in the high-current regions. Calculations based on these data yield a power loss of 5 kW when a current of 4000 A is switched on. The results indicate the feasibility of commutating a power higher than 10^7 W within a time shorter than 10^{-7} s, inasmuch as breakdown in a microwave field inhibits current localization. Figures 5; tables 1; references: 4 Russian.
[141-2415]

CONDITIONS FOR EXCITATION OF RECOMBINATION WAVES IN BOUNDED SEMICONDUCTORS

SABLIKOV, V. A., Institute of Radio Engineering and Electronics, USSR Academy of Sciences, Moscow

[Abstract] A complete theoretical study is made of the conditions for excitation of recombination waves in a bounded homogeneous semiconductor with weakly injected contacts. The analysis involves calculation of the semiconductor impedance Z and determining the natural frequencies from the Kirchhoff equation $Z + R_L = 0$ (R_L - load resistance) with appropriate boundary conditions, deviations of all quantities from their steady-state values being assumed to be exponential functions of time e^{st}. After the equations for the distributions of excess electron and hole concentrations have first been solved, with $\Delta n = \Gamma(s)\Delta p$ where $\Gamma(s)$ is a whole function determined by the trap spectrum, the solution to the Kirchhoff equation is tested for absolute instability and convective instability. The conditions for convective instability are established on this basis. The corresponding cubic equation for the critical electric field intensity has three roots, one of them to be discarded as inconsistent with the premise of an existing resonance region and the two others defining the range between them where convective instability can occur. There also exists a threshold length of semiconductor specimen. The ranges of values of semiconductor parameters (ratio of steady-state electron and hole concentrations n_0/p_0, ratio of electron and hole entrapment frequencies ν_n/ν_p) depend on the semiconductor length and the load resistance. The author thanks V. B. Sandomirskiy for discussing the study. Figures 5; references 7: 6 Russian, 1 Western.
[141-2415]

EFFECT OF MAGNETIC FIELD ON RELAXATION OF ELECTRICAL CONDUCTIVITY OF WARM
CHARGE CARRIERS IN GERMANIUM

DENIS, V., MARTUNAS, Z. and TVARDAUSKAS, G., Institute of SEmiconductor
Physics, LiSSR Academy of Sciences, Vilnius

[Abstract] An experimental study was made concerning the electrical con-
ductivity of warm charge carriers in n-Ge and in p-Ge in crossed fields,
a weak alternating electric field and a constant magnetic field. The
frequency of the electric field was varied over a wide range. Necessary
data were obtained by two methods: mixing of harmonics (fundamental fre-
quency 10 GHz) and measuring the frequency dependences of the effective
nonlinearity coefficient

$$\alpha^* = (\frac{1}{\sigma_0 E_0} - 1)\frac{\sigma_0}{P} \quad (j - \text{mean current density in both}$$

constant electric field E_0 and high-frequency electric field $E_m \cos\omega t$, σ_0 -
electrical conductivity in weak electric field, P - power of high-frequency
field absorbed by unit semiconductor volume). Specimens with Hall geometry
were made of germanium with electrical resistivity ρ = 40 ohm.cm, 20 mm long
for mixing of harmonics and 3.4 mm long for measuring the $\alpha^*(\omega)$ character-
istic. The charge carriers were heated in the <100> direction. The magnetic
field was varied, for measurement of the $\alpha^*(\omega)$ characteristic at various
levels of magnetic induction as well as for measurement of the energy
relaxation time and the conductivity relaxation time, both in the phenomeno-
logical approximation, as functions of the magnetic induction. The results,
confirmed by numerical analysis of the theoretical model at T = 78 K with
E = 30 V/cm by the Monte Carlo method, indicate that a magnetic field enhances
the energy transfer from electrons to lattice through optical scattering with
concurrent inelastic acoustical scattering. Interband redistribution of
holes is more sensitive to a magnetic field than is that of electrons and,
therefore, the relaxation process is more intricate in p-Ge than in n-Ge.
Conductivity relaxation of heavy holes depends not only on the inertia of
energy dissipation but also on some other much faster process not yet
fully explored. Figures 5; references 16: 9 Russian, 7 Western.
[141-2415]

ELECTRICAL PROPERTIES OF EPITAXIAL GaAs LAYERS WITH ISOVALENT Sb AND In
IMPURITIES

SOLOV'YEVA, Ye, V., MIL'VIDSKIY, M. G. and GANINA, N, V., Scientific Research
and Design Institute of the Rare Metals Industry, Moscow

[Abstract] An experimental study was made of homoepitaxial n-GaAs layers
grown from a gallium solution-melt on high-resistivity substrates at 900-
650°C, then doped with antimony or indium. The layers were 100-170 µm
thick with impurity concentrations $[Sb] = (0.3-9) \cdot 10^{19}$ cm^{-3} and $[In] =$
$= (2-5) \cdot 10^{19}$ cm^{-3}, inversion of the conductivity type occurring in the
transition region at the layer-substrate interface, The density of disloca-
tions, measured by the etching method under an optical microscope, was far
below 10^6 cm^{-2} and, therefore, their contribution to electron scattering
negligible. A special control GaAs layer was left undoped, The concentration
profile of ionized scattering "Coulomb" centers over the thickness of doped
layers, determined from the electron mobility and compared with the profile
in the undoped layer, reveals that the concentration of these centers is
decreased by addition of antimony and increased by addition of indium. This
is attributed to changes in the state of residual impurities and of struc-
tural point defects, Into account must also be taken interlinking of
vacancies by isovalent impurity atoms (antimony in gallium and indium in
arsenic) as well as interaction of residual amphoteric silicon atoms in
gallium and arsenic sublattices with antimony and indium respectively. The
electrical conductivity and the Hall coefficient were measured in the n-type
layer as well as in the p-type sublayer, their temperature dependence in the
latter found to be determined by the deep center. The authors thank
T. G. Yugova for performing metallographic examinations and N. S. Rytova for
many discussions. Figures 3; tables 2; references 14: 10 Russian, 4 Western.
[141-2415]

ENERGY DISSIPATION AND INTERVALLEY REDISTRIBUTION OF ELECTRONS IN GERMANIUM
AND IN SILICON IN STRONG HIGH-FREQUENCY FIELDS

ALYAKNA, Yu., GINTILAS, Sh. and DENIS, V., Institute of Semiconductor Physics,
LiSSR Academy of Sciences, Vilnius

[Abstract] The most effective recently developed method of generating and
amplifying electric high-frequency oscillations utilizes the properties of a

hot plasma of free charge carriers in semiconductors, examples of such devices being Gunn-effect and IMPATT diodes. While much information is available on the dependence of electron heating and intervalley redistribution on the electric field intensity, hardly any is available with respect to dependence on the frequency of a strong electromagnetic wave. Therefore, a study was made of the effect of changes in the frequency of a strong electric field on the flow of a weak direct current in n-Ge and n-Si. Specimens in the form of square bars ($3.4 \times 0.5 \times 0.5$ mm^3) with contacts at both ends, electrical resistivity of the material $\rho = 40$ ohm.cm (germanium and $\rho = 200$ ohm.cm (silicon), were placed inside a waveguide in an electric field $E = E_0 + E_1 \cos \omega t$ ($E_0 \ll E_1$) at liquid-nitrogen temperature. The mean current density was measured at frequencies $\omega = 3, 10, 37$ GHz, the inertia of electrical conductivity being negligible throughout this range. Measurements, as well as numerical simulation and analysis by the Monte Carlo method, indicate that the number of charge carriers traversing a passive region of k-space without collisions varies with the frequency of the heating electric field and so does the rate of energy dissipation. When the frequency is so high that inertia of momentum relaxation becomes significant, it is necessary to increase the electric field intensity in order to maintain the rate of energy dissipation. The discrepancy between calculations and measurements does not exceed 15%, if the proportionality $\Delta\sigma \alpha \sqrt{\overline{\Delta<\epsilon>}}$ ($\Delta\sigma$ - change in electrical conductivity, $\overline{\Delta<\epsilon>}$ - average-in-time change of mean energy) and scattering by ionized impurities are taken into account. Intervalley redistribution of electrons was determined from the anisotropy of mean current flow in variously oriented crystals in parallel electric fields ($E_0 || E_1$). The results indicate that the mean probability of electron transitions from hot to cold valleys increases much faster with increasing electric field intensity than does the mean probability of reverse transitions. These probabilities and consequently the respective electron concentrations n_{hot}, n_{cold} also depend on the frequency of the electric field. At low frequencies the redistribution process is inertialess at any electric field intensity E_1. On the other hand, in weak fields with little heating ($n_{hot} \approx n_{cold}$) the two probabilities do not differ much and their ratio is not frequency-sensitive. In strong fields, however, a frequency will be reached at which transition from hot to cold valleys still proceeds without inertia, while depletion of cold valleys is already delayed and less probable. Here, therefore, the ratio $\bar{n}_{hot}/\bar{n}_{cold}$ increases with increasing frequency, approaching the value which corresponds to the population of valleys in a constant electric field of intensity E_1. Figures 3; references 9: 4 Russian, 5 Western. [141-2415]

P-N JUNCTIONS IN GaAs-GaSb SOLID SOLUTIONS

VUL', A. Ya., KARYAYEV, V. N., PETROSYAN, P. G., POLYANSKAYA, T. A., SAYDASHEV, I. I. and SHMARTSEV, Yu. V., Physico-Technical Institute imeni A. F. Ioffe, USSR Academy of Sciences, Leningrad

[Abstract] An experimental study was made of p-n structures of $GaAs_{1-x}Sb_x$ (x < 0.2 $\pm$ 0.005) solid solutions. Specimens with a dislocation density not exceeding $2 \cdot 10^4$ cm^{-2} were produced by the liquid-phase epitaxial process on (111)A n-GaAs substrates from a solution-melt of gallium, undoped n-GaAs + + As source, and undoped p-GaSb + Sb source. Both type-1 triple-layer structures (n-GaAs/n-GaAs$_{1-x_1}$Sb$_{x_1}$/n-GaAs$_{1-x_2}$Sb$_{x_2}$/.../n-GaAs$_{1-x_k}$/p-GaAs$_{1-x_n}$Sb$_{x_n}$

(x_n x_{n-1}) were produced and tested. Electrical and photoelectrical properties were measured on photolithographic "mesa" structures, and current-voltage characteristics were measured by the bridge method at a frequency of 30 kHz. The forward branches of the current-voltage characteristics follow closely the classical relation $j \propto e^{e_0 U/\beta kt}$ with β = 1.8-2.2, which corresponds to current flow activation with recombination in the space-charge region. Their reverse branches have three distinct ranges. The first range is linear (U < 0.1 V) and yields a differential resistance $R_g = (dU/dI)_{U=0} = 10^7 - 10^8$ ohms. In the second range (0.1 $\leq$ U $\leq$ 1-3 V) the current is proportional to the square root of the voltage and depends exponentially on the temperature ($j \propto e^{-Eg(T)/kT}$), which corresponds to generation-recombination in the space-charge region. In the third range (U > 5 - 10 V) the reverse current increases sharply, which corresponds to either avalanche or tunneling breakdown. In this way the current-voltage characteristics of such p-n junctions reveal the effect of mismatch between lattice parameters in the structure. Figures 4; references 24: 10 Russian, 14 Western (2 in translation). [141-2415]

ACOUSTOELECTRIC WAVE IN PIEZOSEMICONDUCTOR WITH SCHOTTKY BARRIER

LETNIK, D. A. and POPOV, V. V., Omsk State University

[Abstract] A piezosemiconductor device is considered which has one ohmic contact and a Schottky barrier as the other contact. Acoustoelectric

instability occurring in such a device upon application of a constant bias voltage is examined, considering that an acoustoelectric wave modulates not only the charge carrier concentration at the potential barrier but also the height of the barrier. An n-type device occupying a region $-a<x<a+b$ and homogeneous in the $-a,a$ region (b- length of barrier depletion region) is assumed. The analysis is based on the linearized equations of piezoacoustics with both diffusion of charge carriers and the effect of the static pulling field on drift of charge carriers disregarded. The dispersion equation for oscillations outside the barrier is derived accordingly, its general solution containing four contsants obtainable from the boundary conditions. The current flowing across the barrier is calculated in accordance with diode theory. No instability occurs with zero bias at the barrier or with a barrier impervious to electrons. When instability occurs, it is caused by modulation of the charge carrier concentration in the $x=a$ plane of the ohmic contact. An analysis of the results indicates an appreciable transfer of oscillation energy to higher-order harmonics, making the oscillations highly nonsinusoidal, with a limited buildup of the amplitude. The authors thank M. K. Balakirev, V. L. Bonch-Bruyevich and I. A. Gilinskiy for helpful discussions. References 4: 3 Russian, 1 Western (in translation). [141-2415]

TRANSIENT DISTRIBUTION OF RECOMBINATION-WAVE INTENSITY IN BOUNDED SEMICONDUCTOR

KARPOVA, I. V., SABLIKOV, V. A. and SYROVEGIN, S. M., Institute of Radio Engineering and Electronics, USSR Academy of Sciences, Moscow

[Abstract] Recombination waves excited in a semiconductor cause the latter to become nonhomogeneous so that the average-in-time electric field acquires a sharp peak in the vicinity of one of the contacts. Here the process of formation of the active region during the transient period following application of a voltage pulse is analyzed in the linear approximation. The distribution of recombination-wave intensity in an initially homogeneous specimen of finite dimensions is calculated as a function of time, two recombination waves being excited simultaneously and a convective instability building up near the excitation threshold in long specimens with a small load resistance. In that case one of the waves is amplified along its propagation path, becoming the dominant one, while the other wave decays within a short distance from the other contact. Experiments were performed with a movable probe in a specimen of Ge doped with Mn, voltage oscillograms being photographed at various instants of time with the probe in various locations. Measurements were made with slow and fast recombination waves in an electric field of 42.5 V/cm (threshold intensity 18 V/cm). The agreement between experimental and theoretical data is fair for slow waves, closest with

$n/p = 1.5$, $\nu_p/\nu_n = 2$, $\nu_n = 1.5 \cdot 10^5$ s^{-1} (n,p electron and hole concentration; ν_n, ν_p frequencies of electron and hole entrapment), worse for fast waves. The results suggest that peaking of the electric field intensity near formation of the active region during the initial transient period is associated directly with the recombination waves and represents one of the nonlinear effects accompanying their evolution. Other evidence supporting this hypothesis is that appearance of an active region accompanies excitation of recombination waves, as demonstrated in a magnetic field which alters the excitation threshold, and that the active region remains at the same location near one end of a semiconductor specimen as the length of this specimen is even appreciably reduced. Figures 6; references: 10 Russian. [142-2415]

EVOLUTION OF SIGNAL SPECTRUM DURING MULTITRANSIT GENERATION OF ACOUSTIC WAVES IN PIEZOSEMICONDUCTORS

MANSFEL'D, G. D. and RUBTSOV, A. A., Institute of Radio Engineering and Electronics, USSR Academy of Sciences, Moscow

[Abstract] Multitransit generation of acoustic waves in a crystal occurs when the half-period of the alternating electric field is equal to the time of one transit of acoustic waves across the crystal so that, upon each reflection at either crystal boundary, they can be amplified by an attendant supersonic electron drift. The evolution of the oscillation spectrum during nonlinear amplification of acoustic fluctuations was studied experimentally in n-InSb crystals of various lengths with electron concentration $n = (0.3-2) \cdot 10^{14}$ cm^{-3} and electron mobility $\mu = (3-5) \cdot 10^5$ $cm^2/V.s$) at liquid-nitrogen temperature (77 K). Acoustic waves were generated in a magnetic field of $H = 1-3$ kOe intensity, with $qR_c \ll 1$ (q- acoustic wave vector, R_c- cyclotron radius) and propagated along the piezoactive axis. The microwave signal generated by acoustic waves in a receiver was determined from the current-voltage characteristic, upon application of a drift field. During the transient period, lasting for 500-800 μs, the initially wide spectrum (several hundred mega-hertz) with maximum intensity at the center frequency was found to become successively narrower with an increasingly sharp peak at the center but with the integral intensity (area under the curve) remaining constant. The final steady-state width of this narrow peak or cluster of several peaks, depending on the resolution, depends on the number of reflections in a drift field and its frequency band depends on the electron concentration in the crystal. The spectral components here form a sequence with nonmonotonically differing amplitudes, as has been established by a Fourier analysis of the spectrum. In long crystal specimens there were many more transits required before steady state was reached with a stable current-voltage

characteristic, but the total length of the transient period was almost the same as in short crystal specimens. The authors thank Yu. V. Gylyayev for his interest and support, also V. L. Gurevich as well as other participants of the seminar chaired by him and M. K. Balakirev for helpful discussions. Figures 4; references 10: 7 Russian, 3 Western.
[142-2415]

EFFICIENCY OF INJECTION OF PARAMAGNETIC DEFECTS INTO SILICON DURING NEUTRON IRRADIATION

ANTONENKO, A. Kh., DVURECHENSKIY, A. V., SMIRNOV, L. S. and KHARCHENKO, V. A., Institute of Semiconductor Physics, Siberian Department, USSR Academy of Sciences, Novosibirsk

[Abstract] An experimental study was made of the buildup of paramagnetic centers in silicon crystals during irradiation with neutrons. Specimens of both n-Si and p-Si with electrical resistivity $o = 1 \cdot 10^{-1} - 5 \cdot 10^{3}$ ohm·cm were grown by the Chochralski method and by zone refining. The specimens at a temperature not exceeding 60°C, were irradiated in a VVR-ts water-moderated water-cooled reactor with a nearly continuous neutron spectrum, with thermal neutrons being cut off, when necessary, by means of cadmium filters. The neutron dose was increased beyond levels corresponding to strong overlap of displacements produced by primarily ejected atoms. Measurements were made with an electron-paramagnetic-resonance spectrometer at 77 K and at 300 K. The concentration of paramagnetic centers was determined from the intensity and the width of the derivatives of absorption lines, the form of these lines assumed to be Gaussian. Because of insufficient spectral resolution, only the concentrations of tetravacancies P3 $(V_4)^0$, twin interstices P6 $(I_2)^+$, interstitial atom complex A5 $(I_2)^0$, and "two vacancies + oxygen" complex A14 $(V_2-O)^0$ could be determined reliably. The concentration of each type of center was found to increase proportionally with the neutron irradiation dose up to an integral neutron flux density $0.5 \cdot 10^{18}$ cm^{-2} and then at a decreasing rate to a saturation level ($2 \cdot 10^{16}$ cm^{-3} for P6 and P3, $1 \cdot 10^{16}$ cm^{-3} for A14, $2 \cdot 10^{15}$ cm^{-3} for A5). Interstitial defects saturate sooner than vacancy-type defects. The results indicate that silicon crystals stabilize under neutron irradiation and cannot be amorphized by this method. The authors thank V. D. Akhmetov and V. V. Bolotov for supplying data on the concentration of divacancies in the silicon specimens used in this study. Figures 1; references 15: 6 Russian, 9 Western (1 in translation).
[142-2415]

PHOTOCONDUCTIVITY OF STRONGLY-DOPED COMPENSATED SEMICONDUCTORS

OSIPOV, V. V. and FOYGEL', M. G., Scientific Research Institute of Physics,
Odessa State University imeni I. I. Mechnikov, Odessa

[Abstract] A theory of intrinsic photoconductivity is developed for strongly-
doped compensated semiconductors, assuming that recombination occurs through
deep centers. A semiconductor is considered which has been strongly doped with
fine donors ($N_{Da_e}^3$, $Nr_0^3 > 1$, $\gamma_0 > I_D$) but not at deep acceptor recombination
levels ($Na_i^3 < 1$)·(N_D, N concentrations of fine donors and of deep centers;
a_e, a_i localization radii of corresponding charge carriers; r_0 characteristic
radius; γ_0 scale of impurity potential fluctuations; I_D donor ionization
energy). The role of recombination processes in such a semiconductor during
exposure to light is analyzed, assuming a quasi-equilibrium distribution of
charge carriers in allowed bands and with electron tunneling included but
hole tunneling disregarded as negligible. The recombination rate is calculated,
using the Fermi integral $\emptyset_{1/2}$ and an exponentially decaying barrier distribu-
tion function. At low temperatures $T_2 < T < T_1$ (luminous flux density $J > J_1$)
tunneling is dominant and the recombination time does not depend on the tempera-
ture. At a temperature $T \approx T_1$ tunneling is insignificant and thermal activation
processes govern the recombination. At temperatures $T < T_2$ the carrier dis-
tribution in allowed bands is not a quasi-equilibrium one and the intrinsic
photoconductivity is a "jumping" quantity. The authors thank A. Ya. Shik,
B. I. Shklovskiy and I. S. Shlimak for discussing the results.
References 11: 10 Russian, 1 Western.
[142-2415]

SURFACE RECOMBINATION WAVES IN SEMICONDUCTORS

KLIMOVSKAYA, A. I., Institute of Semiconductors, UkSSR Academy of Sciences, Kiev

[Abstract] Possible existence of recombination waves in the space-charge
region of a semiconductor is examined, with surface states playing the role
of deep centers here and the space-charge field regulating the carrier
fluxes into surface states. A semiconductor is considered which has been
doped with fine donors, and the effect of a small random electron-hole
fluctuation in the surface layer of the space-charge region is analyzed.

The differential equations of continuity for the space charge, with appropriate boundary conditions and with a negligible divergence of the net electron-hole diffusion-drift current, are converted to integral form. Equations for the carrier concentrations and the electric field intensity are obtained on this basis, and a corresponding dispersion equation. The latter, unlike that for volume recombination waves, contains two new frequencies which depend on the surface state and appear with an exponential factor $e^{\pm Y_s}$ (Y_s deflection of energy bands at the semiconductor edge y = 0). The potential profile at the surface is assumed to be linear and diffusion of electron-hole pairs into the semiconductor bulk is assumed to be negligible. Taking into account some volume recombination in the space charge region will add correction terms to the equations for carrier concentrations and electric field intensity based on surface recombination alone. Surface recombination waves can exist on various interphase boundaries such as those in heterojunctions, also on semiconductor-oxide or semiconductor-electrolyte interfaces as well as in structures with layerwise nonuniform concentration distribution and current flowing along layers. Their characteristics, unlike those of volume recombination waves, can be controlled externally by means which effect changes in the surface state. The author thanks O. V. Konstantinov and V. I. Perel' for discussing and improving the contents of this article. Figures 1; references: 5 Russian.
[142-2415]

LUMINESCENCE OF STRONGLY SILICON-DOPED EPITAXIAL GALLIUM ARSENIDE

KOVALENKO, V. F. and PROKHOROVICH, A. V., Institute of Semiconductors, UkSSR Academy of Sciences, Kiev

[Abstract] A study of the luminescence characteristics of epitaxial GaAs strongly-doped and compensated with silicon has revealed a nontrivial dependence of the location of the photoluminescence peak on the excitation photon energy. Specimens of p-GaAs(Si) were produced by the liquid-phase epitaxial process from a solution of arsenic in gallium melt containing 0.1-1 wt.% silicon. A halogen lamp (KIM-100) with a monochromator (MDR-3) were used for analysis of the photoluminescence spectrum. The anomalous trend is attributed to the behavior of excess electrons. When the energy of these electrons after luminous excitation exceeds the conduction level and during subsequent recombination drops to that level, then the photoluminescence peak does not depend on the excitation photon energy until the latter reaches the conduction level. Electrons excited into states below the conduction level recombine radiatively from those states, in which case a decrease of the excitation photon energy causes the photoluminescence peak to shift into the low-energy range. This hypothesis is confirmed by the fact that the

photoluminescence peak decreases linearly with increasing rms fluctuation of the impurity (silicon) potential, an increase of this potential causing a decrease of the conduction level and a shift of the photoluminescence peak into the low-energy range. Figures 2; references: 4 Russian. [142-2415]

MECHANISM OF BREAKDOWN IN InAs DIODES AND REVERSE BRANCH OF THEIR CURRENT-VOLTAGE CHARACTERISTIC

SMIRNOVA, N. N., SLOBODCHIKOV, S. V. and TALALAKIN, G. N., Physico-Technical Institute imeni A. F. Ioffe, USSR Academy of Sciences, Leningrad

[Abstract] An experimental study was made of the mechanisms of reverse current conduction and of breakdown in $A^{III}B^V$-compound diode structures, specifically InAs Diodes. Specimens of such structures were produced by the epitaxial process so as to make zinc diffuse from the liquid phase into the n-InAs substrates, the electron concentration in them varying from $2 \cdot 10^{16}$ to $4 \cdot 10^{17}$ cm^{-3}, and to contain the entire p-n junctions in those substrates. An In+ 0.5% Zn tab was fused into the p-region to form a nonrectifying contact and an In tab was soldered onto the n-region. The diode structures had areas from $3 \cdot 10^{-3}$ to 10^{-2} cm^2. The reverse branch of their current voltage characteristic was measured with direct current at small bias viltages and with pulse current before and at breakdown, to avoid heating. Diode specimens without microplasma and with the highest breakdown voltages were selected for this test. The breakdown voltage was determined in two ways, first as the voltage at which the current density had reached 1 A/cm^2 and then by extrapolation of the resistive-current segment of the reverse characteristic to the voltage axis at reverse bias voltages exceeding the breakdown level. The impurity distribution in the space-charge region was linear in all structures, as indicated by their capacitance-voltage characteristics, but the impurity concentration gradient was varied to cover the grad n = $1.5 \cdot 10^{19} - 2 \cdot 10^{22}$ cm^{-4} range. The current in all diodes was larger than it would be if determined by thermal activation processes, being instead proportional to the diode area, in a strong electric field, and thus determined by bulk properties of the p-n junction. The temperature dependence of the reverse current in InAs diodes with various concentration gradients was measured over the 77-250 K range and the current was found to remain almost constant from 77 to 170-180 K but increase fast from 170-180 to 250 K. This trend indicates a tunnel mechanism of current flow. The temperature dependence of the breakdown voltage, different for diodes with different concentration gradients, indicates an avalanche breakdown mechanism in the case of low concentration gradients and a tunneling breakdown mechanism in the case of high concentration gradients. Figures 4; tables 1; references 15: 2 Russian, 13 Western. [146-2415]

EFFECT OF ELECTRIC FIELD ON BUILDUP AND ANNEALING OF RADIATIVE DEFECTS IN
GALLIUM ARSENIDE

MAMONTOV, A. P., PESHEV, V. V. and CHERNOV, I. P., Scientific Research
Institute of Nuclear Physics at Tomsk Polytechnic Institute
imeni S. M. Kirov, Tomsk

[Abstract] An experimental study was made of radiative defects in gamma-
irradiated gallium arsenide. Specimens were irradiated with γ-quanta
($3.7 \cdot 10^{16}$ - $1.4 \cdot 10^{17}$ cm^{-2}) from a cobalt-60 source at various temperatures
ranging from 20 to 300°C with and without an electric field applied. The
concentrations of N_{E3} centers in the neutral region and in the space-charge
region were measured as functions of the irradiation temperature. At room
temperature the defect concentration was approximately twice as high in the
space-charge region than in the neutral region, indicating an absence of
defect migration even in a strong electric field. The defect concentration
in the neutral region decreased monotonically with increasing temperature,
first slowly and then rapidly to zero at 220-250°C. The defect concentration
in the space-charge region first increased to a maximum within the 220-250°C
range and then decreased rapidly. Specimens were annealed isothermally at
220°C in an electric field (V = 30 V) and without one (V = 0), the fraction
of residual defects decreasing linearly with time in each case but at a
slower rate whenever the electric field was applied. The results reveal that
an electric field affects the mechanisms of radiative defect buildup and
annealing. Isochronous annealing at higher temperature in the space charge
region than in the neutral region and peaking of the defect concentration
here indicate that at higher temperatures, at which migration of N_{E3} centers
is possible, a change occurs in the charged state of these centers and a new
reaction enters into the play which inhibits their annealing. Figures 2;
references 5: 3 Russian, 2 Western.
[146-2415]

ELECTROABSORPTION IN CHROMIUM-DOPED p-GaAs

MOROZOVA, V. A., OSTROBORODOVA, V. V. and SHEREMET'YEV, V. N., Moscow State
University imeni M. V. Lomonosov

[Abstract] Electrical modulation of optical absorption in p-GaAs doped with
neutral chromium Cr^{3+} atoms was measured in an alternating electric field
of a capacitor (intensity E $\lesssim$ 2.10^4 V/cm, frequency f = 400 Hz), over the

80-300 K temperature range and the 0.5-1.5 eV range of incident radiation energy. The specimens were specially nonoriented, with a chromium concentration $N_{Cr} \approx (1.5-2.5) \cdot 10^{17}$ cm^{-3} and fine-donor concentration $N_d < 10^{16}$ cm^{-3}. The modulation spectra have a sharp peak, or two neighboring peaks, within the 0.61 ± 0.01 eV band at the 1A energy level of Cr in GaAs, analogous to the peak within the 0.8-0.9 eV band in the case of n-GaAs(Cr). An analysis of the temperature dependence and of the dependence on polarization and field intensity indicates that the Pockels effect is operative here. A second peak is sometimes detected within the 0.8 eV band in specimens with a low ratio C = n/p slightly above 10^{-3} and always within the 0.75-0.83 eV band in speciemns with a medium ratio within the $10^{-3} < C < 1$ range, attributable to ejection of electrons from Cr^{2+} into the conduction band. Figures 2; references 15: 10 Russian, 5 Western.
[146-2415]

FORMATION OF CURRENT FILAMENT AT SURFACE OF DIODE STRUCTURE OF GLASSY SEMICONDUCTOR IN MAGNETIC FIELD

AMPILOGOV, V. N., VIKHROV, S. P., GLEBOV, A. S. and KADUSHKIN, V. I., Ryazan Institute of Radio Engineering

[Abstract] The current-voltage characteristic of monolithic-planar $Ge_{15}Te_{81}As_4$ (glassy chalcogenic semiconductor material) diode structures capable of switching with memory were measured in a magnetic field and without one, while the trajectories of the surface current channels were traced photographically. Bending of the current filament is explained by thermomagnetic effects (Ettingshausen effect), according to the theory of current filament motion in homogeneous crystalline semiconductors with S-form current-voltage characteristics. The different behavior of a current filament in glassy semiconductors than in homogeneous crystalline ones, in a magnetic field, is attributable nto the difference in mechanisms of its motion but to the difference in mechanisms of its formation. One such mechanism lies in the potential barrier at the semiconductor-electrode interface which even a magnetic field cannot overcome. The filament moves until structural-phase transformations such as crystallization occur in the current channels, whereupon the filament will stabilize at the surface. Figures 1; references 10: 8 Russian, 2 Western.
[146-2415]

INTERACTION OF RADIATIVE DEFECTS AND IRON IMPURITY IN GaAs CRYSTALS

TESLENKO, V. V., BRAYLOVSKIY, Ye. Yu., KONOZENKO, I. D. and PAMBUKHCHAN, N. Kh.,
Institute of Semiconductors and Institute of Nuclear Research, UkSSR Academy
of Sciences, Kiev

[Abstract] Interaction of radiative defects and iron impurity in GaAs<Fe>
during electron bombardment and during subsequent annealing is analyzed on
the basis of EPR measurements. Electron bombardment at 77 K decreased the
concentration of Fe^{3+} ions in gallium interstices. During bombardment with
any dose within the $(5-10) \cdot 10^{17}$ electrons/cm^2 range the Fermi level in GaAs
stabilized regardless of their initial doping level. Isochronous annealing
revealed two ranges in the temperature dependence of $N_{Fe^{3+}}$-centers concentra-
tion, a further drop of the latter in four steps (at 120, 210, 330, 405 K)
up to 420 K and its more gradual restoration above 450 K. No annealing
occurs below 200 K. Bombardment at 300 K affects the $N_{Fe^{3+}}$ concentration more
strongly, indicating a more intense bonding of Fe atoms into complexes with
radiative defects and thus a radiation-stimulated migration of these defects
in GaAs. At annealing temperatures above 500 K these complexes vanish and
the initial $N_{Fe^{3+}}$ concentration is reached again at 920 K, which is consistent
with the recovery by GaAs crystals of their electrical properties and
luminescence. One such complex (Fe1) was found to produce an EPR spectrum
with the parameters s = 7/2, g-factor 2.09 ± 0.03, ratio D/h = 49.5 ± 0.5 GHz
of the axial crystal field with <111> -type axial symmetry. This complex
does not form during bombardment at 77 K, forms partly at 300 K and completely
only at 400 K. The authors thank K. D. Glinchuk for discussing the results.
Figures 2; references 8: 4 Russian, 4 WEstern.
[146-2415]

CONDITIONS FOR DOMAIN SUPPRESSION IN GUNN-EFFECT DIODE OPERATING IN RELAXATION
MODE

NAZAROV, V. B. and PALSHKOV, V. V.

[Abstract] The operating range of Gunn-diode oscillators can be extended,
with their output power increased and their efficiency raised, by limiting
the voltage caused by space charge. This requires domain suppression, a

condition for which is a sufficiently high rate of change of diode voltage. An analysis of the corresponding relaxation mode of operation includes determining the dependence of domain formation in a Gunn-effect diode on the rate of change of the externally applied voltage, which is done here on the basis of an equivalent circuit containing the reactances of the diode housing and a crystal in parallel with the capacitance of an LC series circuit. Solution of the first-order differential circuit equation and the second-order differential field equation for the linearizable negative range of the current-voltage characteristics, with the appropriate initial conditions, yields the domain suppression characteristics and the necessary rate of change of diode voltage at the threshold voltage level. The results indicate that this rate of change of diode voltage should be much lower than the rate of domain buildup (initial rate of change of domain voltage) and in real devices is approximately equal to the rate of change of bias voltage. Figures 3; references 4: 1 Russian, 3 Western (2 in translation).
[127-2415]

ANALYTICAL METHOD WITH USE OF FIELD PHASE JUMP FOR CALCULATING SUPPRESSION OF SELF-EXCITATION ON BACKWARD HARMONIC IN TRAVELING-WAVE TUBE

MALIVANCHUK, V. I.

[Abstract] An analytical method is outlined for calculating the design parameters of traveling-wave tubes with suppressed self-excitation on the first-order backward harmonic. The method, derived from that for backward-wave tubes, involves solving the matrix equation $dX/d\theta = AX$ where $X = \begin{Vmatrix} F \\ I \\ U \end{Vmatrix}$

and $A = \begin{Vmatrix} -jr & 1 & 0 \\ 0 & 0 & j \\ 1 & jq & 0 \end{Vmatrix}$ with complex amplitudes of the high-frequency field

intensity F, of the alternating component of the convection current I, and of the kineatic potential U, with the slip parameter b, the loss parameter d, $r = b - jd$, the space-charge parameter q, and the normalized length $\theta = Cz/v_e$ (C- gain parameter, v_e - quiescent electron velocity). The relation between output variables and input variables is $X_{out} = e^{A\theta out}\emptyset e^{A\theta in}X_{in}$ where

$\emptyset = \begin{Vmatrix} e^{-j\Delta\varphi} & 0 & 0 \\ 0 & 1 & 0 \\ 0 & 0 & 1 \end{Vmatrix}$ with the field phase jump $\Delta\varphi$. With the order of the A-matrix

determined according to the Sylvester rule and assuming a small space-charge

parameter q > 1, theoretical relations for the length of the acceleration
path and for the slip parameter (oscillation frequency) are reduced
to practical engineering formulas for design and optimization of traveling-
wave tubes with nonhomogeneous structure. Figures 1; references 7:
6 Russian, 1 Western.
[134-2415]

NOISE CHARACTERISTICS AND THRESHOLD SENSITIVITY OF SILICON MAGNETODIODES

GASANOV, L. S., KARBA, L. P., POROVSKIY, G. S. and SOKOLOV, Yu. I.,
Moscow Institute of Electronic Technology

[Abstract] Measurements of KD-301 open-construction magnetodiodes were made
in order to determine the frequency dependence of their noise factor at
various d.c. current levels from 10^{-5} to $2 \cdot 10^{-3}$A without a magnetic field
and in a transverse magnetic field. In the low-frequency operating range
($f < 10^3 - 10^4$ Hz) the noise factor saturates with the frequency approaching
$f = 0$, while the intrinsic noise level exceeds the thermal noise level by
several orders of magnitude at an operating current $I \approx 10^{-3}$A. In the high-
frequency range ($f > 10^3 - 10^4$ Hz) the noise factor decreases to 1.0 at
$f \approx 10^7$ Hz. As the operating current increases, the frequency characteristic
changes from linear to sublinear, especially in the high-frequency range.
A transverse magnetic field raises the noise level, which in turn determines
the threshold magnetic sensitivity of a diode, while its equivalent resistance
and with the thermal noise level also increase so that the noise factor
remains almost unchanged. The article was recommended by the Department
(Kafedra) of General Physics. Figures 4; references 7: 6 Russian, 1 Western
(in translation).
[145-2415]

NEW MEASURING INSTRUMENTS

Staff Report

[Abstract] New measuring instruments now commercially available include: 822 analyzer of pulse code sequences, operating as a pseudo-random sequences receiver and produced by the Ministry of Communication Equipment Industry; VSKM-12 humidity meter for structures, products, and materials; ATL titro- metric-type fluid analyzer for measuring the oxygen deficiency in stagnant waters; GVP generator of video-pulse and interference pairs for checking geophysical instruments used in oil and gas drilling; Spektropir 9 spectral- ratio pyrometer for processing of data on color temperature or true tempera- ture of objects. The latter three instruments are produced by the Ministry of Instrument Making, Automation Equipment and Control Systems. [136-2415]

ELECTRONIC COMPONENTS OF DIGITAL THERMOPHYSICAL INSTRUMENTS

KOZIN, V. M., KUREPIN, V. V. and OLEYNIK, B. N., Leningrad Technological Institute of the Refrigeration Industry

[Abstract] A device is described which ensures linear heating of the calori- metric cell in thermography over the temperature range from -200 to +400°C. The device includes a Chromel-Alumel thermocouple as a primary temperature transducer with a temperature-dependent sensitivity $S_T(T)$ = (23-38) K/mV and an electronic digital temperature setter, as well as a voltage (thermal emf) amplifier with a gain G = 250, a smoothing filter, an analog-to-digital converter, a register, and a digital computer with read-only memory. The temperature setter consists of a pulse generator and a 12-digit binary counter, with a temperature-difference register, a 6-digit analog-to-digital (tempera- ture difference to voltage) converter, and a corrector with power amplifier

for proportional-integral-differential regulation. A performance analysis, with 3-10 K segments of the temperature curve approximated with second-degree parabolas for monotonic heating, indicates that the heating rate of a calorimetric cell is read accurately within 1.5% over the entire temperature range. The article was recommended by the Department (Kafedra) of Physics. Figures 1; references: 2 Russian.
[145-2415]

HIGH-SPEED SPECTROMETER FOR ANALYSIS OF RADIATION SOURCES WITHIN SELECTED RANGES OF SPECTRUM

DMITRIYEVSKIY, O. D., KAVERIN, L. V., KISELEV, B. A., KLEMENT'YEV, V. G., KUZNETSOV, A. I. and PUSHKIN, Yu. D.

[Abstract] A photoelectric spectrometer has been built which measures contours of spectral lines of fast-varying plasmas within the 200-1100 nm range of wavelengths, with a 0.006-2.0 nm spectral resolution and a 10^{-5} s time resolution. This SP-181 instrument has three channels: one for simultaneous measurement of the spectral intensity of a radiation source within two preselected ranges of the spectrum (channel I), two for simultaneous measurement of the contours of two spectral lines with 0.006-0.066 nm resolution (channel II) and with 0.066-2.0 nm resolution (channel III). The optical part of the instrument includes a two-channel diffraction-type monochromator, taken from the high-speed two-channel SDS spectrometer, an IT-223 Fabry-Perot high-speed scanning interferometer (in channel II), and a slotted-disk modulator (in channel III). Other components are two calibrating radiation sources, two fixed mirrors, four rotating mirrors, three collimating objectives, three projecting objectives, a diaphragm (in channel I), an iris (in channel II), a power supply, a synchronizer, and a two-beam oscillograph. The monochromator has two interchangeable gratings with 1200 lines/mm, one with maximum energy concentration at $\lambda \approx 300$ nm wavelength (for the 200-434 nm range) and one with maximum energy concentration at $\lambda \approx 600$ nm wavelength (for the 420-1100 nm range); its aperture has a fixed height (12.5 mm) and a variable width (0-4 mm). The modulator disk (three interchangeable disks with different slot patterns) is driven by an electric motor, the latter equipped with a tachometer and a milliammeter. The spectrometer can operate as a spectrograph, with a special two-slot camera and three photomultipliers. The peak power requirement for operating this instrument is 3.5 kW. Figures 4; tables 1; references 4: 2 Russian, 3 Western.
[143-2415]

SMALL-SIZE INTERFEROMETER FOR FOURIER SPECTROMETRY

ARKHIPOV, V. V. and YEZHEVSKAYA, T. B.

[Abstract] A small-size interferometer has been built for use in Fourier
spectrometry. It consists of two identical coaxially mounted confocal
planoconcave spherical mirrors with a parallel light-splitter plate half-way
between them. A displacement of this plate along the axis by $\pm\Delta$ from the
center produces a difference between total paths of light rays in two compart-
ments equal to $\pm4\Delta$. Two holes in the splitter equidistant from the axis
and one hole in each mirror at the axis have been made for passage of light
rays. A light ray, upon entering the interferometer, is reflected inside
three times in a "cat's eye" pattern before leaving. All components have been
designed and produced to proper dimensions, with necessary and feasible toler-
ances. The interferometer, with a rotatable plane mirror in front on one
side and with an electrodynamic displacement mechanism (magnet, coil, spring
and clamp), has been tested in a small mock-up Fourier infrared spectrometer.
Its performance characteristics, particularly insensitivity to misalignments
and small angle of vision, make it suitable for airborne astronometry. Its
spectral range depends on the splitter material and on the type of photo-
receiver, but its performance is best in the visible and near-infrared
range. Two other important features are spatial separation of splitting
and interfering light beams at the splitter, which saves 50% of the radiation
loss, and allowance for adding other source channels such as for a reference
beam or white light without complicating the construction. Figures 4;
references: 2 Russian.
[144-2415]

HEATING OF TRANSDUCER IN PONDEROMOTIVE MICROWAVE WATTMETER

SHPAGIN, Yu. V. and MARTYNENKO, L. G.

[Abstract] Ponderomotive wattmeters for measuring superhigh microwave power
include transducer probes which heat up to levels which affect the instrument
accuracy. Design and operation of such wattmeters must take this heating
into account, which has been done in the case of dielectric probes but not
in the case of metal ones. The temperature field can be calculated on the
basis of the law of energy conservation for a model representing the probe
as a thin disk inside a rectangular H_{10}-mode waveguide, with the center of the

disk on the axis of the waveguide. An analytical solution of the problem involves simultaneously solving the equations of the electromagnetic field, the equations of heat propagation through gas and solid, and the equation of motion. This has not yet been done for the general case, because of tremendous difficulties, but can be simplified by assuming that the disk does not perturb the electromagnetic field, that the temperature at any point of the disk remains constant, and that heat transfer from the disk surface proceeds according to Newton's law. An expression for the steady-state temperature rise was derived on this basis, with the heat transfer coefficient to be determined experimentally. The results were verified experimentally on a constantan disk inside a waveguide transmitting a power of 10 W at the 3.2 cm wavelength, the measured rise of disk temperature not exceeding (2.1 ± 0.2) K. Figures 1; references: 6 Russian.
[136-2415]

X-RADIATION DETECTORS USING CHARGE-COUPLED DEVICES

KORZH, V. I., KUSKOV, V. Ye. and STENIN, V. ya.

[Abstract] Charged-coupled devices based on MOS structures, with a surface channel or volume channel and of the "brushfire" type in the form of a transistor series bank, are adaptable for use as x-radiation detectors and measuring the space distribution of the latter. All the necessary characteristics of these devices, namely quantum efficiency, quantum yield, sensitivity, resolution, dynamic range and radiation resistance are adequate for this purpose. The radiation resistance can be improved by using Si_3N_4 or vacuum evaporated SiO rather than SiO_2 as a dielectric and by recognizing that a p-type surface channel and an n-type surface channel are more radiation-resistant alternatives, as well as by making all electrodes of one material, preferable aluminum, with a uniform thickness of the dielectric underneath so as not to distort the surface potential profile and by configuring them without overlap so as to facilitate monitoring the potential in the interelectrode regions. Devices doped by ion implantation under the gates meet these requirements. Experimental devices of this kind with surface channel on an n-Si substrate have partially overlapping electrodes but do not require compensation of the shift of threshold voltage over a wide range of radiation doses (up to 10 Mrad). "Brushfire" devices have similar characteristics as well as the additional feature of being less sensitive to rising density of surface traps. Devices with a volume channel are the most promising of all. Here the dielectric-semiconductor interface does not participate in the transfer of signal charge and the dielectric does not constitute a barrier between charge carriers and control electrode so that it can be replaced with a reverse-biased p-n junction or a Schottky barrier.

Charge-coupled devices compare competitively with other x-radiation detectors such as diode arrays, gas-filled chambers and photoemulsion films. They can be assembled in linear as well as two dimensional arrays and interfaced with a computer or microcomputer. Figures 16; tables 2; references 43: 14 Russian, 29 Western (3 in translation).
[140-2415]

JOINT ACTIVITY OF SOVIET UNION AND GERMAN DEMOCRATIC REPUBLIC IN AREA OF HIGH-VOLTAGE MEASUREMENT TECHNIQUES

LOBZHANIDZE, N. G., TAVDGIRIDZE, L. N., MEGRELIDZE, K. I. and MCHEDLIDZE, G. V., USSR, BARTZ, I. U., SOLGA, H., TIPNER, W. and VOGEL, H., GDR

[Abstract] As a result of joint activity of USSR organizations (All-Union Scientific Research Institute of Metrology imeni D. I. Mendeleyev, All-Union Scientific Research Institute of Metrological Service, All-Union Scientific Research Institute of Means and Methods of Automation) and the GDR organization ASMW (Administration for Standardization, Metrology and Product Inspection) during the 1975-80 period, the following have been developed: 1) Design of a permanent high-voltage inspection laboratory (total floor area 590 m^2, area occupied by high-voltage booths 480 m^2, height 10 m, available power 200 kVA) for testing a.c. voltage dividers (accuracy class 0.01), a.c. voltmeters, voltage transformers, electromagnetic a.c. current comparators, d.c. voltmeters, capacitors, wtih top capability $330\sqrt{3}$ kV - 50 Hz and 100 kV d.c., a 35 kV - 400 Hz motor-generator set also being available; 2) Design of a movable high-voltage inspection laboratory for periodic testing offvoltage transformers with an electromagnetic current comparator and a gas-filled capacitor, its equipment including an automatic loading machine with special truck and trailer, also facilities for testing current transformers; 3) A high-voltage instrument capacitor with computable voltage dependence ofthe capacitance. Reciprocal arrangements have been made for comparing International System etalons of up to 36 kV by means of a Soviet-made ILL-35 transformer (accuracy class 0.2 secondary voltage $100/100\sqrt{3}$ V, burden 5 VA, $\cos\varphi = 0.8$). References 5: 4 Russian, 1 East German.
[136-2415]

REFERENCE-VOLTAGE SUPPLY

ALEKSEYEV, V. P., VIBE, P. F. and GOL'DSHTEYN, Ye. I.

[Abstract] A new 1-10 V reference-voltage supply pack has been made available
for high-stability measuring instruments and analog-to-digital converters as
well as for high-precision automatic and radioelectronic devices. It is
produced by hybrid/thick-film technology and consists of a two-channel
voltage stabilizer with operational amplifiers in the feedback loop. The
substrate temperature is maintained within 0.8 K over the 213-378 K range by
means of resistive voltage dividers and holding stabilizers. The PSON-3
pack has power components, low-power components, and thermal stabilization
circuitry in three separate modules. It is also equipped with overload pro-
tection and a logic for fault indication. The nominal load current is 0.15 A.
The maximum total instability of the output voltage (during ±15% fluctuation
of the input voltage, current dumping from full load to zero, and temperature
change through the 213-378 K range) is ±0.02%, its fluctuations are within
0.2 mV. The warm-up time is 60 s, the voltage drift does not exceed 0.01%
within 8 h of operation. A photograph of the PSON-3 pack is shown.
Figures 1.
[140-2415]

EQUIPMENT AND PROCEDURE FOR OBJECTIVE EVALUATION OF CHARACTERISTICS OF
ELECTRON-OPTICAL CONVERTER

MATSKOVSKAYA, Yu. Z., EDEL'SHTEYN, Yu. G., SAVENCHUK, N. A. and
KOLESNIKOV, V. Ye.

[Abstract] An instrument has been developed for measuring the signal-to-
noise ratio of electron-optical converters and correlating it with the
threshold characteristics, namely resolution and threshold contrast, of these
devices with background quantum noise. The signal-to-noise ratio is defined
as the ratio of mean brightness level of a uniformly luminous screen to the
rms deviation from this mean level. The cathode of a converter is uniformly
illuminated by a light source with a color temperature of 2850 K. The image
is transmitted by an OM-5 microscope objective from the screen through an
analyzing diaphragm (several interchangeable diaphragms of various sizes are
available) to an FEU-51 photoreceiver. The constant component of the

photoreceiver output signal is measured by an ShCh 1513 digital voltmeter directly. The variable component is measured by the same digital voltmeter, as noise, after being amplified by a low-pass filter with a passband the same as that of an eye (0.1-20 Hz), then detected (rectified) and integrated. Measurements are made first with the cathode open and then with an opaque disk in front of it. The data are processed in terms of the product of signal-to-noise ratio by the contrast transmission coefficient at a certain space frequency, the latter being determined by the converter magnification, the objective magnification, and the slot width. With catalog data given and known measurement parameters, including sensitivity and noise factor was well as noise space-filtration coefficient, one can determine the frequency-contrast characteristic of the tested electron-optical converter. Figures 2; references 6: 3 Russian, 3 Western (1 in translation). [144-2415]

UDC 621.387

MULTICHANNEL INDICATOR FOR CONTROL PANEL FOR PHYSICAL EXPERIMENTS

MIKHAYLOV, V. G., REZVOV, V, A. and YUDIN. L. I.

[Abstract] A panel of gas-discharge-tube indicators for display of data is described. This GIP-10000 panel uses IMG-1 devices with built-in control circuitry. The data field covers 100x100 points spaced 1 mm apart. The panel consists of two mutually orthogonal arrays of electrodes, eight vertical cathodes for image sweeping and eight horizontal anodes for data input, separated by a dielectric plate with holes where anodes and cathodes cross. When a crossing anode-cathode pair is under voltage, from a 250 V source, then discharge with orange-red glow occurs in the corresponding cubicle of space between the electrodes. Each electrode array is connected to a commutator, a protective circuit between cathode commutator and anode commutator preventing overload in the absence of a sweep. Both commutators are made of K1NT661A switching transistors. The cathode commutator also contains a decoder and is controlled from a duodecimal counter in the 1-2-4-8 code. With a 10 kHz frequency of the generator driving the cathode commutator, all data will be repeated at a frequency of 100 Hz. In the anode commutator the emitter circuits are lumped into groups of 10 and the base circuits remain free so that 110 inputs become available for incoming data. A typical operation of this panel is to display data in the form of histograms, with resistor pairs appropriately connected into the base circuits and the transistors correspondingly controlled for this purpose. The display system with inputs 1,2,...,100, strobing input and input from an address decoder also includes an analog commutator, a d.c. amplifier, a generator of linearly varying voltage and a comparator which together with an AND gate and a register form an analog-to-digital converter, a master oscillator and a buffer register feeding into the anode commutator. While the screen of this

panel is not as information-intensive as that of a cathode-ray-tube panel, it is more reliable and simpler in construction, being also smaller in size and not requiring a high-voltage supply. A photograph of the equipment is shown, Figures 5; references: 4 Russian.
[140-2415]

METHOD OF CALCULATING EXPECTED INTENSITY OF BACKGROUND MOONSHINE FOR PLANNING ASTRONOMICAL OBSERVATIONS

VERESHCHAGIN, S. I. and LIKHOMANOV, S. A.

[Abstract] Most astronomical observations are made during moonless nights, but some can also be made with the moon shining - below a certain intensity level. Here a method is proposed for preliminary estimating what the background moonshine intensity will be within a given region of the sky. The method, based on theoretical analysis and experimental data, utilizes the analogy between already well known brightness distributions over the sky in daylight and at moonlit nights. A semi-empirical expression is used for the mean sky brightness, taking into account the dependence of local brightness on the elevation angle as well as the changes in brightness caused by changes in the sun's position. These two factors appear as normalized functions. Transparence of the atmosphere and albedo of the ground surface are lumped together into a single coefficient. The mean intensity of background moonshine, as a function of the moon's phase, is evaluated by the method of polynomial approximations. A computer program IZOLI has been devised which yields the space-time distribution of moonshine intensity and plots it in the form of isophots on a sky map representing a region bounded by space and time coordinates δ_{min}, t_{min} and δ_{max}, t_{max} with the date also marked. The coefficient is evaluated in a separate program, by the method of least squares. Figures 2; tables 1; references 10: 7 Russian, 3 Western.
[144-2415]

OPTIMIZATION OF DATA RECORDING PROCESS ON MEMORIZING CATHODE-RAY TUBE WITH
SELF-ERASURE

ASADOV, Kh. G., Azerbaijan SSR

[Abstract] Use of memorizing cathode-ray tubes for identification and
measurement of fast processes is considered, taking into account the self-
erasure effect with attendant narrowing of the dynamic range and resulting
loss of data. Calculations based on signal analysis and the minimum read-
able signal indicate the conditions for retention of the maximum amount of
data and yield the payoff of a recording system optimized accordingly.
Figures 3.
[135-2415]

ESTIMATION OF PROBABILITY OF SIGNAL DETECTION DURING IMAGE IDENTIFICATION BY
GEOMETRICAL APPROACH

RAKCHEYEV, D. P. and TOLSTIKOV, A. S., Leningrad

[Abstract] Some problems of image identification, when the variance of reali-
zations relative to the mean etalons is very small, can be solved without
minimization of Euclidean distances. Images can then be classified by analog
means, on the basis of comparison with threshold distances and without the
use of a digital computer. Invariance of an image with respect to rotation
and translation can be achieved by means of a spiral television scan with
the center at one of the point objects. Here the probability of detection
of video signals in such an identification process is estimated in terms of
the signal-to-noise ratio and on the basis of the frequency of false alarms,
the false-alarm error being the most dangerous one in image identification
for production control. Calculations indicate that one can increase this
probability by stipulating the signal-to-noise requirements at the input of
the recording instrument and by selecting the optimum relative threshold
level as well as the optimum duration of the programmable sampling strobe.
Statistical accumulation of data will improve the interference immunity.
Figures 3; references 4: 2 Russian, 2 Western (both in translation).
[145-2415]

PHOTOELECTRIC MICROSCOPE WITH DIGITAL READOUT

LEVANDOVSKAYA, N. Ye., MOSKALEV, P. A., FINKEL'SHTEYN, Ye. I., MOVSHEV, A. K., KLABUKOV, A. G., ABLEYEV, V. A. and BEREZOV, V. G.

[Abstract] An improved version of the FEM-2 photoelectric microscope has been developed in which subjective error is eliminated by automatic correction of "null" drift and automatic compensation of displacement of a scale line relative to the viewfinder axis. A mismatch produced in the tracking system by a displacement, or disappearance, of a scale line compensates that displacement and homes the scale line. A "null" drift of the electromagnetic vibrator-scanner is corrected similarly. This FEM-1Ts instrument can also be switched to manual operation. Its basic performance characteristics are: range of measurement 0.1 mm, discreteness of readings 0.05 μm, maximum allowable systematic error $\pm(0.1 + 0.002L)$ μm (L- length to be measured), and rms error of scale line homing 0.05 μm. Readings can be shifted to any point within the range. Readout and indication are digital. The instrument scale is of first or second class accuracy, on glass or metal, with scale lines 4-8 μm thick according to GOvernment STandard 12069-78. As light source serves an OP8-9 lamp operating at partial glow level, which lengthens its life twelvefold beyond nominal. The instrument has been tested and evaluated for accuracy, stability, and reproducibility of readings in transmitted light and in reflected light. Figures 3; references: 1 Russian.
[143-2415]

MAGNETICS

MAGNETIC CIRCUIT OF MAGNETIC-MODULATION TRANSDUCER

IVANOV, M. P., MALESHIN, V. B. and GUSEV, V. G., Ufa Institute of Aviation
imeni S. Ordzhonikidze

[Abstract] Contactless magnetic-modulation transducers are used for trans-
mission of signals from rotating thermocouples, these devices being the only
ones available for operation at ambient temperatures of 300-400°C. Such a
transducer consists of a shell-type magnetic yoke mounted on a shaft and
carrying two identical stationary measuring coils, a rotating signal coil
between them, and a stationary modulating coil embracing all three. Changes
in fluxes and magnetomotive forces during modulation of a signal are cal-
culated by solving the corresponding differential equations for the various
parts of the magnetic circuit. The structure is assumed to be long (large
length-to-diameter ratio) and linear (wide air gap between rotor and stator),
with only the magnetic reluctance of skin layers varying during modulation and
all skin layers having the same saturation depth. The magnetic permeability
of the modulated parts of the circuit is assumed to remain constant and equal
to the initial magnetic permeability of the material. The equations are
solved and the performance characteristics of the transducer, particularly
its sensitivity, are calculated for specific numerical design data. The re-
sults agree within 11% with experimental data. The sensitivity depends
principally on the saturation depth of the part of the structure with
modulated magnetic reluctance. For maximum sensitivity, this depth should
be such as to maintain the relative magnetic permeability within the 10-
100 range during modulation throughout the given temperature range. The
optimum length-to-diameter ratio is 6-8, a further increase of this ratio
not increasing the sensitivity enough and thus not being economical. The
article was recommended by the Department (Kafedra) of Information and
Measurement Engineering. Figures 4; references: 2 Russian.
[145-2415]

MICROWAVE THEORY & TECHNIQUES

ENGINEERING METHOD OF CALCULATING WAVEGUIDE LOADS

USENKOV, V. V., KIM, A. Ch. and ZHAROVA, V. M.

[Abstract] A general method is developed for computer-aided calculation
of waveguide loads in the form of a length of waveguide of variable cross
section filled with a lossy dielectric, where the degree of filling is length-
wise variable. Effects associated with higher wave modes are disregarded, and
it is assumed that the load can be represented by an inhomogeneous transmis-
sion line with distributed losses. The relation between complex values of
the coefficient of reflection, propagation constant and their derivatives
along the transmission line is described by a Riccati equation, which is
numerically integrated. Machine time for carrying out the integration ranges
from 1 minute to 1 hour, depending on the complexity of the system. Some
results are given showing calculation of the standing wave ratio of various
loads. Therresults of the program have been used in designing the MZ-46 and
MZ-47 wattmeter waveguide loads. Figures 3, references: 4 Russian.
[128-6610]

SOLID-STATE HIGH-POWER MICROWAVE PROTECTIVE DEVICES

AKOPYAN, V. A. and LEBEDEV, I. V.

[Abstract] Various solid-state switching diodes are used for protecing the
input of microwave receivers from too powerful transmitter signals as well
as from stray microwave signals. The basic two versions are a switch
blocking a signal only when forward biased and a switch blocking a signal

only when zero or reverse biased. A special case of the latter is a
"resonance diode" passing a signal when forward biased bacause of parallel
resonance between diode output inductance and diode housing capacitance.
An important problem in design and manufacture of such protective devices is
ensuring adequate power capacity, which can be achieved by appropriate
compounding of diode structures and effective heat dissipation. Typical
configurations are reverse-biased diodes in the arms of a waveguide bridge
and a multidiode resonance-type waveguide mesh. The latter, with a large
number of simultaneously operating diodes, can now be produced by application
of the planar-integration technology. With p-i-n switching diodes such devices
are externally controllable, and with limiting diodes they become self-
controllable. Figures 4; references 16: 8 Russian, 8 Western.
[127-2415]

FABRICATION OF STRIPLINE MICROWAVE DEVICES WITH AID OF PULSE-TYPE PLASMA
ACCELERATORS

CHERNYAYEV, V. N., KORZO, V. F. and KONDRASHIN, A. A.

[Abstract] Deposition of thin conductor-metal (Cu, Ag, Al) films on dielectric
substrates with the aid of a pulse-type plasma accelerator eliminates the
need for adhesive refractory-metal (W, V, Cr, Mn) interlayers in the fabrication
of stripline microwave devices. The main advantage of this method is deposi-
tion of high-energy metal atoms and ions, the energy of ions being controll-
able so as to ensure good adhesion without buildup of structural defects in
the boundary layer. Other advantages include high deposition rate (up to
0.1 µm/s) with controllable degree of ionization (10-90%), high metal-vapor
utilization factor (20-50%), and highly accurate control of metal evaporation.
A production set has been designed and built which provides these features
without the disadvantages caused by nonuniform erosion of the accelerator
cathode and the presence of liquid drops in the plasma stream. Its structure
is based on UVN-2M-3 equipment with a cylindrical cold cathode made of the
metal to be evaporated and operating in the vacuum-arc mode. Adequate pulse
power is provided by a capacitor bank with a rectified 380 V supply. The
equipment was tested in deposition of 2-7 µm thick copper films on glass-
ceramic substrate with an adhesion strength of correspondingly 104-432
kgf/cm^2. The adhesion strength remains almost at the top level as the film
thickness increases to 8 µm and then begins to decrease as the film thickness
further. An electron-microscope examination of copper films on Polycor sub-
strate has revealed films up to 1.5 µm thick have an amorphous structure and
thicker films have a granular structure, with the grain size increasing with
higher deposition temperature as well as with larger film thickness but

leveling off as the film thickness exceeds 5 μm. The method and equipment are practical for deposition of 0.1-10 μm thick copper and other films with adequate adhesion strength and stability. Figures 3; tables 1; references 8: 6 Russian, 2 Western (1 in translation).
[134-2415]

HIGHER GAIN STABILITY OF TRAVELING-WAVE MASER

PARKHOMENKO, M. V. and STETSENKO, A. I.

[Abstract] Gain stability of a traveling-wave maser within its tuning range requires a stable magnetic Q-factor of the paramagnetic crystal and a stable dispersion characteristic of the electrodynamic retarding system. Although the feasibility of eliminating the causes of Q-factor instability has already been established both theoretically and experimentally, there is still a problem with the electrodynamic system. A study has revealed that its dispersion characteristic can be stabilized by reliable fixation of the row of pins in the periodic comb structure (which also includes a row of ferrite beads parallel to the row of pins along the active element inside the pumping waveguide) for the entire temperature range from 290 K (room) to 4.2 K (liquid helium). This was done by filling the space between the pins with cast II-bars of a dielectric (polymer) material, polyethylene. The structure was temperature cycled, to simulate conditions of intermittent operation. The signal slowdown with respect to group velocity was measured by the Nyquist method. Presence of the polymer material was found to shift the high-frequency cutoff toward longer waves and thus increase the slowdown while narrowing the tuning range, but not to increase losses throughout the entire transmission band. A traveling-wave maser for the 4-cm wave band was built with such a retarding structure and tested over the entire tuning range with temperature cycling, its gain stability remaining very high throughout. Figures 2; references 9: 5 Russian, 4 Western (1 in translation).
[134-2415]

UDC 621.385.6

ADDITIONAL NOISE SOURCES IN MICROWAVE DEVICES WITH CROSSED FIELDS

Kiev IZVESTIYA VYSSHIKH UCHEBNYKH ZAVEDENIY: RADIOELEKTRONIKA in Russian
Vol 25, No 10, Oct 82 (manuscript received 3 Jul 81) pp 88-91

NIKITIN, A. A., STAL'MAKHOV, V. S. and SHAPOVALOV, A. S.

[Abstract] An evaluation is made of noise sources which are usually not taken into account in the analysis of microwave M-type electron-beam devices with crossed fields. The principal such sources are fluctuations of the electron drift velocity, calculated here together with their spectral density for a rectilinear ribbon beam of finite thickness between two parallel infinitely long plates. The calculations are based on the Laplace equation for the two regions without space charge (between the beam and each plate) and the Poisson equation for the two regions with space charge (layers of the beam, each of half the total thickness). Other heretofore unaccounted for noise sources are current subsidence and consequent secondary electron emission, both irremovable, and causing additional fluctuations of the space-charge density and of the electron drift. Expressions are derived for calculating the effect of these fluctuations on the various noise parameters of such devices. Figures 1; references 5: 4 Russian, 1 Western.
[127-2415]

POWER ENGINEERING

UDC 621.313.13-133.32

CONTROL MODULE FOR STEPPER MOTOR

SALOSIN, V. N., KOSHEVOY, Yu. V. and GUSHCHIN, Ye. A., Institute of
Biophysics, USSR Academy of Sciences, Pushchino

[Abstract] A universal control module has been developed for stepper motors
in various applications ranging from microbatchers and microcompressors to
automatic control of biological processes. It consists of a master pulse
generator which converts voltage to frequency, a pulse shaper which converts
input pulses of arbitrary form to rectangular pulses of required duration,
a commutator which converts a unitary code to a 4-phase voltage signal, and
a power amplifier which energizes the control winding of the motor. The
master pulse generator contains a K140UD2A operational amplifier and a
KT117V transistor with a 0.1 nF capacitor in the collector circuit which
serve as a wideband current generator, followed by a KT117V-KT117V
transistor-pair threshold device. The voltage-to-frequency conversion is
linear within ±1% over the 1.35-0.0313 V range and the error of the master
pulse generator does not exceed 2.5% as the temperature rises from 15 to 40°C.
The module is supplied through a transformer and a rectifier with a stabilizing
circuit. It has been tested with a ShDA-3F stepper motor. Figures 1;
references: 4 Russian.
[140-2415]

UDC 621.315

LOW-INDUCTANCE CABLE-TYPE COLLECTORS FOR CAPACITIVE ENERGY STORAGE DEVICES

GRIGOR'YEV, A. V. and DASHCHUK, P. N., Leningrad Polytechnic Institute

[Abstract] Collectors serve as matching elements between a capacitive energy
storing device and a small-size load, usually an inductive one, and their

inductance must be minimized for maximizing the output power. The equivalent inductance of a collector consisting of an array of coaxial cables can be decreased by increasing the number of such cables, but without excessively increasing the mean distance from load to cable connection. Here two variants of a low-inductance collector are proposed. In the first one the load is connected coaxially at the center of a circular cable array, in the second one the load is connected at one side of a rectangular cable array. The pothead is designed accordingly and the main polyethylene insulation here is coated with a semiconducting material so as to form a 1.5 mm thick monolithic layer with highly anisotropic electrical resistivity and high radial electric strength. The voltage rating can be further increased, up to twofold, by adding a 0.5-1.0 mm thick layer of dielectric material or slipping on dielectric washers. A circular 1 MJ - 150 kV collector with an inductance of 5 nH equal to 14% of total inducatnce and a rectangular 18 kJ - 50 kV collector with an inductance of 1.95 nH equal to 4% of total inductance have been designed on the basis of these principles. Figures 3; references 10: 9 Russian, 1 German.
[140-2415]

WIDEBAND POWER DIVIDERS-ADDERS USING ASYMMETRIC DIRECTIONAL COUPLERS

GORBACHEV, A. P., NEVEROV, S. G. and ROMANOV, A. N.

[Abstract] Binary power dividers-adders using asymmetric stepped directional couplers on coupled transmission lines operate over a wide frequency range without excessive unbalance, while minimization of losses is ensured by phasing of signals in the load. The principle is demonstrated here on a device for identical amplifiers with Chebyshev frequency characteristics, its performance being analyzed as that of a linear multipole network. An eight-channel power divider-adder was built using two-segment directional couplers, with FAF-4 material as dielectric (ϵ = 2.3). It was tested over a frequency range with 2.5 overlap, within whichiits efficiency did not drop below 0.87 and the total power of 5 W octave amplifiers reached 36 W with 0.4 dB unbalance. Figures 3; references 5: 3 Russian, 2 Western.
[134-2415]

CONTROL SYSTEM MODULE FOR POWER PLANTS OPERATING IN PULSE MODE

AZIZOV, E. A., VOROB'YEV, V. A., GENDEL', Yu. G., NEKHAYEV, V. I. and
YAROSH, A. M.

[Abstract] A logic module has been developed for a reliable control system
in nuclear fusion plants with inductive pulse-type energy sources storing
10^7 J or more energy. It ensures rigorous execution of a given operations
program, actuation of all servomechanism components in proper sequence,
monitoring of plant performance and state during an operating cycle, and
continuance of operations in a field of strong electromagnetic interference,
as well as interruption of the program and actuation of protective equipment
in case of abnormal deviations. The module is connected to two input devices
and three output pulse shapers. One input signal coincides in time with the
signal for a servomechanism component to be switched on, the other input
signal corresponds to actuation of that component. The module consists of
18 series K155LA3/4 microcircuit AND gates, five KT201 transistors, seven
D9 diodes, four AL307B light emitting diodes, and two MIT-3 input transformers
with four KS139A stabilitrons. Two extra inputs are tapped in for interlock-
ing with other system modules. Two output signals are formed in response to
input signals from sensors. The third output signal is formed through a
delay device. The module prevents emergency shutdowns and "burst" release
of energy. Figures 4; references: 1 Russian.
[140-2415]

MATCHING CIRCUITS OF OVERHEAD LINES WITH CABLE INSERTS

VELIKZHANIN, N. K., senior lecturer, Ural Electromechanical Institute of
Railroad Transportation Engineers, and KHRIPUNOVA, I. V., assistant

[Abstract] Expansion of railroad stations and junctions along with expansion
of electric transmission networks necessitates coupling of cable inserts with
overhead line segments. The segments of such an electrically nonhomogeneous
line require matching, for which a device is proposed consisting of a set of
matching four-pole impedance networks with a series reactance on each side.
The components of this device are designed for given frequency bands in the
voice spectrum, where an overhead line segment is in effect capacitive and
attenuation in a cable insert increases with increasing frequency. Accordingly,
a compensating element must be inductive and a coil wound on an iron ring-core

fits this requirement. Design calculations are aided by curves representing the frequency characteristics of input impedances and of attenuation for various cable lengths. Figures 11.
[139-2415]

INTRODUCTION OF 'ELEKTRONIKA S5' MICROCOMPUTER INTO SYSTEMS OF LOSS OF ELECTRIC ENERGY ACCOUNTING AND AUTOMATIC RESERVE SWITCHING

LESIN, N. M., engineer, and FAYBISOVICH, V. A., candidate of technical sciences, Belenergoremnaladka (Belorussian Regional Administration of Power Equipment Repair and Adjustment)

[Abstract] The family of "Elektronika S5" microcomputers has been designed for application in power system automation. Such a microcomputer operates with digital input and output, an "Elektronika S5-121" functional module being available for analog-to-digital conversion, signal commutation, and input of analog d.c. signals. In the first stage of introducing the "Elektronika S5-11(12)" microcomputer into electrical automation of the Belorussian power system, it has been assigned two tasks to perform: accounting of energy losses in the high-voltage transmission lines and high-speed automatic reserve switching. It has been programmed to implement the corresponding algorithms, with the aid of analog-to-digital conversion in the aforementioned functional module and with input data from a.c. current and voltage transducers, as well as a temperature transducer. A read-only memory or preferably an energy-independent semipermanent memory is provided in order to avoid intermittent failures or erasures in the main memory when the supply voltage drops too far below 220 V. Interference immunity of the microcomputer is ensured by appropriate special-purpose hardware and software. Peripheral equipment includes an STA-2M telegraph set which operates with a five-element code in the teletype dispatcher mode, magnetic tape for data storage, and means of signal simulation for debugging and testing. Figures 2; references: 4 Russian.
[138-2415]

COMPENSATION OF SCANNER ERROR

GALUYEV, S. V., MIKHEYEV, V. P., ROZOV, B. S. and SHMELEV, S. I.,
Moscow Institute of Engineering Physics

[Abstract] Static and dynamic errors of an optomechanical laser-mirror
scanner which sweeps $5°$ angles along each coordinate independently, with a
0.1" discreteness, can be compensated optically with the aid of a high-speed
auxiliary deflector. This is demonstrated on the basis of the approximate
transfer function of such a scanner as control object with two oscillaotry
elements. The equipment also includes, in addition to this auxiliary deflec-
tor, the servomotor-driven main deflector (mirror), a focusing carrier, an
interference-type displacement transducer, a comparator, and a control
mechanism driving the auxiliary deflector. As a correcting deflector can
serve an optoelectric, optoacoustic, magnetoelectric, or piezoelectric device,
each type with its peculiar transfer function and all having a narrow dynamic
range. Errors from any source are compensated here, the degree of compensa-
tion limited by the inaccuracy of the auxiliary deflector plus one reading
of the laser interferometer. Such a compensation of dynamic errors increases
the scanner response speed to anywhere between 7 and 22 times the response
speed with logic-law control without optical correction. Magnetoelectric
galvanometers, with a somewhat wider dynamic range, increase the scanner
response speed by a factor of 14. The article was recommended by the
Department (Kafedra) of Automation and Telemechanics. Figures 2;
references: 3 Russian.
[145-2415]

HETEROJUNCTION PHOTOTRANSISTOR FOR INTEGRATED OPTICS

BORODULIN, V. I., ZVERKOV, M. V., KONYAYEV, V. P., PASHKO, S. A., SIMAKOV, V. A.
and SHVEYKIN, V. I.

[Abstract] It has been found feasible to produce a laser+phototransistor
device by conventional zinc diffusion technology for application in monolithic
integrated optics including an injection laser and a photoreceiver with
control and stabilization of laser radiation power. The phototransistor
is built on a heterostructure with widened optical waveguide, a stack of five
heteroepitaxial layers on an n-GaAs substrate: $n\text{-}Ga_{0.7}Al_{0.1}As$, $n\text{-}Ga_{0.9}Al_{0.1}As$
(0.3 μm thick), p-GaAs base (0.2 μm thick with $p = 5 \cdot 10^{17} cm^{-3}$),
$n\text{-}Ga_{0.5}Al_{0.5}As$, and n-GaAs contact. The current conducting region adjacent
to the p-GaAs layer is formed by two-stage zinc diffusion. The breakdown
voltage of both emitter-base and collector-base p-n junctions is 5-5.5 V.
An injection laser is built into the same crystal. The steady-state photo-
current was measured as a function of the incident radiation power for a
common-emitter circuit with a continuous-wave injection laser (862 nm) as
radiation source. With $V_{CE} = 3.0$ V and $I_B = 0$ and $I_B = 1.5$ μA the sensitivity
was found to be 27 and 19 A/W respectively, with $V_{CE} = 2.5$ V and $I_B = 1.5$ μA
the sensitivity decreased to 5.6 A/W. The sensitivity remains high even under
nonoptimum conditions of irradiation. The photocurrent increases almost
linearly with the radiation power, at least up to 1.2 mW. Figures 2;
references 6: 3 Russian, 3 Western.
[134-2415]

SOLID STATE CIRCUITS

INJECTION TRANSISTOR ASSEMBLIES

IGUMNOV, D. V., KOSTYUNINA, G. P. and MASLOVSKIY, V. A.

[Abstract] The authors analyze circuits called injection transistor
assemblies in which NPN transistors are connected in parallel with the load,
the negative side of the input going to the emitter of the first stage,
while the positive signal is applied to the base. Transistors of succeeding
stages have their bases common with the input, and are connected collector-
to-emitter, the load being connected between the collector and base of the
output stage. The output voltage is the injection voltage. It is shown that
such assemblies can be used for decoupling electric control circuits, and
also in electronic power supplies. This type of circuit can be easily
realized as a silicon chip. The optimum semiconductor devices for injection
assemblies are transistors with variable-conductivity base region.
Figures 4; references 3: 1 Russian, 2 Western.
[128-6610]

INTEGRATION OF SOLID-STATE MICROWAVE CONTROL AND PROTECTIVE DEVICES

LEBEDEV, I. V., ALYBIN, V. G. and KUPTSOV, Ye. I.

[Abstract] Outfitting and packaging of solid-state control and protective
microwave devices are based on essentially the same principles as those for
their gas-discharge and vacuum-tube analogs, the miniaturization index
serving as a convenient criterion of effectiveness in terms of weight and
size. A typical illustration are cutout switches and limiters. Most

suitable and promising for circuit integration of centimeter-wave and
millimeter-wave devices are planar components, use of quasi-T modes without
cutoff in microstrip lines being an outstanding example. Various methods
of increasing both the integration density and the power capacity are
available, among the use of "multistory" circuit boards and unsing both sides
of the dielectric substrate. Hybrid integration of millimeter-wave devices
is still a tradeoff between microstrip lines and fin lines. Alongside have
also developments been made in circuit integration and miniaturization with
bulk devices. Altogether computer-aided analysis and synthesis are very
helpful, especially when number of samples and number of errors can be
minimized. Much attention in future planning should be paid to "exotic"
monolithic and quasi-monolithic circuit configurations. Figures 10;
references 72: 30 Russian, 42 Western.
[127-2415]

STATE OF ART AND MAIN PROBLEMS IN DEVELOPMENT OF MICROWAVE TRANSISTORS
(SURVEY)

MURAV'YEV, V. V. and NAUMOVICH, N. M.

[Abstract] The appearance of new semiconductor microwave devices and their
subsequent improvements make it possible to replace gradually vacuum-tube
devices such as reflex klystrons, low-power low-noise traveling-wave tubes
and wideband backward-wave tubes. These semiconductor devices include IMPATT
and Gunn-effect diodes, bipolar and field-effect transistors. Functionally,
i.e., with respect to their basic application and performance characteristics,
transistors fall into two categories: low-noise amplifier transistors for
linear amplification of small signals and power oscillator transistors for
generation or amplification of large signals. Existing bipolar transistors
are designed with comb, multiemitter, cellular or rhombic structure, the three
semiconductor materials used for them being silicon, GaAs and InP. They can
operate at frequencies up to 14 GHz (power devices) and 4 GHz (low-noise
devices). Microwave field-effect transistors come in two versions. Those
with a Schottky barrier use GaAs or InAs as basic material and can operate
at frequencies up to 30 GHz, at high efficiency and without secondary break-
down. Those with an insulated gate use silicon as basic material and can
operate at frequencies up to 4 GHz, with excellent linearity and thermal
stability. An important problem in design and manufacture is the transistor
housing, beryllium ceramic (oxide) being so far the best material for a crystal
holder with adequately high elasticity, flexural strength, electrical resistivity
and thermal conductivity. All microwave transistors are being adapted for
circuit integration, until recently primarily for hybrid circuit integration
but also increasingly for monolithic circuit integration. Further developments

aim, most importantly, at higher reliability and ensuring it by producing devices with internal matching components immune to mismatch of output channels, as well as extending the frequency range and improving other performance characteristics. Photolithography and ion implantation as well as novel technological processes are being extensively researched. Figures 6; tables 4; references 67: 27 Russian, 40 Western.
[127-2415]

TEMPERATURE DEPENDENCE OF NOISE PARAMETERS OF MICROWAVE TRANSISTORS

IVANOV, N. I. and YURCHAK, N. S., Physico-Technical Institute of Low Temperatures UkSSR Academy of Sciences, Kharkov

[Abstract] Noise characteristics of n-p-n germanium transistors for microwave wide-band amplifiers and narrow-band oscillators were measured with cooling, for the purpose of determining their temperature dependence and the feasibility of noise reduction at low temperatures. The noise factor of GT329 and GT341 transistors with $\omega_\alpha \sim 2.5 - 4$ Ghz, measured over the $0.1 - 2$ GHz frequency range in an aperiodic common-emitter amplifier circuit with mica capacitors and varnished metal-film heat-resistant resistors, was found to be minimum (1.8 - 2 dB) at 150 ÷ 170 K. These temperatures do not coincide with temperatures at which the gain is maximum. The noise temperature of these transistors was measured in a grounded-base oscillator circuit. The momentary frequency instability of such an oscillator was measured by the method of a time window and found to decrease with decreasing temperature and to drop to its residual level within 1 s (10^{-6} with transistor and tank circuit at 170 K, $10^{-10} - 10^{-9}$ with transistor at 170 K and tank circuit at 4.2 K). Figures 2; references 7: 6 Russian, 1 Western in translation.
[140-2415]

INTERFERENCE IMMUNITY OF OPTOELECTRONIC SYSTEM WITH SECTORAL SCANNER

KAZAKOV, V. A. and SHUMOV, A. P., Ryazan Institute of Radio Engineering

[Abstract] An optoelectronic instrument with a sectoral scanner is used for determining the coordinates of a randomly moving small object. Measurements

104

by this method are subject to additive intrinsic noise in the receiver of
radiant energy, additive noise caused by jitter of the moving object, and
multiplicative signal amplitude fluctuations (fadeout). The interference
immunity of such an optoelectronic device converting continuous radiation
to radiation pulses is evaluated here in terms of the signal-to-noise ratio,
with the parameters of the electric signal pulse at the receiver output
precisely defined. The analysis is based on the filtration algorithm for
readings of the coordinates (normal Markov process), with parameters of the
signal pulses nonlinearly dependent on these readings. Calculations for
various numbers of equal alternating transparent and opaque sectors on the
disk ($n = 24$, 4) and for various time quantization ratios reveal that signal
fadeout does not, on the average, affect the accuracy of data processing in
such an instrument with an optimum radiation receiver. The article was
recommended by the Department (Kafedra) of Radio Control and Communication.
Figures 3; references: 4 Russian.
[137-2415]

SONICS & ULTRASONICS

LASER-RESONANCE OPTOACOUSTIC GAS ANALYZER FOR MONITORING IMPURITIES IN
ATMOSPHERE

DOLGIY, S. I., IPPOLITOV, I. I., KHMEL'NITSKIY, G. S. and SHUBIN, S. F.,
Institute of Atmospheric Optics, Siberian Department, USSR Academy of
Sciences

[Abstract] A high-sensitivity gas analyzer for use in oil and gas explora-
tion through the "gas cap" above ground has been developed at the Institute
of Atmospheric Optics, as a special-purpose version of a gas analyzer for use
in pollution control. It consists of a resonance-type optoacoustic spectrom-
eter with a set of two lasers discretely tunable by means of a diffraction
grating, namely a low-pressure CO_2 laser and an LG-126 He-Ne laser, and a
microcomputer-based data processing system with time tracking by means of
an electronic clock. The method of measurements is based on absorption of
monochromatic radiation from the lasers, the latter being tuned to the fine
absorption lines of the gases sought. The instrument includes aamodulator
with motor drive and control, a control-pulse shaping circuit with frequency
meter, a spectrophone chamber, a microphone, a selective amplifier, an
attenuator, two digital voltmeters (analog-to-digital converters), and a
control module for interfacing with the "Elektronika" BZ-21 microcomputer.
The spectrophone chamber is an acoustic resonator tuned to 860 Hz. The gas
pressure in it varies at the frequency of laser modulation and its readings
are converted to gas concentration. The wavelength of the He-Ne laser can
be tuned for water vapor (1.15 micrometer) and lighter hydrocarbons beginning
with methane (3.39 micrometer). The wavelength of the CO_2 laser can be
tuned from 9.1 to 10.9 micrometer for heavier hydrocarbons, ammonia, ozone,
carbon dioxide, and Freon-12. The minimum concentration measurable by this
instrument varies from $0.001 \cdot 10^{-6}$ atm (Freon-12) to $30 \cdot 10^{-6}$ atm (carbon
dioxide), far below the corresponding maximum permissible levels. Figures 1;
tables 1; references 6: 4 Russian, 2 Western.
[137-2415]

NEW ACTIVITIES: MISCELLANEOUS

DEVELOPMENT OF COMMUNICATION FACILITIES IN KIRGIZIA: PROBLEMS AND OUTLOOK

TYUREBAYEV, V. N., minister of com unications, Kirghiz SSR

[Abstract] The communication system in Kirgizia have undergone intensive
development, particularly during recent years. The latest achievements in-
clude expansion and automation of the telephone network, the number of
interurban lines having increased threefold since 1971, and of the public
telegraph network, introduction of phototelegraphic newspaper teleprinting,
modernization of rural communication facilities, installation of powerful
television transmitters ("Yakor", "Zona", "Len") as well as of 100 W tele-
vision relays and of facilities for reception of broadcasts via satellite,
addition of color to black-and-white television broadcasting, simultaneous
high-quality broadcasting of First and Second radio programs (Republican),
and initiation of electronic postal service. For the remainder of the
current Five-Year-Plan period further improvement and expansion of all
communication services are scheduled, with particular emphasis on targeted
installation and use of computer facilities, completion of the automated
control system for communications (OASU-Svyaz'), and in particular extension
of the electronic postal service to 25 new rural offices. According to the
1982 status reports, these goals are expected to be met. Figures 3.
[126-2415]

ELECTRICAL EQUIPMENT INDUSTRY IN SOVIET UNION

MAYORETS, A. I., minister of the Electrical Equipment Industry

[Abstract] Development of the Soviet electrical equipment industry is
reviewed historically, from V. I. Lenin's plan for the State Commission on
Electrification of Russia set forth in 1920 to product sophistication and
production levels in the current eleventh Five-Year-Plan. Landmark contribu-
tions by scientific, engineering and manufacturing organization are traced

through the 60 years of the Soviet Union (1922-82), with credit given to outstanding individuals in the field of electrical engineering. Cooperation between the various Soviet republics and since 1945 with other socialist countries, especially Poland and the German Democratic Republic, is also mentioned as an important contributing factor. The present status is reported in broad outlines, which include electrical equipment now produced which ranges from components for nuclear power plants and high-voltage power systems to components for computers and communication systems (e.g., satellite communication systems), from heavy rotating machines and transformers to optoelectronic devices and integrated circuits, and high-volume general purpose equipment to low-volume special-purpose equipment. The report also covers economic and human aspects of progress in the electrical equipment industry, stimuli and incentives, management and educational support, and the growing trend toward meeting the demand for consumer goods.
[138-2415]

ELECTRICAL COMMUNICATION IN ESTONIA

KALDMA, A. U., minister of communications, Estonian SSR

[Abstract] Tremendous strides have been made in improving and expanding the electrical communication systems in Estonia during the past two Five-Year-Plan period and the first 2 years of the present one. They include a 58% increase of the number of telephone subscribers to 16 sets per 100 inhabitants, automation and better control of telephone exchange offices, modernization of intraurban and interurban telegraph lines, the Tallinn-Narva line being the principal one, inclusion of rural areas in the telegraph network, introduction of stereophonic FM radio broadcasting of four programs from MCh-ChM and MV-ChM stations, increase of television transmitter power ("Il'men" decimeter-wave transmitter to be installed in Kikhtla-Yarve), and extension of the television broadcast range to cover 80% of the republic's population. These achievements are made possible by developments in engineering and manufacturing of better, more, and new equipment. It is expected that the goals of the current Five-Year-Plan will be continue being met as successfully. Figures 4.
[126-2415]

COMMUNICATION FACILITIES IN ARMENIA

POGOSYAN, L. I., deputy minister of communications, Armenian SSR

[Abstract] The telephone network in Armenia has expanded tremendously from 1921 (when the Yerevan telephone exchange office operated with only two switchboards and served only 250 subscribers) to 1981 (when installation of a new coaxial cable trunk with additional 300 intrazonal and 600 interzonal telephone channels was completed). It now also covers interurban and rural lines with the total number of subscribers reaching 110 thousand in Yerevan alone, with 7.95 sets per 100 inhabitants (ranking third highest in the Soviet Union). The telegraph system has developed alongside. Television in Armenia has also expanded tremendously since 1956 (when the Yerevan television center covered a radius of 60 km and reached only 48% of the republic's population), now covering 93.4-98.2% of the population with the First Central and Republican programs, 65.7-68.4% of the population with the Second Central and Republican programs, and includes broadcasting in color as well as in black-and-white. Radio broadcasting has expanded alongside. These achievements were primarily made possible by adaptation and extension of facilities to higher elevations above sea level in the republic's mountainous territory, and through appropriate design, installation and operation of equipment. The trend is expected to continue throughout the present Five-Year-Plan period so that the established goals will be met. Figures 5.
[126-2415]

PROGRESS IN RADIO ENGINEERING IN GEORGIAN SSR DURING 60 YEARS SINCE FOUNDING OF SOVIET UNION

SANADZE, T. I., associate member, GSSR Academy of Sciences, and NAMICHEYSHVILI, O. M., Georgian SSR

[Abstract] Radio engineering in the Georgian SSR has progressed from the electron-tube radio telegraph station built in 1923, one of the first in the Soviet Union, to the unique general-purpose microcomputer built recently with tunable standard PS-300 structures. Contributors to this progress have been the Institute of Communication Engineers, transferred from Leningrad to Tbilisi during the Great Patriotic War [World War II], the Tbilisi State University with its Department (Kafedra) of Radio Engineering (since 1948) and Department (Kafedra) of Radiophysics (since 1960), the Georgian Poly- technic Institute (since 1965), and the Institute of Control Systems at the GSSR Academy of Sciences (since 1956, until 1970 called Institute of Electronics, Automation and Telemechanics). Achievements during the first 30 years were made particularly in the areas of radio interference abatement, including use of autoparametric filters, ionosphere probing, transmitter and antenna design and technology. Achievements in the last thirty years were made particularly

in the areas of microwave electronics, television and x-ray measurements and flaw detection, microelectronics, biomagnetism, quantum radiophysics, diffraction of electromagnetic waves (including development of the method of orthogonal functions), electron-paramagnetic resonance, optoelectronics, automation and reliability assurance. The first general-purpose digital computer in the Georgian SSR ("Delisi" model) was developed during the 1957-62 period. A scientific research laboratory for ionosphere study, the only one in Transcaucasia and located under the focus of ionospheric dynamio currents, has been in existence since 1962. Transition from ideas and concepts to prototype construction and subsequent series manufacture is facilitated by engineering organization and scientific-industrial associations such as the Tbilisi "Analitpribor" at the USSR Ministry of Communications, the Scientific-Industrial Association "Elva" (since 1971) based on the Tbilisi Scientific Research Institute of Instrument Design and Automatic Equipment (since 1956), and the Scientific Research Institute "Avtomatprom" (since 1956). [135-2415]

DEVELOPMENT OF RADIOELECTRONICS IN UZBEKISTAN

SADYKOV, A. S., president, UzSSR Academy of Sciences

[Abstract] Developments in radioelectronics in Uzbekistan began on an intensive scale in 1943, when the UzSSR Academy of Sciences was founded. There are now 43 higher educational institutions in the Uzbek SSR engaged in basic and applied research, including the Department of Thermophysics with the status of an institute, and several institutes (Physico-Technical Institute, Institute of Nuclear Physics, Institute of Electronics, Institute of Cybernetics) at the UzSSR Academy of Sciences, Tashkent University, Tashkent Institute of Electrical Engineering of Communications, Tashkent Polytechnic Institute, Tashkent Pedagogical Institute, Fergano Pedagogical Institute, and Samarkand University. Achievements have been made in four major areas: 1) Physical electronics (secondary electron emission, ion scattering, diffusion and scattering in crystals, sorption and adsorption processes), including development of the double-modulation method and special ion-bombardment techniques; 2) Semiconductor electronics (industrial production of extra-pure silicon, theory of deep impurity levels, high-frequency barrier effects); 3) Quantum electronics (light scattering, interaction of laser radiation and vapors of alkali metals at two-photon resonance, effect of laser radiation on surface thermodynamics, on dielectrics, semiconductors, and metals), including development of small low-noise CO_2-laser with transverse high-frequency pumping; and 4) Communication and computer technology (optical fibers, integrated optics, interference-immune digital data transmission, optimization of computer-based automatic control systems, improvement of quality of television images through optimum signal correction). References: 32 Russian.
[135-2415]

SCIENTIFIC-TECHNICAL SEMINAR ON METHODS OF MATHEMATICAL MODELING AND MACHINE DESIGN OF LASERS

MIKAELYAN, A. L. and KOBLOVA, M. M.

[Abstract] The second scientific-technical seminar of the quantum radio-optics section of the Scientific and Technical Society of Radio Engineering, Electronics and Communications imeni A. S. Popov was held 8-9 September 1982 at the Tomsk Institute of Automated Control Systems and Radio Electronics. The seminar dealt with problems of mathematical modeling of laser processes. Reports were heard and discussed by specialists from Moscow, Minsk, Novosibirsk, Tomsk and other cities. The reports were given in two groups: 1) particulars of constructing mathematical models for specific laser processes; and 2) introduction and practical development of methods of machine design based on sound mathematical models. The titles and authors of some of the papers are listed together with a brief overview of contents. [128-6610]

METHODS OF PRODUCING DIAMOND-LIKE FILMS AND THEIR PROPERTIES

BALAKOV, A. V. and KONSHINA, Ye. A.

[Abstract] Diamond-like carbon films can be produced by all known ion-plasma deposition methods. These can be classified into two groups: graphite atomization (Penning cell with ions of inert gas in low-pressure plasma in longitudinal magnetic field; deposition on solid substrate under superhigh vacuum with a duoplasmatron; condensation of plasma stream from vacuum arc between graphite cathode and metal anode with curvilinear separator; Finkelstein cell with two ion guns for atomization of graphite and buildup of carbon films, respectively, with ions of inert gas) and decomposition of hydrocarbons (d.c. glow discharge; high-frequency discahrge; gas ionization with magnetron-type ion source). These authors have produced diamond-like carbon films by decomposition of acetylen from a 50:50 acetylen-krypton plasma and gas ionization with a magnetron-type ion source. The structure and the phase composition of carbon films depend on the process conditions, mainly on the energy of deposited particles, but also on the energy of non-carbon particles involved in the process as well as gas pressure, deposition rate, substrate temperature and substrate dimensions. Carbon films have been produced with macroscopic properties approaching those of diamond electrically (resistivity, mechanically (hardness), optically (emission and absorption spectra), and chemically (resistance to aggressive media such as inorganic

acids and alkalis, organic solvents). The microhardness of the softest carbon films, produced by decomposition of hydrocarbons in glow discharge, exceeds that of silicon carbide. The microhardness of the hardest carbon films exceeds that of natural diamond. Carbon films can be identified and classified on the basis of these measurable properties. For use as protective coating, a quasi-amorphous film has better microscopic properties than a polycrystalline one. Both can be used for protecting the surface of laser windows against oxidation. An important other application of superhigh-hard carbon films is as abrasive on tools for surface finish treatment. Figures 10; tables 2; references 49: 21 Russian, 28 Western (2 in translation).
[144-2415]

SCIENTIFIC-TECHNICAL PROBLEMS AND DEVELOPMENT TRENDS IN ROBOTICS

YUREVICH, Ye. I.

[Abstract] A special resolution of the CC CPSU adopted on 31 July 1980 set forth the following goals for development of robotics: larger production volume of standard high-quality industrial robots and their components; delivery of self-contained robotized technological complexes, general-purpose and special-purpose, to new industrial enterprises; construction and duplication of "flexible" complexly automated model plants; extension of robotics application to other than machine manufacturing industries; complete standardization of robotics producer goods; further improvement of industrial robots, including construction and production of new generations. Currently built industrial robots with automatic manipulators have a hierarchical modular structure consisting of problem-oriented or function-oriented modules with structural-logical correspondence, not closed so as to allow for expansion. An important feature is inclusion of microprocessors and microcomputers for control and automation. The main problems in installation of robotized technological complexes are ensuring adequate floor space and transportation facilities, ensuring full and efficient utilization with maximum economy and reliability, and ensuring high productivity through high-speed operation with high load capacity. Introduction of industrial robots with automatic manipulators into a production process requires analysis of plant sites from the standpoint of automation, productivity of basic tools, and stability of operation. Their first application is loading-unloading, and their next application is handling semiautomatic equipment. Scientific-technical activities in robotics development during the eleventh Five-Year-Plan period will be: developing principles of adaptive modular robot design; developing principles of flexible robotized production automation; constructing standard robotized complexes for new technologies such as plasma treatment, powder metallurgy, thermocyclic treatment, and processes which utilize superplasticity ;

studying the socio-economic aspects of robotization and developing methods of measuring them. Recently bilateral and multilateral agreements with other CEMA countries have been reached on cooperation in the field of robotics, an important general one in 1982. Figures 1; references: 2 Russian.
[145-2415]

SPLIT SUPERCONDUCTING DIAPHRAGMED WAVEGUIDE

KAMINSKIY, V. L., NOVIKOV, S. A., SAMOYLENKO, G. M. and YUSHKOV, Yu. G.

[Abstract] A superconducting diaphragmed waveguide is described where no high-frequency current flows through the contact between its components. The disadvantage of electron-beam welded joints is buildup of thermal stresses and attendant field emission during operation at high power levels. A split coupling has been designed instead with all dimensions fixed for given performance requirements, except the depth of the coaxial groove. The latter could be varied to optimize the structure and ensure a zero azimuthal magnetic field component of the accelerating wave at the contact. Calculations were made according to available programs for azimuthally symmetric structures with arbitrary form of inside boundary. A prototype consisting of two segments, both made of niobium, was built and tested. The experimental data (f_0 = 4968.5 MHz and $Q_0 = 10^6$ with a 1.5 cm deep groove, f_0 = 4952.02 MHz and $Q_0 = 10^7$ with 1.72 cm deep groove) agreed with the design data within 0.11%. The results indicate that the gap between waveguide segments does not distort the axial profile of the longitudinal electric field ocmponents and that it may be feasible to attain $Q_0 = 10^9$ by special treatment of the superconducting waveguide structure. Figures 2; references 6: 3 Russian, 3 Western.
[127-2415]

STANDARDIZATION OF NORMS FOR MANUFACTURE OF ELECTRICAL EXPLOSION-PROOF AND MINING EQUIPMENT

KAYMAKOV, A. A., candidate of technical sciences, LYAGIN, B. S., engineer, OSIPOVICH, V. T., engineer, POPOV, V. V., engineer, PYATETSKIY, G. Yu., engineer, TORGASHOV, V. S., candidate of technical sciences, KHORUNZHIY, M. V., engineer, and SHILOV, V. V., candidate of technical sciences, All-Union Scientific Research Institute of Electrical Explosion-Proof and Mining Equipment (VNIIVE)

[Abstract] Soviet norms for manufacture of electrical explosion-proof and mining equipment, established during the 1950-63 period and enforced through-out the nineteen seventies, are technically lower than IEC norms enforced in most industrial countries as well as some recommended by CEMA. Existing specifications are being upgraded, therefore, so as to reflect progress in manufacturing of such equipment and, at the same time, contribute to standardization and trade agreements. The upgrading process is a difficult one and new specifications necessarily include some with no IEC and CEMA equivalents typically for standard ore mining equipment, thus requiring appropriate adjustments. The new requirements and corresponding test methods are formulated in GOST 22782.0-81 (general technical requirements and test methods), GOST 22782.1-77 (protection: housing filled with oil), GOST 22782.1.77 (protection: housing filled with quartz), GOST 22782.3-77 (protection: special form), GOST 22782.4-78 (protection: housing filled or scavenged under subgauge pressure), GOST 22782.5-78 (protection: spark-proof electric circuit), GOST 22782.6-81 (protection: explosion-proof housing, and GOST 22782.7-81 (protection: "f"). In addition GOST 12.2.020-76 covers equipment terminology and definitions, GOST 12.021-76 covers sequence of documentation matching, GOST 12.1.011-78 covers classification of hazardous mixtures from standpoint of equipment selection, GOST 24719-81 covers require-ments and isolation, and GOST 24754-81 covers requirements and testing of standard ore mining equipment.
[138-2415]

- END -